IntechOpen

Modified Asphalt

Edited by Jose Luis Rivera-Armenta and Beatriz Adriana Salazar-Cruz

MODIFIED ASPHALT

Edited by **Jose Luis Rivera-Armenta**
and **Beatriz Adriana Salazar-Cruz**

Modified Asphalt
http://dx.doi.org/10.5772/intechopen.71157
Edited by Jose Luis Rivera-Armenta and Beatriz Adriana Salazar-Cruz

Contributors

Farzaneh Tahmoorian, Bijan Samali, John Yeaman, Ragab Abd Eltawab, Ahmet S. Karakas, Faruk Ortes, Vladislav Podolski, Dmitry Chernousov, Alexandr Lukashuk, Bagdat Teltayev, Russell Chianelli, Eva Deemer

Notice

Statements and opinions expressed in the chapters are these of the individual contributors and not necessarily those of the editors or publisher. No responsibility is accepted for the accuracy of information contained in the published chapters. The publisher assumes no responsibility for any damage or injury to persons or property arising out of the use of any materials, instructions, methods or ideas contained in the book.

First published in London, United Kingdom, 2018 by IntechOpen
eBook (PDF) Published by IntechOpen, 2019
IntechOpen is the global imprint of INTECHOPEN LIMITED, registered in England and Wales, registration number: 11086078, The Shard, 25th floor, 32 London Bridge Street
London, SE19SG – United Kingdom
Printed in Croatia

British Library Cataloguing-in-Publication Data
A catalogue record for this book is available from the British Library

Additional hard and PDF copies can be obtained from orders@intechopen.com

Modified Asphalt
Edited by Jose Luis Rivera-Armenta and Beatriz Adriana Salazar-Cruz

p. cm.

Print ISBN 978-1-78923-726-9

Online ISBN 978-1-78923-727-6

eBook (PDF) ISBN 978-1-83881-523-3

Meet the editors

José Luis Rivera-Armenta was born in Tampico, Mexico, in 1971. He has a BSc in chemical engineering (1994), an MSc in Petroleum Technology and Petrochemicals (1998), and a PhD in Chemical Engineering (2002) at the Technological Instituto of Madero City (ITCM). Since 2003 he has been a full-time professor in postgraduate programs at ITCM and project manager of several projects sponsored by the National Technologic of Mexico and CONACYT. Since 2005 he has been a member of the National Research System in CONACYT level 1. He is responsible for the injection and extrusion, and thermal analysis laboratory at the Petrochemical Research Center at ITCM. He has advisored eight PhD, 15 master's degree and three bachelor theses. He also supervised three posdoctorate students. He has had 48 articles and five book chapters published.

Beatriz A. Salazar Cruz, PhD since 2014, has been an associate member of MATCO since 2016, and an associate professor since 2012 of the Technological Institute of Madero City. She has had experience in the chemical process industry from 1995 to 2008 (Dynasol Elastomers) developing projects with SBS, SBR and SEBS polymers, and characterizing and innovating the quality of products in a wide range of applications: asphalts, adhesives and compounds. She is the author or coauthor of several scientific publications in English and Spanish, and author or coauthor of several book chapters. She has taught several rheology courses and is a collaborator of several projects supported by the National Technologic of Mexico and CONACYT. She has advisored a master's degree thesis and also supervised engineering students.

Contents

Preface

This book presents specific information on asphalt modifications, which has become an interesting area in recent years, due to the relevance of these kinds of materials for applications in roads and highways. The current requirements in terms of the capacity to withstand greater loads on roads and highways make it necessary to develop more resistance asphalt with better properties, for instance deformation resistance at high temperatures, low-temperature cracking, and fatigue cracking, with the aim of meeting the needs of different geographical areas.

Asphalt is a byproduct of oil refinery and is a complex mix of hydrocarbons. Because it has a varied composition that mainly consists of heavy oil fractions, such as saturated asphaltenes, resins, and aromatics, and depending on its origin, the proportions of these fractions can vary to make asphalt heavier.

The main problems with modified asphalts are phase separation and thermal stability, which are responsible for failures such as ruts, fractures, and cracks, among others. Depending of the environmental conditions of use, these failures can increase in some cases, so it becomes necessary to use modifier agents that improve the characteristics of asphalts.

Asphalt modifiers by excellence are elastomers, mainly styrene-butadiene; however, even modified asphalt with these kinds of elastomers have fallen short in fulfilling their main purpose, which is why it is necessary to look for new modifiers and especially new developments to adapt and evaluate the performance of modified asphalts.

Among the main properties that a modified asphalt must have are mechanical properties, since final performance depends on their supporting the loads and conditions to which they are subjected during their application.

In recent years, environmental issues have become an important aspect of caring, so not only should modified asphalts allow for lower fuel consumption, but also the modifying agents such as polymers or natural products can be recycled, because in this way natural resources would be used less and less pollution would be generated.

This book is divided into two sections: the first “Asphalts with Environmental Focus” and the second “Evaluation of Asphalt Performance.” The objective of presenting in this way is to analyze the options to generate modified asphalts using environmentally friendly materials and, on the other hand, to analyze the performance of modified asphalts with conventional agents such as rubbers, polymers, or clays, or to evaluate properties such as fatigue failures or thermal properties.

This book is a compilation of work that studies how modified asphalts are developed using unconventional materials that can be environmentally friendly and, on the other hand, work where the performance of modified asphalts is evaluated mainly for their mechanical properties, due to the relevance of these areas in the applications of modified asphalts.

Dr. José Luis Rivera-Armenta and Dr. Beatriz Adriana Salazar-Cruz
National Technologic of Mexico (TecNM)
Technological Institute of Madero City, Mexico

Section 1

Asphalts with Environmental Focus

Chapter 1

Asphalt Modified with Biomaterials as Eco-Friendly and Sustainable Modifiers

Ragab Abd Eltawab Abd El-latief

Additional information is available at the end of the chapter

http://dx.doi.org/10.5772/intechopen.76832

Abstract

High construction costs, when combined with awareness regarding environmental stewardship have encouraged the use of waste and renewable resources in asphalt modification. Increasing energy costs and the strong worldwide demand for petroleum have encouraged the development of alternative binders to modify or replace asphalt binders. The benefits of using alternative binders are that they can help save natural resources and reduce energy consumption while maintaining and in some cases improving asphalt performance. Common alternative binders include engine oil residue, bio-binder, soybean oil, palm oil, fossil fuel, swine waste, and materials from pyrolysis. Chemical compositions of the majority of these alternative binders are similar to those of unmodified asphalt binders (e.g. Resin, saturates, aromatics, and asphaltene). On the other hand, tests indicate the wide variability in the properties of alternative binders. Also, the chemical modification mechanism for asphalt with alternative binders depends clearly on the unmodified asphalt and is consequently not well understood. For energy sustainability, environment-friendly materials and an urgent need for infrastructure rehabilitation that more research is needed to evaluate the alternative binders for use in asphalt modification. The alternative binders should have moisture resistance and good aging characteristics.

Keywords: asphalt, sustainable, alternative binders, biomaterials, eco-friendly, bio-binder

1. Introduction

1.1. General introduction

Bio-materials that are used as binders in asphalt mixtures are termed "bio binders" [1]. The interest on using bio-binders in pavement engineering has significantly grown over the last decades due to the increasing scarcity of raw materials and environmental concerns about the use of non-recoverable natural resources.

Common alternative binders include engine oil residue, bio-binder, soybean oil, palm oil, fossil fuel, swine waste, and materials from pyrolysis [2]. Chemical compositions of the majority of these alternative binders are similar to those of unmodified asphalt binders (e.g. Resin, saturates, aromatics, and asphaltene) [3]. On the other hand, tests indicate the wide variability in the properties of alternative binders. Also, the chemical modification mechanism for asphalt with alternative binders depends clearly on the unmodified asphalt and is consequently not well understood [4, 5]. For energy sustainability, environment-friendly materials and an urgent need for infrastructure rehabilitation that more research is needed to evaluate the alternative binders for use in asphalt modification. The alternative binders should have moisture resistance and good aging characteristics [6].

2. Bio binder's definition and resources

2.1. Definition

Bio-binder is an eco-friendly asphalt binder alternative obtained from non-petroleum-based renewable resources, which should not rival any food material. From the definition, bio-binder can be described as dark brown, high flow, organic liquids that are comprised mainly of highly oxygenated compounds [7–10].

2.2. Bio-binder material sources

A range of different vegetable oils has been investigated in recent times, through the application of scientific research and development, to determine their physical and chemical properties to study their applicability to be used as bio-binders in the pavement industry [11–13]. Bio-oils are produced from plant matter and residues, such as municipal wastes, agricultural crops, and byproducts from agricultural and forestry [8]. Other biomass sources include molasses and rice, sugar, potato starches and corn, gum resins and natural tree, vegetable oils and natural latex rubber, cellulose, lignin, waste oil of palm, peanut oil waste, coconut waste, potato starch, canola oil waste, dried sewerage effluent, and others.

Utilize this bio-binder can be a great potential as a modifier for asphalt binder because of similar chemical properties when compared with crude petroleum as shown in **Table 1**.

Currently, bio-binder is the second leading renewable energy in the nation after hydropower [14, 15].

Physical property	Value
Percent of moisture (wt %)	15–30
pH	2.5
Specific gravity	1.2
Elemental composition (H, C, O, N) (wt %)	(5.5–7.0, 54–58, 35–40, 0–0.2)
Distillation residual (wt %)	Up to 50
Viscosity @500°C (pa)	40–100

Table 1. Typical characteristics of wood-based bio-oils.

3. Materials used for the production of bio-binder

3.1. Bio-oil

Bio-Oil is the liquid produced from the rapid heating of biomass in a vacuum condition [17]. There are many advantages for bio-oils over asphalt from crude oil as they are environment-friendly, renewable, present a great economic opportunity, and provide energy security.

3.1.1. Bio-oil sources and production

3.1.1.1. Thermochemical liquefaction

To obtain more gasoline and other liquid fuels, the quality of the bio-oil is improved by using processes such as thermal cracking and hydrogenation [16, 17]. Upon fractionation, the light hydrocarbon fraction can be used as fuel. The remaining heavy residue called bio-binder can be used as an asphalt binder modifier.

3.1.1.2. Pyrolysis process

Fast pyrolysis is a thermal decomposition process that requires a high heat transfer rate to the biomass particles and a short vapor residence time in the reaction zone [8], which is a high-temperature process for the production of vapors, aerosols and some coal-like char where biomass is quickly heated in the vacuum and then decomposes. The dark brown mobile fluid (bio-oil) is formed after cooling and condensation of these vapors and aerosols. When organic matter is biomass, consisting of biopolymers (such as cellulose, hemicelluloses, and lignin), the oils produced are called bio-oils. Generally, fast pyrolysis is used to obtain high-grade bio-oil. Fast pyrolysis processes produce 60–75 wt% of liquid bio-oil, 15–25 wt% of solid char, and 10–20 wt% of non-condensable gases. Fast pyrolysis initially starts with slow heating rates, and then involves a rapid heating rate of the biomass, that can reach up to 300°C/min, but not as fast as flash pyrolysis.

Fast pyrolysis design variables include, but are not limited to the following ones reported by [8]: feed moisture content, particle size, pretreatment, reactor configuration, heat supply, heat

transfer, heating rates, reaction temperature, vapor residence time, secondary cracking, char separation, ash separation, and liquid collection.

3.1.2. Importance of using bio-oil in the modification of asphalt

The bio-oil obtained from waste biomass at low cost is an environmentally friendly material containing the natural antioxidant lignin, bio-renewable asphalt modifier and asphalt substitutes potential to be successfully applied as an antioxidant additive in asphalt pavements. The other various chemicals that using as antioxidant additives are not environmentally and economically preferable [18].

3.2. Biopolymers

Bio-plastics or organic plastics are a form of plastics derived from renewable biomass sources, such as vegetable oil, corn starch, pea starch, or microbiota. Some of its advantages are often biodegradable, not toxic to produce and alternative to traditional plastics this is included in the definition of biodegradable polymers mentioned in [19]. Biopolymers are an alternative to petroleum based polymers produced by living organisms. The field of biopolymers is still in its early stage but is growing in popularity every day. Biodegradable polymers are produced by using micro-organisms, plants and animals (biological systems), or biological starting materials, which have been synthesized chemically from (e.g. starch, sugars, oils or natural fats, etc.). The biopolymers are biodegradable most of them and water-soluble some of them. Most of the biopolymer are compostable or will decompose in landfills, but the time can vary from a few days to even years, and will eventually decompose [20]. The natural rubber is the best example classified as a biopolymer. The natural rubber is the most common elastomer in almost all human activities due to its unique characteristics, raw or combined with synthetic elastomers. This elastomer has the ability to improve pavements performance and durability for being applied in road pavements as a recycled material from tires [21].

3.2.1. Importance of using the biopolymers

The bitumen degree controls the performance of the pavement mixture during the service temperature. In many cases, bitumen properties need to change to enhance their flexible characteristics at low temperatures to withstand adequate cracking and increase shear resistance through high-temperatures and continuous loads to resist corrosion. With the addition of SBS polymers, the physical properties of polymers are usually modified to produce an improved asphalt grade that improves the performance of hot mix asphalt. In 2008, there was a shortage of type spherical polymers for the asphalt industry forcing asphalt mixing producers and owner/agencies to search for different products that could be used as bitumen [21]. With expectations of increased demand from soft asphalt in the next time, the need for viable asphalt is cost-effective that can be used instead of typical spike-type rates will still strong. Of asphalt-modified polymer mixture, nearly 80% of the polymer modified asphalt uses the SB type polymers. Thus there is a great market opportunity to create new polymers that can complement and/or replace the type SBS polymers used in asphalt paving. The researchers of chemistry and engineering are currently working to obtain chemicals and polymers from

renewable raw materials, composite materials and manufactured products known as "biological materials." When deliberating biomaterials, it is noteworthy that there are no direct negative effects caused by plants on the ecosystem, they can recycle carbon dioxide for the Earth's crust, grow in different climatic zones, and much work on soil fertility improvement [22].

3.2.2. Bio-elastomers

Elastomers materials, or rubber materials, have a cross-linked structure. Natural and synthetic rubbers are both common examples of Elastomers [23]. Elastomer is a polymer with viscoelasticity property in general, especially at low Yung's modulus, and high yield strain compared to other materials. The plastics are very flexible and flexible, which means they can undergo large elastic deformities without rupture and greatly restore the shape and size after removal has been removed. Plastics are usually resistant to oil and fuel, not permeable to liquids and gases, but tend to deteriorate by oxidation [23]. Furthermore, plastics are either thermoplastic (can be thawed) or thermoplastic (which cannot be melted). The use of plant-derived triglycerides is a substance used in the production of plastics because it provides two interactive sites, the double bond in the series of unsaturated fatty acids, and the ester group [24].

3.2.3. Using of bio-elastomers in asphalt modification

The introduction of crumb rubber in the production of asphalt-rubber mixtures for road pavement should be considered a sustainable technology that turns unwanted residues into a new mixture with high resistance to fatigue and breakage. According to ASTM D 6814–02, rubber is a synthetic or natural synthetic rubber that can be chemically cross-linked/vulcanized to enhance its useful properties. Rubber or elastic joints across the link are three-dimensional molecular networks, with long molecules held together by chemical bonds. It absorbs solvents and swells but does not melt. Moreover, it cannot be reprocessed simply by heating [25–27].

3.3. Waste cooking oil

The amount of waste cooking oil collected every year from food shops and restaurants is found to be 3 billion gallons; this is according to the U.S. Environmental Protection Agency (2011) [28]. This can be treated by polymerization and used as an alternative to bitumen [29].

The researchers investigated the potential use of cooking oil waste as an approved bitumen rejuvenation agent [30, 31]. The result was very promising because of the successful application of waste cooking oil with bitumen as an activated agent for used bitumen or older leads to an economical and environmentally friendly solution. More modification and research is needed to obtain more efficient and effective results.

3.3.1. Problems caused by waste cooking oil and its treatment methods

In general, the dumping of untreated waste into a land fill or river leads to a negative environmental impact. One of the main environmental issues arises the enrichment process that occurs when there is an obstacle to sunlight to penetrate the surface of the river caused by

the blocking of a thin layer of oil. Ultimately, oxygen supply to aquatic life is disturbed when nutrient enrichment occurs in the river [32, 33]. The balance of the water ecosystem balance in the lake or river has also affected water quality. Engine oil from vehicles or cooking oil waste from residential areas contributes to the main source of river pollution. The responsibility to overcome high construction costs and reduce waste disposal issues has begun to practice the recycling of waste as an alternative and an alternative way to prevent these problems [32]. According to Hamad et al. [33] and Singhbando and Tezuka [34], only the designated licensed companies responsible for collecting cooking waste World Customs Organization (WCO) from the food industry and especially the fast food restaurant before being sent to the recycling centers.

3.3.2. Production of waste cooking oil

Waste cooking oil originates from frying activity at high-temperatures during food preparation, usually in the food industry, restaurants, hotels, and residences. The application of global customs organizations is diverse, for example, the use of yellow grease [35, 36], potential as a fuel source in biodiesel production [37], animal food [38], and making soap production [37]. Despite efforts to collect up to 15 million tons of WCO annually, only a small amount of cooking waste is properly managed through the recycling process [38]. Regular monitoring and management of the WCO creates a challenge to be addressed and becomes the primary consideration for overcoming serious dumping problems that eventually lead to serious water pollution [39]. **Figure 1** shows the total production of the WCO by States. The production of 10 million tons of WCO per year, accounting for 55%, makes the United States the highest producer of the WCO.

A large amount of vegetable oil consumption about 17 million tons causes a huge amount of waste that has reduced the production of oil resources, and this amount increases about 2%

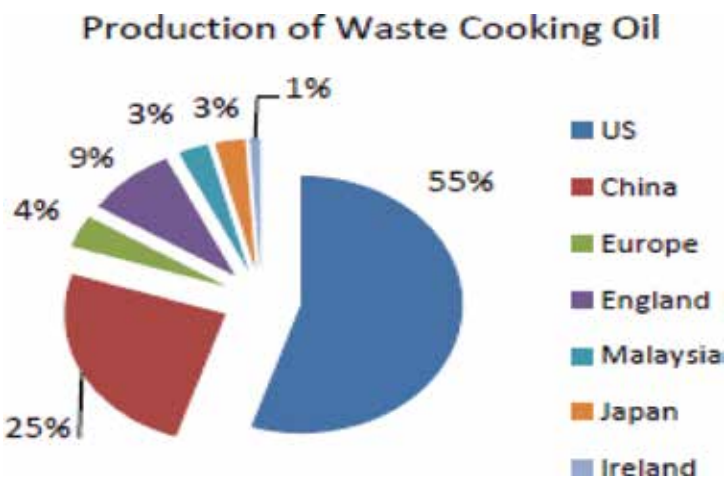

Figure 1. Production of cooking oil based on the country [36, 40, 41].

every passing year [42]. According to the food and drug administration (FDA) report [42, 43], 40% of the sewage system is blocked with frying oil which is cast in the kitchen sink.

3.3.3. Chemical properties and characterization of waste cooking oil

Chemical properties gas chromatography–mass spectrometry test (GCMS) is one of the chemical tests that are used for the purpose of the identification of chemical compound in unknown waste cooking oil. Based on the observation, the major chemical compound identified in the WCO is oleic acid, which represents 43.67% of the entire compound. Meanwhile, palmitic acid represents for 38.35% whereas 11.39% is recorded linoleic acid as shown in **Table 2**.

Due to long chain of palmitic acid and oleic acid [44], the potential of being cracked is high by thermal cracking or catalytic cracking process. Based on the research conducted by Zahoor et al. [45], the properties of unused oil is differ from used cooking oil especially in term of density, kinematic viscosity, and moisture content which presented in **Table 3**.

3.3.4. Experimental application of bio-binders

The main field of application of bio-binders is in the paving industry. However, market opportunities exist in housing products via roofing shingles and sealants [46]. There are three ways that a bio-binder reduces the use of bitumen from fossil fuels (as shown in the percentage) [8].

1. Directly alternative (75–100% bitumen substitute.
2. Bitumen extender (10–75% bitumen substitute)
3. Bitumen modifier (<10% bitumen substitute)

Free fatty acid's type	**Waste cooking oil %**
Heneicosanoic acid	0.08
Cis-11-Eicosenoic acid	0.16
Linolenic acid	0.29
Palmitic acid	38.35
Linoleic acid	11.39
Stearic acid	4.33
Myristic acid	1.03
ɣ-Linolenic acid	0.37
Lauric acid	0.34
Oleic acid	43.67
Total	100

Table 2. Chemical properties of waste cooking oil [44].

Properties	Used cooking oil values	Unused cooking oil values
Acid value (mg KOH/gm)	4.03	0.3
Calorific value (J/gm)	39,658	—
Saponification value (mg KOH/gm)	177.97	194
Peroxide value (meq/kg)	10	< 10
Density (gm/cm^3)	0.9013	0.898
Kinematic viscosity (mm^2/s)	44.956	39.994
Dynamic viscosity (mpa.s)	40.519	35.920
Flash point (°C)	222–224	161–164
Moisture content (wt. %)	0.140	0.101

Table 3. Comparison between properties of unused oil and used cooking oil.

In almost, all the road construction has been used modifiers in conventional bitumen binder. To decrease the demand for petroleum-based bitumen research is being done on bitumen extender as 100% replacement of bitumen. Additives are the resin, emulsions, crumb rubber, polymer and so on. Waste materials like waste cooking oil, waste engine oil and so on, may be the promising alternatives [47, 48].

4. Overview of the results of using of bio-modified asphalt

4.1. Predictable overall specifications

Asphalt is a mixture of moderately molecular weight hydrocarbons, aliphatic, and aromatic hydrocarbons containing moderate amounts of sulfur, small amounts of oxygen and nitrogen, and other rare elements including transitional metals. The physical and chemical properties of asphalt are results of their chemical composition. Large changes in chemical composition may lead to changes in unexpected physical properties. Bio-binders are at best linked to performance, so important chemical changes may give a false test. There are many noticeable, tacit assumptions about asphalt to consider:

- Expected aging characteristics.
- It is expected to have rheological properties.
- Will have the characteristics of the expected adhesion to aggregates.
- Has the expected coating behavior in the mixing plant.
- Have predictable flow characteristics throughout construction.

There are many other less obvious predictions:

- Predictable outflow characteristics.
- Expectable water solubility.
- Expected interactions with fuels, oils, and so on.
- Predictable environmental characteristics.
- It will have a predictable smell.
- It will have a predictable mixing with a virgin binder as a reclaimed asphalt pavement
- It will have a predictable interaction with contiguous mixtures.
- Will be available in large quantities upon request.

4.2. Aging

Rolling thin film oven test (RTFO) and pressure aging vessel (PAV) may not sufficiently represent plant and field aging because an alternative binder may have significantly different aging characteristics. Start by identifying an aging index to compare with unmodified asphalt is suggested in experimental respects. RTFO It should be operated over a variety of times and temperatures to see if normal temperature correspondence is still present. The same is true for PAV. Use PAV at 60°C for excessive times and compare output performance with results in standard conditions.

4.3. Rheological properties of bio-modified asphalt

Bio-binder may it may completely break down or give suggestively different time-temperature relationships. A clear example is an alternative bond with a fine melting point. A binder with a melting point at 73°C may be well suited for use in heavy road traffic in the PG 64 environment, but the dynamic shear rheometer (DSR) test at a specific grade of 76°C will give inappropriate results.

4.4. Strength properties and cracking

While strength characteristics and cracking are precarious to pavement performance, they are controlled by the total and the gradient and the effect of the alternative binder properties is not easily expected. Unlike low-temperature characteristics, it may be necessary to reduce the mixture test to explain the effect of a new material on cracking and strength properties.

4.5. Rutting performance at high-temperature

As illustrious above, bio-binder may have a different shape to the master curve. They may also have varied stress tolerance. For more than a few reasons, the creep compliance is

unrecoverable, Jnr, from the multiple creep and recovery creep (MSCR), is a better choice than the G */sin δ of the oscillating DSR to describe the performance of high-temperatures. MSCR is run at the expected high pavement temperature and therefore, does not depend on the time-overlay overlap. Jnr has been shown to be well correlated with the actual progressive performance of a larger group of substances from G */sin δ. Finally, stress tolerance is already a unit for MSCR testing. However, it would be practical to check the range of temperatures and pressures to look for unusual behavior that may affect progressive performance. The mixture test is also strongly recommended.

4.6. Cracking in cold climates

Cold climates tensile and crack the characteristics of a bio-binder may differ from conventional asphalt, so testing the bending beam rheometer (BBR) may not be sufficient. A fracture test such as a direct tensile test or asphalt cracking will provide information on low-temperature break characteristics. If there is a significant difference in expected temperatures, the fracture test results can still be used to re-evaluate the BBR results to simplify the test over the long term. One more caution, these still only characterize one single thermal cracker. May not adequately address fatigue at low-temperatures.

4.7. Fatigue performance

There is currently a no good way to characterize a binder for fatigue performance, although there are some talented tests in development. The G * sin δ from DSR has been included in the superpave specification to control the shape of the main curve, and as mentioned above, it may or may not be suitable for a substance different from asphalt. There are differences in mixing tests that are related to fatigue performance, and at least today, this is the only correct position to handle fatigue performance.

5. Comparison between bio-modified asphalt binders and unmodified ones

The temperature range of viscous behavior for bio-oils may be lower than the virgin asphalt rate, by about 30–40°C. The rheological properties of the original bio-binder differ from those of the asphalt, but the rheological properties of these modified biological bonds vary greatly when polymer rates are added. For the developed bio-binders the high-temperature performance grade may not vary significantly from that of the asphalt binders, nevertheless, the low-temperature performance grade may vary significantly [6].

5.1. Structure of bio-oil compared with asphalt

The chemical properties indicated that the amount of furfural and phenols were varying due to the different aging processes and intervals.

The chemistry of bio-oils is complex, similar to asphalt; thus, a complete chemical characterization is difficult or practically impossible. The complication of chemical characterization or analysis resulted from the attendance of high molecular weight of phenolic species [4]. In addition, the fragmented oligomeric products occur with different numbers of phenolic and carboxylic acids, and hydroxyl groups as well as aldehyde, alcohol, and ether purposes. Thus, phenolic species occur as different hydrogen-bonded aggregates, micelles, droplets, and gels.

5.2. Temperature of performance

In general, the mixing and compaction the temperature range for bio-oils may be lower than bitumen inhibitors at about 30–40°C.

- The flow characteristics, that is, the temperature and shear, of the biomedical biomaterials of the bio-oils differ from those of the asphalt, but when adding the polymer hosts, the rheological properties of these modified biomarkers change dramatically.
- Polymers should be carefully chosen because the temperature range of the bio-groups established differs from the polymers used extensively in the asphalt industry.
- The high-temperature performance of biologically determined groups may not change significantly from sediment deposits. However, the low-temperature performance level may change significantly because of the high oxygen content in biomaterials compared to typical asphalt volumes.

5.3. Comparison from viewpoints of environment, economy, and energy

Significantly, The United States is working to create a biobased economy that generates energy from renewable organic matter rather than fossil fuels. Because of access to large amounts of vital sources such as triglycerides, proteins, starch, and other carbohydrates from various plant sources, there are interesting technical and economic forecasts for their use to produce vital bonding materials. At present, research on the application of bio-oils has focused on their use as bio-defense fuel to replace fossil fuels. Based on the findings of these surveys, the use of bio-oils as asphalt metal is very promising.

On the other hand, no research has yet been conducted on the feasibility of using bio-oils as an alternative to asphalt (replacing 100%) for use in the paving industry. As a result, there is a lack of data demonstrating the development of biomaterials from essential oils. Biomass boxes (artificial bonding materials) can be used in three different ways to reduce the demand for fossil-based asphalt compounds.

6. Conclusion

High construction costs, when combined with awareness regarding environmental stewardship have encouraged the use of waste and renewable resources in asphalt modification.

Increased energy costs and strong global demand for oil have encouraged the development of alternative bonding materials to modify or replace asphalt bonding materials. The benefits of using alternative bonding materials are their ability to help conserve natural resources and reduce energy consumption while at the same time improving asphalt performance.

The use of alternative (or secondary) materials in asphalt mixtures may be one of the most complex methods of highway use. It is not a matter of throwing alternative materials into the mixture and coating them with cement. The best use should be designed and used, including the design of the mixture itself, and the effects of alternative materials on the behavior of the asphalt binder, and the pavement to be incorporated into it. It is necessary to know how to test the resulting mixture in order to conform to the specifications; in some cases, this knowledge is lacking. Also, the expected finding from this chapter is as follows:

- Bio-Binder modified asphalt is capable to change rheological properties of the asphalt binder which will improve the performance against pavement distress
- The bio-binder will increase viscosity of the asphalt binder at high service temperature
- The binder test will show that the addition of bio-oils is expected to improve the rutting performance
- Most of the bio-oil modified asphalt mixture has higher fatigue lives than the control asphalt mixture.
- The addition of bio-modified asphalt with asphalt binder reduced the PG of the base binder, representing an increased resistance to thermal cracking, nevertheless reduced resistance to rutting.
- The adding of bio-modified asphalt reduced the crack energy at middle temperatures when compared to unoriginal asphalt under monotonic loading, representing reduced resistance to fatigue cracking.
- The dynamic modulus of hot mix asphalt (HMA) reduced with addition of bio-modified asphalt.
- The flow numbers of the bio-modified asphalt HMA mixes were lower than those of unoriginal mixes. This finding indicated that bio-modified asphalt HMA mixes are more disposed to rutting than unoriginal mixes.
- The cracking energy reduced with addition of bio-modified asphalt in the HMA and crack work obtained from IDT testing at intermediate temperatures, indicating that the bio-modified asphalt mixes are disposed to fatigue failure as soon as compared to control HMA.
- Thermal cracking energy increased with addition of bio-modified asphalt in the HMA, which indicating that an improved resistance to low-temperature thermal cracking. Bio-modified asphalt mixes are highly elastic even at lower temperatures than unoriginal mixes.
- Overall bio-modified asphalt can be a promising applicant for low-temperature behavior. However, further modification of bio-modified asphalt for higher temperature is essential to increase its performance against rutting.

It will be a positive step in the direction of achieving mixture modified with bio-binder that has similar or improve performance when compare to conventional mixtures.

Author details

Ragab Abd Eltawab Abd El-latief

Address all correspondence to: chemragab83@yahoo.com

Asphalt Lab, Petroleum Applications Department, Egyptian Petroleum Research Institute (EPRI), Cairo, Egypt

References

[1] Jiménez del Barco-Carrión A, Pérez-Martínez M, Themeli A, Lo Presti D, Marsacb P, Pouget S, Hammoum F, Chailleux E, Airey GD. Evaluation of bio-materials' rejuvenating effect on binders for high-reclaimed asphalt content mixtures. Materiales de Construcción. 2017;**67**:327

[2] Yang X, You X, Dai Q. Performance evaluation of asphalt binder modified by bio-oil generated from waste wood resources. International Journal of Pavement Research and Technology. 2009;**6**(4):431-439

[3] Walters RC, Fini EH, Abu-Lebdeh T. Enhancing asphalt rheological behaviour and aging susceptibility using bio-char and nano-clay. American Journal of Engineering & Applied Sciences. 2014;**7**(1): 66-76

[4] Mohammad LN, Elseifi MA, Cooper SB, Challa H, Naidoo P. Laboratory evaluation of asphalt mixtures containing bio-binder technologies. 92nd Transportation Research Board Annual Meeting; 2013

[5] Huang SC, Salomon D, Haddock J. Alternative binders for sustainable asphalt pavements. In: Laboratory of Waste Cooking oil Based as sustainable binder for hot-mix asphalt. Washington, D.C: Papers from a Workshop; January 22, 2012. p. 625

[6] Peralta J, Raouf MA, Tang S, Williams RC. Bio-renewable asphalt modifiers and asphalt substitutes. In: Sustainable Bioenergy and Bioproducts, Green Energy and Technology. London: Springer-Verlag London Limited; 2012. DOI: 10.1007/978-1-4471-2324-8_6

[7] Asokan P, Firdoous M, Sonal W. Properties and potential of bio fibres, bio binders, and bio composites. Review on Advanced Materials Science. 2012;**30**:254-261

[8] Mohan D, Pittman CU, Steele PH. Pyrolysis of wood/biomass for bio-oil: A critical review. Energy & Fuels. 2006;**20**(3):848-889

[9] Oasmaa A, Czernik S, Johnson DK, Black S. Stability of wood fast pyrolysis oil. Biomass Bioenergy. 1999;**7**:187-192

[10] Oasmaa A, Sipil K, Solantausta Y, Kuoppala E. Quality improvement of pyrolysis liquid: Effect of light volatiles on the stability of pyrolysis liquids. Energy & Fuels. 2005;**19**(6) 2556-2561

[11] Airey GD, Mohammed MH. Rheological properties of polyacrylates used as synthetic road binders. Rheologica Acta. 2008;**47**:751-763

[12] Shields J. Adhesives Handbook. London: Butterworth; 1976

[13] Tan CP, Che Man YB. Comparative differential scanning calorimetric analysis of vegetable oils: Effects of heating rate variation. Phytochemical Analysis. 2002;**13**:129-141

[14] Urbanchuk JM. Biomass energy resources. US Department of Energy LECG LLC. February 19, 2007

[15] Xiu SN, Zhang Y, Shahbazi A. Swine manure solids separation and thermochemical conversion to heavy oil. BioResources. 2009A;**4**(2):458-470

[16] Ancheyta J, Speigh JG. Hydroprocessing of Heavy Oils and Residua. CRC Press; 2007

[17] Gevert BS, Otterstedt JE. Upgrading of directly liquefied biomass to transportation fuels-hydroprocessing. Biomass. 1987;**13**(2):105-115

[18] Williams RC, Peralta J, Ng Puga KL. Development of non-petroleum-based binders for use in flexible pavements—Phase II. Final Report. 2015

[19] Goyal HB, Seal D, Saxena RC. Bio-fuels from thermochemical conversion of renewable resources: A review. Renewable and Sustainable Energy Reviews. 2006;**12**:504-517

[20] Liu M, Ferry MA, Davidson RR, Glover CJ, Bullin JA. Oxygen uptake as correlated to carbonyl growth in aged asphalt and corbett fractions. Industrial & Engineering Chemistry Research. 1998;**37**:4669-4694

[21] Ouyang C, Wang S, Zhang Y, Zhang Y. Improving the aging resistance of styrenebutadiene-styrene tri-block copolymer modified asphalt by addition of antioxidants. Polymer Degradation and Stability. 2006;**91**:795-804

[22] Lukkassen D, Meidell A. Advanced Materials and Structures and their Fabrication Processes. Book manuscript, Narvik University College, HiN; 2007

[23] Rus AZM. Polymers from renewable materials. Science Progress. 2010;**93**(3):285-300

[24] Hamed GR. Materials and Compounds. Engineering with Rubber: How to Design Rubber Components from Alan N. Gent. Germany: Hanser Publishers; 1992

[25] Rahman MM. Characterisation of dry process crumb rubber modified asphalt mixtures [Dissertation]. University of Nottingham; 2004

[26] Wan Azahar WNA, Bujang M, Jaya RP, Hainin MR, Mohamed A, Ngadi N, Sri Jayanti D. The potential of waste cooking oil as bio-asphalt for alternative binder—An overview. Jurnal Teknologi (Sciences & Engineering). 2016;**78**(4):111-116

[27] U.S Environmental Protection Agency. 2011. [cited 10.7.2011]

[28] Wen H, Bhusal S, Wen B. Laboratory evaluation of waste cooking oil-based bioasphalt as an alternative binder for hot mix asphalt. Journal of Materials in Civil Engineering. 2012;**25**(10):1432-1437

[29] Asli H, Ahmadinia E, Zargar M, Karim MR. Investigation on physical properties of waste cooking oil—Rejuvenated bitumen binder. Construction and Building Materials. 2012;**37**:398-405

[30] El-Fadel M, Khoury R. Strategies for vehicle waste-oil management: A case Study. Resources, Conservation and Recycling. 2001;**33**:75-91

[31] Hamad BS, Rteil AA, El-fadel M. Effect of used engine oil on properties of fresh and hardened concrete. Construction and Building Materials. 2003;**17**:311-318

[32] Singhabhandhu A, Tezuka T. The waste-to-energy framework for integrated multi-waste utilization: Waste cooking oil, waste lubricating oil, and waste plastics'. Energy. 2003;**35**(6):2544-2551

[33] EPA. 2011. Available from: http://www.epa.gov/region9/waste/biodiesel/questions.html [Accessed: August 2011]

[34] Gui MM, Lee KT, Bhatia S. Feasibility of edible oil vs. non-edible oil vs. waste edible oil as biodiesel feedstock. Energy. 2008;**33**(11):1646-1653

[35] Peiro LT, Lombardi L, Méndez GV, Durany XG. Life cycle assessment (LCA) and exergetic life cycle assessment (ELCA) of the production of biodiesel from used cooking oil (UCO). Energy. 2010;**35**:2:889-893

[36] Castellanelli CA. Analyzes of the used oil under environmental perspective and its possibilities for production of biodiesel. Courtesy of UFSM—Federal University of Santa Maria; 2007

[37] Math MC, Kumar SP, Chetty SV. Technologies for biodiesel production from used cooking oil—A review. Energy for Sustainable Development. 2010;**14**:4:339-345

[38] Kulkarni MG, Dalai AK. Waste cooking oil—An economical source for biodiesel: A review. Industrial & Engineering Chemistry Research. 2006;**45** 9:2901-2913

[39] Moghaddam TB, Karim MR, Abdelaziz M. A review on fatigue and rutting performance of asphalt mixes. Scientific Research and Essays. 2011;**6** 4:670-682

[40] Agriculture and Food Development Authority, Waste Oils and Fats as Biodiesel Feedstocks. 2000. An assessment of their potential in the EU, ALTENER program NTB-NETT phase IV, Task 4, Final Report. March 2000

[41] Sanli H, Canakci M, Alptekin E. Characterization of waste frying oil obtained from different facilities. Linkoping, Sweden: World Renewable Energy Congress 2011-Sweden; 8-13 May 2011

[42] Khalisanni K, Khalizani K, Rohani MS, Khalid PO. Analysis of waste cooking oil as raw material for biofuel production. Global Journal of Environmental Research. 2008;**2**(2):81-83

[43] Zahoor U, Mohamad AB, Zakaria M. Characterization of waste palm cooking oil for biodiesel production. International Journal of Chemical Engineering and Application. 2014;**5**(2):134-137

[44] Md Maniruzzaman AA, Md Tareq R, Mohd. Rosli H, WAWA Bakar. An overview on alternative binders for flexible pavement Construction and Building Materials. 2015;**84**:315-319

[45] Raouf MA, Williams RC. Temperature susceptibility of non-petroleum binders derived from bio-oils. In: The 7th Asia Pacific Conference on Transportation and the Environment Semarang, Indonesia. 2010

[46] Demirbas M, Balat M. Recent advances on the production and utilization trends of bio-fuels: A global perspective. Energy Conversion and Management. 2006;**47**(15):2371-2381

[47] Rahman MT, Aziz MMA, Hainin MR, Bakar WAWA. Impact of bitumen binder: Scope of bio-based binder for construction of flexible pavement. Jurnal Teknologi. 2014;**70**(7): 105-109

[48] Kluttz R. Considerations for use of alternative binders in asphalt pavements: Material characteristics transportation research circular E-C165: Alternative Binders; 2012

Section 2

Evaluation of Asphalt Performance

Chapter 2

Aging Effects on Mechanical Characteristics of Multi-Layer Asphalt Structure

Ahmet Sertac Karakas

Additional information is available at the end of the chapter

http://dx.doi.org/10.5772/intechopen.75698

Abstract

This chapter focuses on Asphalt ages during construction, transportation, application phases and service life, as well. Exposure of environmental conditions such as traffic and climate is one of the prominent reasons aging in asphalt. The most common mechanism of aging is the degradation in the chemical structure of the binder by oxidation. Asphalt aging could cause several serious issues on the pavement such as stiffening, stripping that accelerates fatigue cracking and different moisture-induced problems such as raveling and potholes. Therefore, various additives are used as modifiers to improve the mechanical properties of asphalt. The most commonly used modifiers are polymers. Styrene butadiene styrene (SBS) polymers are utilized to prevent from deteriorating against external factors during its service life and to delay its aging in asphalt pavement. In the scope of this study, it was aimed to provide the general perspectives on mechanical characteristics of multi-layer asphalt structure under the aging effects besides traffic conditions.

Keywords: asphalt, SBS, aging, polymer additive, numerical approach

1. Introduction

Asphalt ages during construction, transportation, application phases and during service life. One of the biggest causes of aging in asphalt is caused by exposure to environmental conditions such as traffic and climate. The most common type of degradation is the degradation of the chemical structure of the binder by oxidation. Some serious problems can be seen in the asphalt coating as a result of the aging of the asphalt. Oxygen, moisture, ultraviolet irradiation, heat radiation and traffic action ultimately lead to the changes in the molecular structures and chemical functional groups of asphalt. The consequence of asphalt aging can be several serious issues in the pavement, such as stiffening, stripping; that accelerates fatigue cracking, and

different moisture induced distresses such as raveling, potholes, respectively. Therefore, various additives are used as modifiers to improve the engineering properties of the bitumen material. The most commonly used modifiers are polymers.

The investigations in asphalt pavement technology and its application fields have enabled the development and practical use of polymer modifiers. A number of researches have been carried out to investigate in asphalt pavement [1–15].

Various additives which are called modifiers have been contributed binder to increase the performance of asphalt. Modifiers are provided long term service life of asphalt and prevented them long term aging [17–20].

Polymer has been used commonly with asphalt for nearly 50 years as of additives. Many tests are being applied for increasing the properties of asphalt combination. [3].

The traffic load and temperature cause the asphalt coating to lose strength over time. SBS Block Copolymer is used commonly with binders in order to ensure the high quality of materials, increase the endurance of binder and hot mix asphalt pavement. Many studies have been found that Modified asphalt with SBS provided to endurance rutting in high temperature, fatigue behavior and low temperature cracking [17–20].

Hamid et al. determined different types of HMAs which are prepared with grinded and non-grinded SBS polymers. It was seen better result with grinded SBS polymer modifier. According to the test result, it was determined that there was slight increase in the air gap and aggregate volume, and endurance to stresses increased and the density decreased.

Qadi et al. probed the effect of multiple additives and modifiers on asphalt pavement. Polyphosphoric acid (PPA), liquid anti strip (LAS), and hydrated lime were selected for using of laboratory study. It was seen that the moisture sensitivity in asphalt mixtures decreased when used of Liquid Anti Stripe and hydrated lime [21].

Styrene butadiene styrene copolymers (SBSC) are classified as thermoplastic elastomers because of their elastic and thermoplastic characteristics, and are used as modifiers for the bitumen because of their important features contributing to the mechanical properties of the asphalt [22–24].

In numerical studies, it is performed Abaqus and Ansys program are widely used with non-linear viscoplastic finite element model (FEM) analysis. Furthermore; Due to the longitudinal dimension, 2- and 3-dimensional models are generally approved for the design of modeling [25, 26].

2. Aging behavior of asphalt

Most of the coating systems are located at moderate temperatures. The asphalt cement has both a fluid and an elastic solid character. Since the asphalt is an organic material, it reacts with the surrounding oxygen. Oxidation changes the structure and complexity of asphalt

molecules. Oxidation causes to oxidation on the asphalt, aging or hardening, leading to further fractures.

Oxidation occurs more rapidly at higher temperatures. When the asphalt cement is heated, mixed more easily and compressed, the amount of breakage is considerable. The characteristics of asphalt cement under temperature changes and loading rates and aging stages are determined by their ability to perform as a binder in coating systems.

Asphalt cement within the coating; it is hardened under the influence of air, environmental condition and heat during the service life. It is occurred aging hardening and viscosity increase in the bitumen over the time. In the bitumen subjected to aging hardening, lower penetration and higher viscosity are seen, and it is stated that aging hardening results in lower adhesion and brittle fracture.

The aging index of asphalt is shown the following **Figure 1** in term of years.

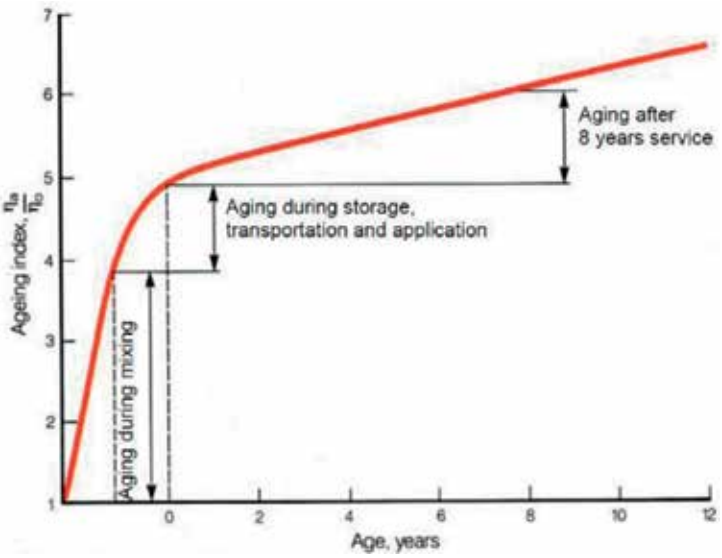

Figure 1. Asphalt aging index by years [27].

3. Factors effect on asphalt aging

As indicated before, asphalt in service condition interacts with many environmental and mechanical factors such as, atmospheric oxygen, dissolved oxygen, moisture, ambient and pavement layer temperatures, UV irradiation, traffic. Therefore, all these factors have minor to very severe effects in physical & chemical characteristics of asphalt, and subsequently these effects are reflected in either increase in viscosity, loosening adhesibility, or changes in moduli.

Stimulate asphalt aging has been shown in **Table 1** and the Petersen's findings have been presented in **Figure 2** respectively.

Factors	Influenced by					Occurring	
	Time	Heat	Oxygen	Sun-light	Beta & gamma rays	At the surface	In mass
Oxidation (in dark)	√	√	√			√	
Photo-oxidation (direct light)	√	√	√	√		√	
Volatilisation	√	√				√	
Photo-oxidation (reflect light)	√	√	√	√		√	
Photo-chemical (direct light)	√	√		√		√	
Photo-chemical (reflected light)	√	√		√		√	√
Polymerization	√	√				√	√
Steric or physical	√					√	√
Exudation of oils	√	√				√	
Changes by nuclear energy	√	√			√	√	√
Action by water	√	√	√	√		√	
Absorption by solid	√	√				√	√
Absorption of components at a solid surface	√	√				√	
Chemical reactions	√	√				√	√
Microbiological deterioration	√	√	√			√	√

Table 1. List of individual factors and conjoint factors that affect asphalt aging [28].

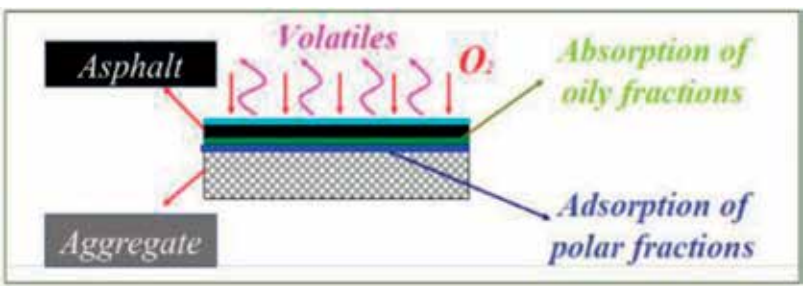

Figure 2. Illustration of asphalt aging process due to volatilization, oxidation, absorption and adsorption [28].

4. Bitumen modification

Bitumen exhibits viscoelastic properties as rheological structure. Bitumen, which plays a major role in many parameters of road performance, mainly cracking and permanent deformation resistance, also causes viscoelastic properties of asphalt mixtures. Generally, the amount of deformation in asphalt coating varies depending on the loading time and the temperature value.

The behavior of bitumen affected by static and dynamic loads is shown in **Figure 3**.

Permanent deformation (creeping), cracking (thermal or fatigue), moisture damage are the most common types of degradation in flexible coatings. Shortening the service life of road coverings under increasing traffic load has necessitated modification of bitumen. In recent years, based on polymers, the use of highly modified bituminous blends and mixtures has been increasing. As polymer additives and non-polymer additives as shown in **Table 2**.

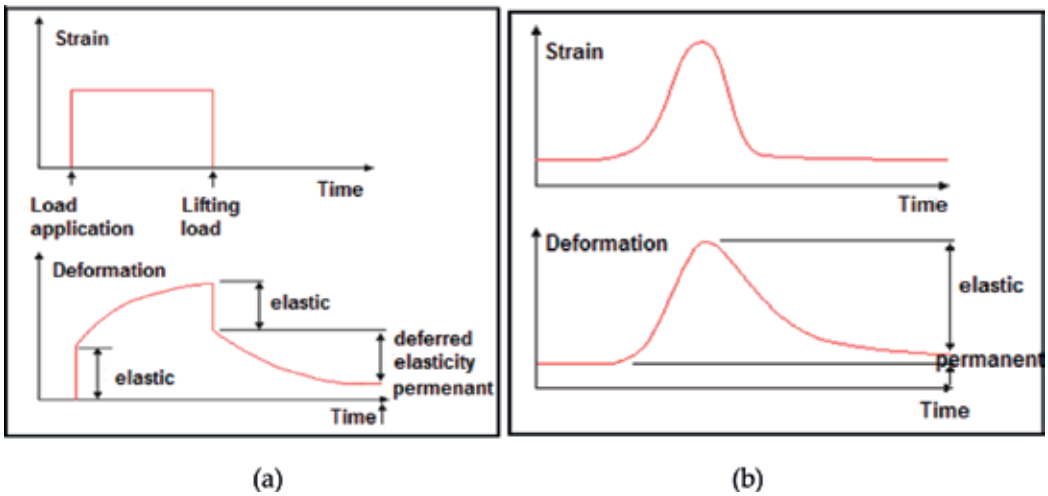

Figure 3. The behavior of bitumen affected by static load (a) and dynamic load (b) [27].

Modification types	Specimens
I. Modification with non-polymer additive	
a. Filler	Clay, black carbon, fly ash
b. Anti-peel additives	Organic Amines and Amids
c. Expander (Extendents)	Lignin and sulfur
d. Antioxidants	Zinc and lead antioxidants, phenolics
e. Organo-metal compounds	Amines
f. Others	Organo manganese compositions
	Organo carbon compositions
II. Modification with polymer additives	
a. Plastics	Polyethylene (PE), polypropylene (PP), polyvinyl chloride (PVC),
1. Thermoplastics	Polystyrene (PS), ethylene vinyl acetate (EVA)
2. Thermosets	Epoxy resins
b. Elastomers	Synthetic butadiene copolymer (SBR), Styrene-butadiene styrene copolymer
1. Natural Rubbers	(SBS),
2. Artificial Elastomers	Ethylene prokplendien harmoliper (EPDM), Isobutene isoprene copolymer
3. Processed Rubbers	(IIR)
4. Fibers	Polyester, fibers, polypropylene fibers
III. Chemical reaction modification	Additive reaction (bitumen + monomer)
	Vulcanization (bitumen + sulfur)
	Nitrogen reaction (bitumen + nitric acid)

Table 2. Bitumen modification types [29].

Usage purposes of modified bitumen applications:

- Control of fatigue cracks,
- Water impermeability,

- Increase of adhesion,
- Reduction of noise,
- Reduction of groove marks on wheel load can be summarized [37, 38].

Additives used in the modification of bituminous and bituminous mixtures and the benefits provided according to their shape of deterioration are shown in **Table 3**.

Modifier	Permanent deformation	Thermal cracking	Fatigue crack	Moisture damage	Aging
Elastomers	+	+	+		+
Plastomers	+				
Processed rubber		+	+		
Black carbon	+				+
Lime					+
Sulfur	+				
Chemical modifier	+				
Antioxidants					+
Hydrated lime				+	+

Table 3. Benefits of different types of modifications [27].

5. SBS polymer modified bitumen and properties

Styrene-butadiene styrene (SBS) polymer additives used as additives in bitumen are one of the most preferred additive materials since they give positive results in physical and mechanical properties of HMA blends.

SBS additive and its three-dimensional structure is indicated in **Figure 4**.

SBS polymers are randomly formed as bond shapes in different forms such as block, styrene, butadiene, and linear.

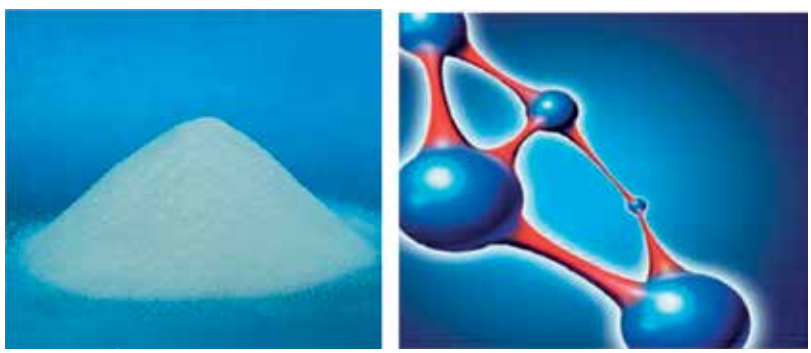

Figure 4. General view of SBS-additive and three-dimensional SBS structure [30].

Molecular structure of SBS additives is illustrated in **Figure 5**.

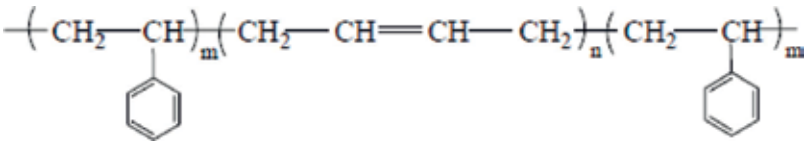

Figure 5. SBS molecular structure [31].

Figure 6 is indicated a three-dimensional view of asphalt-coated SBS molecules and the SBS modified bitumen structure consisting of asphaltic cell form and styrene butadiene bonds.

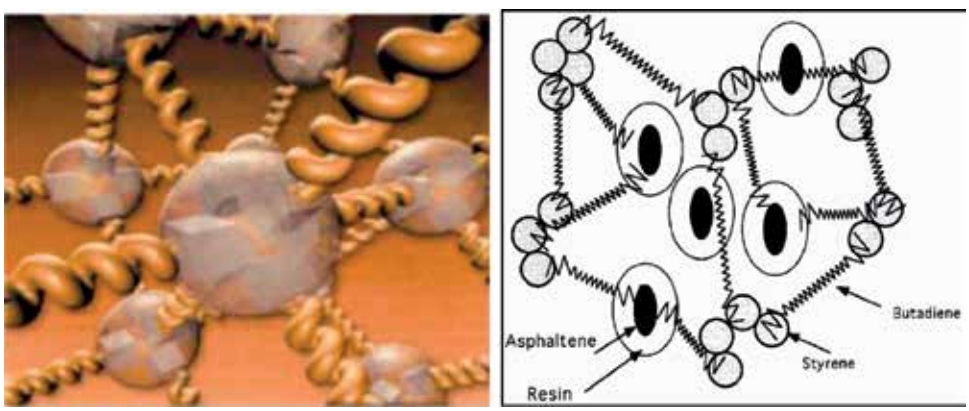

Figure 6. Three-dimensional appearance of asphalt-coated SBS molecules bond structure of SBS coated asphalt film [30, 32].

When the structure of SBS is examined, the following conclusions can be drawn:

- The polystyrene crowlings gives strength by forming physical cross-links.
- The polybutadiene bridges provide elasticity and flexibility.
- At 100°C, the polymer becomes fluid and the three-dimensional network structure recurs. Since the material is a thermoplastic elastomer, it does not lose anything in its heating and cooling properties.
- It maintains its characteristic between −40°C and + 80°C.

6. Materials and methodology

In this study, initially, some conventional tests were applied. The properties of bitumen and aggregates to be used in bituminous hot blends have been examined. In the performance tests; core samples were taken different time in 1 year period (1st, 4th, 8th and 12th months) and tested in **Figure 7**. Core samples achieved from the implementation of asphalt pavement which are prepared with SBS modified and neat bitumen of the asphalt pavement. When taking the

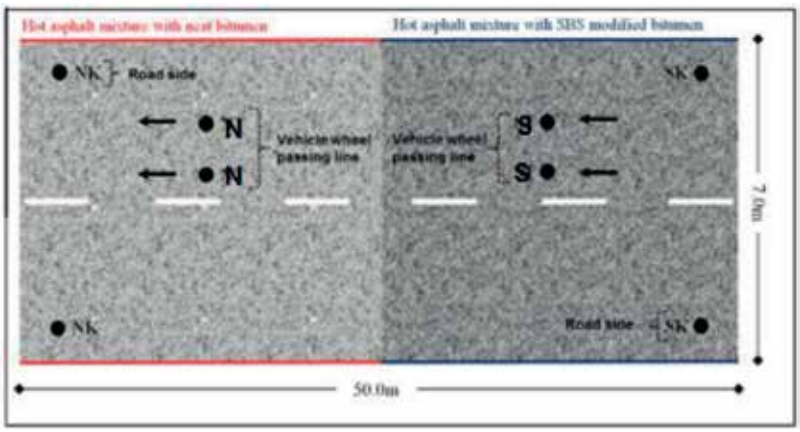

Figure 7. Core samples of hot mix asphalt (HMA) [33].

core samples, the edge of the road and the wheel passage areas are taken into consideration in **Figure 8**. In a one-year time period, 7432 equivalent axle loads were evaluated on trial path. Small axle tracks are not considered and are not taken into consideration because of using a secondary road. The effects of temperature on stability, stiffness, indirect tensile strength and fatigue resistance were investigated. Furthermore, it was examined Von Mises stress and vertical deformation of asphalt pavement on different time period with numerical analysis.

The location of the samples in asphalt and identification of the sample types are given in **Table 4**.

As a neat binder, asphalt binder of B 50/70 type taken from TUPRAS refinery was used. In modification, KRATON D 1101 contains styrene-butadiene styrene (SBS) block copolymer produced by Shell Bitumen was used.

The materials used in the layers that constituted the super structure of the road are; crushed aggregate chosen in the lower base layer, granular crushed aggregate chosen in the base layer, and crushed limestone aggregate chosen in road coating layer.

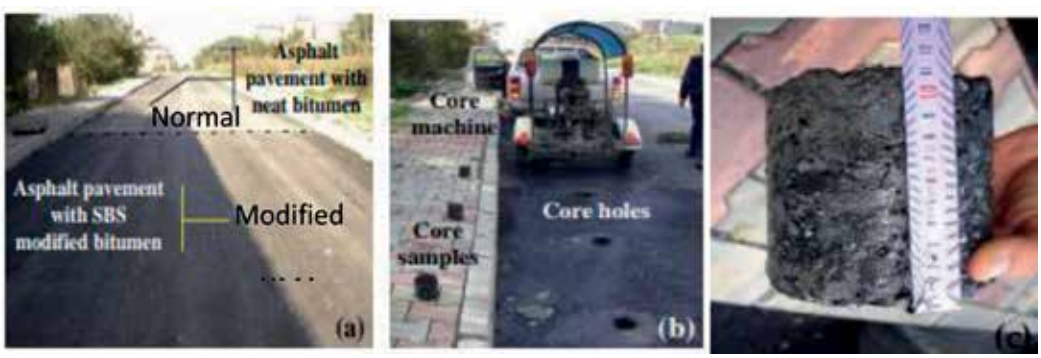

Figure 8. Asphalt pavement type (a), the core holes (b) and core sample (c) [33, 34].

Identification of the samples	State and location of samples
SK	SBS modified samples on road side
S	SBS modified samples on vehicle wheel passing line
NK	Neat samples on road side
N	Neat samples on vehicle wheel passing line

Table 4. Classification of drilling core samples of the HMA mixtures [33–35].

A solid model consisting of superstructure layers was created with namely Ansys using the finite element program. The solid model is designed by using the field parameters obtained by considering the environmental conditions such as traffic and climate. HMA design has been applied in the solid model, and only by doing so could real conditions were simulated with the analyses.

6.1. Numeric analyses

Numerical analyses assure significant advantages in using parameters derived from empirical studies to determine the stress and deformation characteristics of the superstructure of roads, corrosion, binder, base and sublayers, and to make future estimates. The Finite Element Method is often favored among other numerical approaches since it allows to make various changes and provides precise measurements in creating numerical models of physical problems. The Finite Elements Program used in numerical analysis is a numerical solution method developed for the analysis of problems expressed by differential equations. In the program, a continuous medium is branched by finite elements, and the equations are enrolled for one element, and integrated to derived system equations. As a result, complex differential equations considered for continuous media transformed into matrix format and it is reduced to a set of linear equations [36].

6.2. The finite elements method

The Finite Elements Method is a numerical solution method used frequently in engineering practices for the purpose of examining the continuous medium problems by examining them after dividing into a certain number of elements. In the scope of this method, the solution is obtained by dividing a medium or an object by finite elements and writing the rigidity matrix for each element, and then integrating the solutions for all elements. The numerical solutions of the differential equations that express the mechanical behavior of the system in question are written in matrix format. Generally, bigger matrices appear for the geometrical applications that require multiple elements. In solving such problems, the necessary linear algebraic operations are performed via computers.

6.2.1. The advantages of the finite elements programs

- The Finite Elements Formulation may be applied to many problems.

- It ensures the opportunity of speed and optimization that can be analyzed via computer.
- Any types of complex geometrical, material status and loading limit conditions may be defined.
- It facilitates the solution of integrated problems in ways such as tension, shape-shifting (statics) and consolidation (dynamics).
- The primary independent variables like place-shift, flow potential, which are selected, and the secondary unknown factors depending on these such as tension, shape-shifting, speed, and the amount of flow, etc., which are depending on these, are assessed together.
- Results that are close to reality are obtained with adequate element definitions [36].

In this chapter, a finite elements model was developed by using the ANSYS Finite Elements Program for the super-structure of the road. The models, which consist of asphalt coating, the base and sub-base include 79,045 elements and 558,224 nodal point in average.

Different models were prepared for various time periods, which were 1st, 4th, 8th and 12th Months, by considering the multi-layer structure of asphalt, the traffic and the environmental conditions [35].

The Finite element model (FEM) of road is given in **Figure 9**.

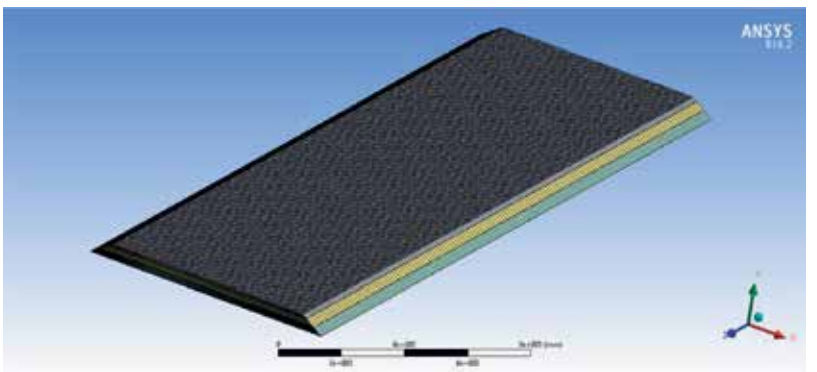

Figure 9. Finite element model (FEM) of road [34].

7. Results and discussion

7.1. Experimental results

Field and laboratory test works were conducted on the super-structure of the road for a time period of 1 year under traffic and environmental conditions. Drilling core samples were taken from the super-structure of the road in certain periods. The experimental part of the study was carried out in two stages. In the first stage, the physical properties of the aggregates and the neat and SBS modified bitumen which are using the asphalt mixture were determined. In the

second stage, various tests performed HMA samples. The mechanical properties of the samples collected from the different asphalt pavement were examined in the 1st, 4th, 8th and 12th months for a one-year period.

7.1.1. Properties of bituminous binders and aggregates

The binder was used in B50/70 class and constituted the building block of the HMA, which was used in the road platform. The characteristics of the pure (neat) and HMA-modified bitumen are given in **Table 5** that the neat and SBS modified bitumen are a little susceptible to temperature in relation to the penetration index and they have a value above the limits of the specification as softening.

The gradation characteristics of the mixture are given in **Table 6**. The physical properties of the aggregate are shown in **Table 7**. It is understood that the aggregates used in the coating layer of HMA are within the limits of the related specifications in terms of their physical properties.

Property	Test method	Neat bitumen	SBS modified bitumen
Specific gravity (gr/cm^3)	EN 15326	1.022	1.017
Penetration (25°C, 0.1 mm)	EN 1426	B-61	B-68
Softening point (°C)	EN 1427	51.7	54.0
Ductility (25°C, cm)	EN 13589	>100	>100
Fraas breaking point (°C)	EN 12593	−17	−17.5

Table 5. The properties of the neat bitumen [34].

Sieve Size (mm)	12.5	9.5	4.75	2.00	0.425	0.18	0.075
Passed (%)	100	90.4	56.6	36.6	18.2	13.0	10.3

Table 6. Aggregate gradation.

Tested property	Standard	Coarse	Fine	Filler	Specification limit
Abrasion Loss % (Los Angeles)	ASTM C 131	20.5	—	—	Max 35
Frost action % (with Na_2So_4)	ASTM C 88	1.20	—	—	Max 10
Peel strength (%)	ASTM D903	60–70			Min 50
Flatness index (%)	BS 812	16.1			Max 30
Water absorption (%)	ASTM C127	0.38	0.88	—	
Specific bulk density (gr/cm^3)	ASTM C127	2.733	—	—	
Specific bulk density (gr/cm^3)	ASTM C128	—	2.678	—	
Specific bulk density (gr/cm^3)	ASTM D854	—	—	2.764	

Table 7. Aggregate characteristics [35].

7.1.2. HMA design properties

In order to determine the HMA design properties, the pure and SBS-modified asphalt concrete coating sample road platform was prepared by taking the aggregate gradation as the basis. The pure HMA optimum bitumen rate was determined as 4.95%, and the SBS-added HMA optimum bitumen rate was determined as 5.24%. The properties of the design criteria are given in **Table 8**, and it is observed that they meet the Conditions List criteria.

From the pavement spread and compacted according to the predetermined design the core samples were taken at three different time periods on the vehicle wheel passing line and banquette of the road. The core samples were sized to those of Marshall samples and they were tested by Stiffness Modulus, Indirect Tensile, Fatigue and Marshall tests.

The average volumetric characteristics of the core samples are given in **Table 9**.

In **Figure 10**, It is indicated that the alteration in the stability of the samples over time. According to the result of the experiment, there have been remarkable increases in the stability with the hardening in the asphalt coating over time. SBS modified specimens were found to have 24% greater stability at 1st month and 72% greater at 12th months, respectively, when compared to neat specimens. The Stability increased 34% in neat mixtures and 76% more in SBS modified mixtures, respectively for 12th month compared to 1st month.

Property	Pure HMA value	SBS modified HMA value
Optimum bitumen rate (%)	4.95	5.24
Practical specific gravity (Gmb, gr/cm^3)	2.415	2.411
Marshall stability (kgf)	1222	1170
Flow (mm)	3.03	3.58
Aggregate void ratio (Vma, %)	15.10	13.9
Asphalt void ratio (Vf, %)	73.93	75.4
Air void ratio (Vh, %)	3.94	3.10

Gmb, bulk specific gravity; Vh, air voids; Vf, voids filled with asphalt; Vma, the void volume between the aggregates.

Table 8. Design properties of pure and SBS-modified HMA [34, 35].

Specimen	Gmb	Vh (%)	Vma (%)	Vf (%)
N	2.267	8.929	19.362	53.899
NK	2.280	8.43	18.92	55.480
S	2.271	8.369	19.457	57.032
SK	2.280	8.004	19.136	58.188

Gmb, bulk specific gravity; Vh, air voids; Vf, voids filled with asphalt; Vma, the void volume between the aggregates.

Table 9. The volumetric characteristics of the core samples in the 1st month [35].

http://dx.doi.org/10.5772/intechopen.75698

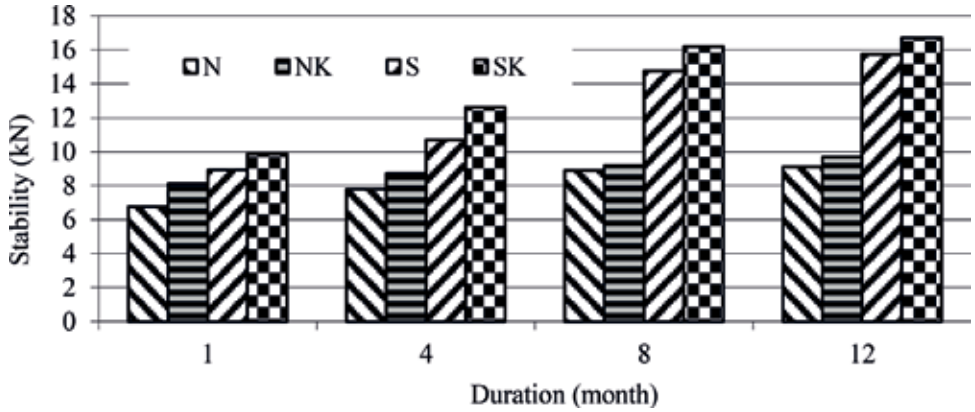

Figure 10. The change of stability in different period [35].

The change of the stiffness modules is illustrated in **Figure 11**.

In **Figure 11**, the stiffness modulus values show significant increase over time. In addition, the stiffness module of the samples taken from the edges and the vehicle wheel pass line of neat and SBS modified asphalt pavement were similarly affected by the time factor. SBS modified sample values increased by 8–27% more than neat sample values. The edge asphalt samples which are taken from banquette value were higher than the vehicle wheel passing. This difference is seen 2.3% to 11.8% in neat specimens and 1.8–10% in modified specimens. The reason for this increase is due to the fact that the samples from the edge are exposed to more water due to the transverse slope of the road [35].

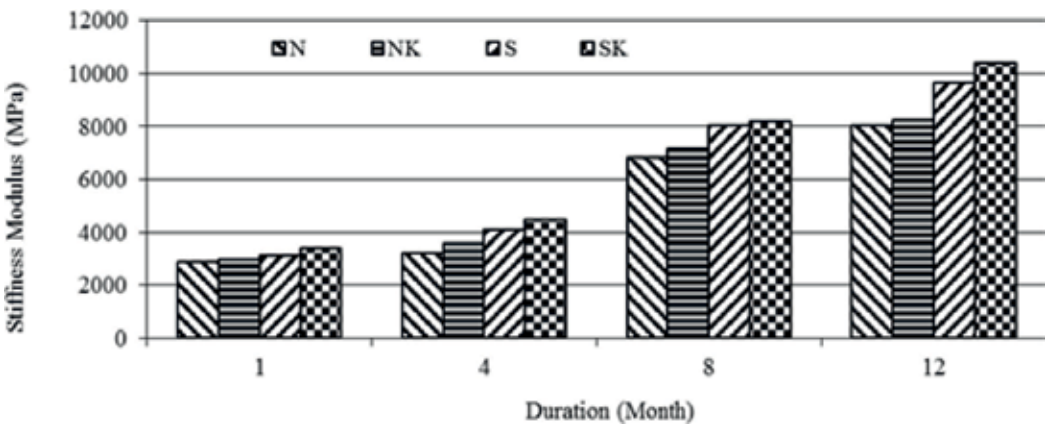

Figure 11. The change of the stiffness modules in different period [35].

The graph in **Figure 12** shows the average test results of the Indirect Tensile Strength Test.

In **Figure 12**, ITS values were found to be lowest at 1st month and highest at 12st months. In terms of monthly periods, ITS values of S and SK type core samples were more than N and NK

type of core samples. It was realized the lowest values in the N type and the highest values in the SK type. The increase of samples from 1st to the 12th month were seen 42.68% NK, 49.89% N, 20.4% SK and 26.93% S type of samples, respectively.

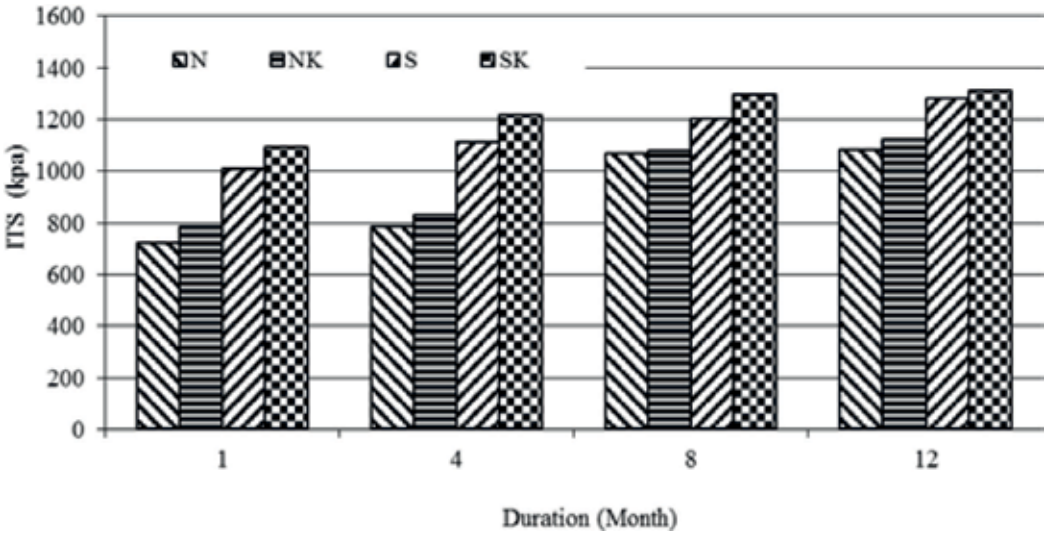

Figure 12. The change of the indirect tensile strengths in different period [35].

The change of fatigue strength in different period is given in **Figure 13**.

In **Figure 13**, it was observed that the loading repetition required for the samples to reach a level of deformation of about 2 mm was significantly increased using the SBS additive material. It was seen that the maximum loading repetition number (Nmax) values were increased after time period. The fatigue resistance of the samples with neat was lower than the SBS ones. The lowest deformation was gained from SK type samples. In the same manner, the highest Nmax values were achieved from SK type samples. It was clearly understood that

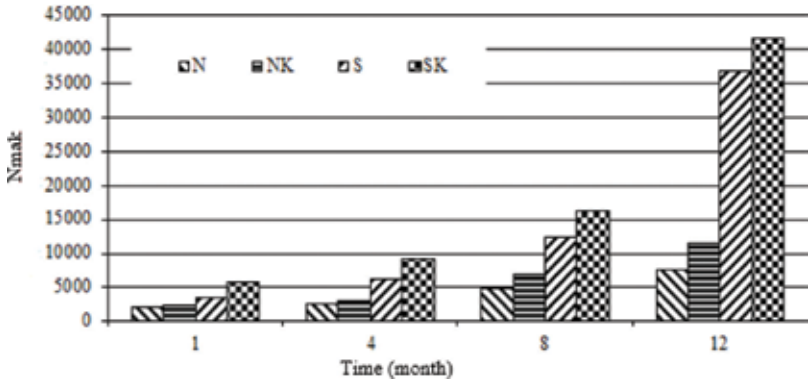

Figure 13. The change of fatigue strength in different period [35].

the flexibility of bituminous hot mixtures decreased after aging and for this reason a more brittle fracture may occupy [35].

7.2. Numeric analyses result

FEM models have been solved to determine the Von Mises stresses besides vertical deformations in super structures of the road, as well.

The FEM models of the Von Mises stresses for one of sample material is given in **Figure 14**.

Numerical analysis was done by applying the finite element method on the super-structure of the road. Von Mises Stress properties of the road super-structure are evaluated in **Figure 15**.

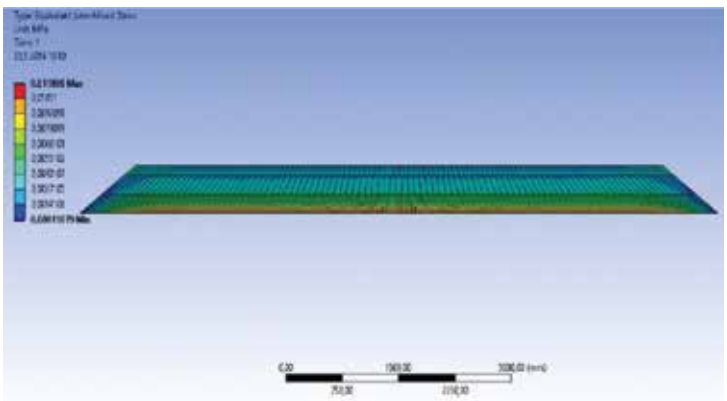

Figure 14. Von Mises FEM model [34].

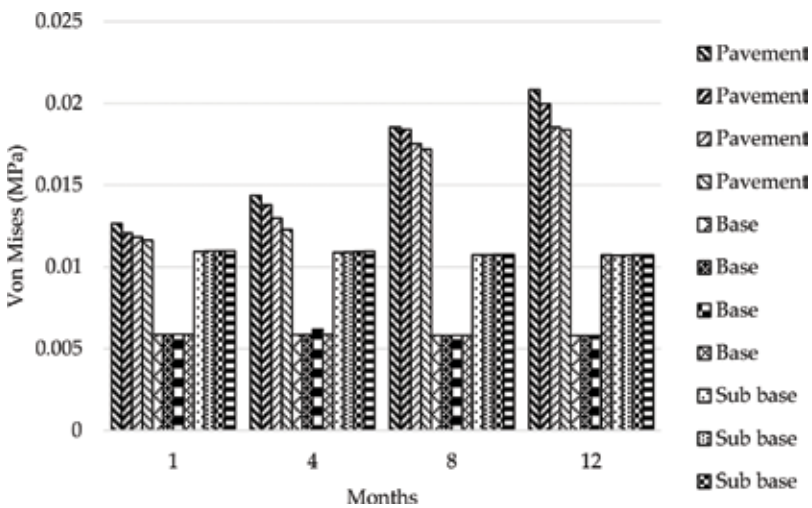

Figure 15. Von Mises tension-time changes of the super-structure of the road [34].

According to **Figure 15**; the highest Von Mises tensions were occurred the coating layer and the lowest values were observed in the base layer. It is fixed that The Von Mises tensions increased in the coating layer within 1 year period. It has been determined that the highest Von Mises tension were in SK type road coating whereas, the lowest Von Mises tensions were in N type coating. The Von Mises tensions of base layer indicated similarity properties and no significant changes were observed [34].

Vertical deformation (y)-time changes of the super-structure of the road is given in **Figure 16**.

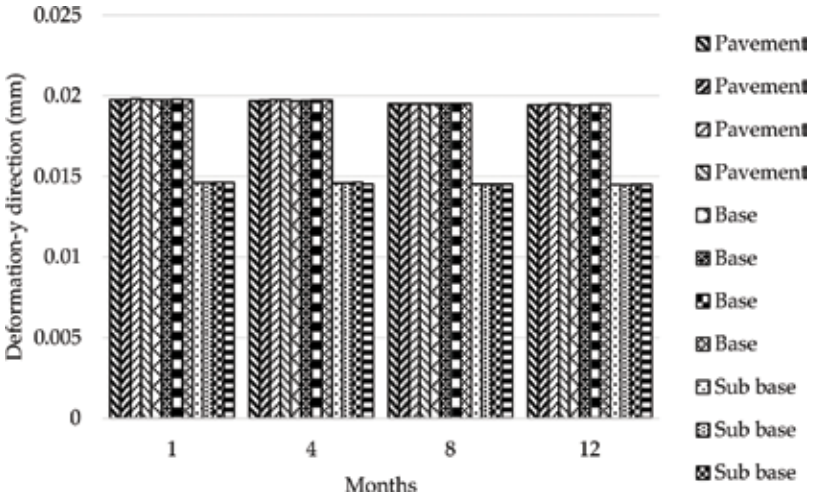

Figure 16. Vertical deformation (y)-time changes of the super-structure of the road [34].

When **Figure 16** is evaluated, it is seen that the highest vertical deformations are found at the base and lower base layers and the lowest deformations are found at the coating layer. Within a year, there have been small deviations in the amount of deformation. The amounts of deformation were confirmed as 0.014492 mm in SK-type, and 0.0145 mm in NK-type in the 12th month [34].

Von Misses stress and vertical deformation function and R^2 values are submitted in **Table 10**.

Layer types	Regression models	Function type			
		Von Mises stress function	R2	Vertical deformation function	R2
Coating	SK	$y = 0{,}0001x^2 + 0{,}0021x + 0{,}0101$	0,977	$y = 1E\text{-}06x^2 – 0{,}0001x + 0{,}0199$	0,9678
	S	$y = -3E\text{-}05x^2 + 0{,}003x + 0{,}0088$	0,9583	$y = -0{,}0001x + 0{,}0199$	0,9329
	NK	$y = 0{,}0099e^{0{,}1654x}$	0,9291	$y = 8E\text{-}06x^2 – 0{,}0002x + 0{,}02$	0,8994
	N	$y = 0{,}0001x^2 + 0{,}0019x + 0{,}0092$	0,9095	$y = -0{,}0001x + 0{,}0199$	0,8744
Base	SK	$y = 6E\text{-}07x^2 – 3E\text{-}05x + 0{,}0059$	0,9683	$y = -0{,}0001x + 0{,}0199$	0,9686
	S	$y = -4E\text{-}07x^2 – 3E\text{-}05x + 0{,}0059$	0,929	$y = -3E\text{-}06x^2 – 1E\text{-}04x + 0{,}0199$	0,9301
	NK	$y = -7E\text{-}05x^2 + 0{,}0003x + 0{,}0057$	0,4428	$y = 6E\text{-}06x^2 – 0{,}0001x + 0{,}0199$	0,9059
	N	$y = 0{,}0012x^2 – 0{,}0047x + 0{,}0096$	0,9282	$y = -3E\text{-}06x^2 – 9E\text{-}05x + 0{,}0199$	0,8785

Layer types	Regression models	Function type			
		Von Mises stress function	R2	Vertical deformation function	R2
sub base	SK	$y = 5E\text{-}06x^2 – 0{,}0001x + 0{,}0111$	0,9683	$y = 2E\text{-}06x^2 – 5E\text{-}05x + 0{,}0147$	0,9645
	S	$y = 5E\text{-}06x^2 – 0{,}0001x + 0{,}0111$	0,946	$y = -1E\text{-}06x^2 – 4E\text{-}05x + 0{,}0147$	0,923
	NK	$y = 3E\text{-}06x^2 – 0{,}0001x + 0{,}0111$	0,8963	$y = 7E\text{-}07x^2 – 5E\text{-}05x + 0{,}0147$	0,8528
	N	$y = -2E\text{-}07x^2 – 9E\text{-}05x + 0{,}0111$	0,8926	$y = 2E\text{-}05x^2 – 0{,}0002x + 0{,}0147$	0,9271

Table 10. Function and regression analyses of the relation between the super-structures of the road vertical deformation time [34].

When **Table 10** is examined, It is understood that R^2 values are close to 1 for all road layers. It has been inferred that numerical analyzes have supported empirical studies because of the strong relationship [34].

8. Conclusion

It came out that the performance characteristics of the SBS-added the HMA are improved due to the use of the SBS polymer material as compared to the unmodified ones. This is because when the SBS polymer is used, the adhesion between the aggregates increases. It has been seen that the flexible structure of asphalt is stiffened due to environmental conditions due to oxidation, which is caused by temperature changes and precipitation during transportation, storage, mixing and production processes. In addition to, as the air void ratio increases, the hardening time decreases due to air contact. The hardening of the asphalt road coating was found to be higher in the coating without additive material and it was appeared that the polymer increased the deformation resistance at high temperatures and increased the tendency to fracture at low temperatures.

Analytical calculations from different material types and different strata in the flexible road coating are complex. The traffic loads and the distribution of pressure on the superstructures of the roads are varied, and different materials are used on each layer, and therefore the mechanical properties and the load distribution ability vary. Climate and various environmental conditions affect the road. Because of these reasons, empirical studies must be promoted with numerical analyzes to establish performance characteristics of the road.

Acknowledgements

The author would like to thank Transportation Laboratory, Department of Civil Engineering, Firat University; Geotechnical &Transportation Laboratory, Department of Civil Engineering, Dicle University, Istanbul University and Bimtas Research Laboratories, Istanbul.

Author details

Ahmet Sertac Karakas

Address all correspondence to: skarakas@istanbul.edu.tr

Istanbul University, Division of Construction and Technical Maintenance, Istanbul, Turkey

References

[1] Shingo K, Shigeru T, Zhang XM, Dong DW, Inagaki N. Compatibilizer role of styrene-butadiene-styrene tri-block copolymer in asphalt. Polymer Journal. 2001;**33**(3):209-213

[2] Airey GD. Styrene butadiene styrene polymer medication of road bitumens. Journal of Materials Science. 2004;**39**(3):951-999

[3] Becker Y, Mendez MP, Rodriguez Y. Polymer modified asphalt. Vision Technologica. 2001;**9**(1):39-50

[4] Behbahani H, Hassan Z, Shams N. The use of polymer modification of bitumen for Durant hot asphalt mixtures. Journal of Applied Sciences Research. 2008;**4**(1):96-102

[5] Awwad MT, Shbeeb L. The use of polyethylene in hot asphalt mixtures. American Journal of Applied Sciences. 2007;**4**(6):390-396

[6] Dong F, Zhao W, Zhang Y, Wei J, Fan W, Yu Y, Wang Z. Influence of SBS and asphalt on SBS dispersion and the performance of modified asphalt. Construction and Building Materials. 2014;**62**(15): 1-7

[7] Prowell BD, Zhang J, Brown ER. Aggregate Properties and the Performance of Superpave-Designed Hot Mix Asphalt. NCHRP Report 539, Transportation Research Board, 2005

[8] Cpatt OV. Investigation of polymer modified asphalt by shear and tensile compliances. Material Characterization for Inputs into AASHTO 2002 Guide Session of the 2004 Annual Conference, Transportation Association, Canada, Québec City; ; 2004. pp. 145–213

[9] Lucena MCC, Soares SA, Soares JB. Characterization and thermal behavior of polymer-modified asphalt. Materials Research. 2004;**7**(4):529-534

[10] Newman K. Polymer-modified asphalt mixtures for heavy-duty pavements: fatigue characteristics as measured by flexural beam testing. 2004 FAA Worldwide Airport Technology Transfer Conference, Atlantic City, New Jersey, USA, 2004

[11] Mohammad LN, Negulescu LL, Wu Z, Daranga C, Daly WH, Abadie C. Investigation of the use of recycled polymer modified asphalt binder in asphalt concrete pavements. Journal of the Association of Asphalt Paving Technologists. 2003;**72**:551-594

[12] Zubeck H, Raad L, Saboundjian S, Minassian G, Ryer J. Performance of polymer-modified-asphalt-aggregate mixtures in Alaska. Journal of Cold Regions Engineering. 2002;**16**:170-190

[13] Masson JF, Pelletier L, Collins P. Rapid FTIR method for quantification of styrene-butadiene type copolymers in bitumen. Journal of Applied Polymer Science. 2001;**79**: 1034-1041

[14] Lu X, Isacsson U. Influence of styrene-butadiene-styrene polymer modification on bitumen viscosity. Fuel. 1997;**76**(14–15):1353-1359

[15] Cavaliere MG, Diani E, Dia MD. Dynamic mechanical characterization of binder and asphalt concrete. In: Proceedings of the Euroasphalt and Eurobitumen Congress, No.5551; 1996

[16] Behbahani H, Ziari H, Noubakhat S. The use of polymer modification of bitumen for Durant hot asphalt mixtures. Journal of Applied Sciences Research. 2008;**4**(1):96-102

[17] Lu X, Isacsson U. Laboratory study on the low temperature physical hardening of conventional and polymer modified bitumens. Construction and Building Materials. 2000;**14**:79-88

[18] Navarro FJ, Partal P, Martinez-Boza F, Valencia C, Gallegos C. Rheological characteristics of ground tire rubber-modified bitumens. Chemical Engineering Journal. 2002;**89**:53-61

[19] Airey GD. Rheological properties of styrene butadienee styrene polymer modified road bitumens. Fuel. 2002;**82**(14):1709-1719

[20] Khattak MJ, Baladi GY. Engineering properties of polymer- modified asphalt mixtures. Transportation Research Record. 1998;**1638**:12-22

[21] Al-Qadi IL, Abuawad IM, Dhasmana H, Coenen AR. Effects of Various Asphalt Binder Additives/Modifiers on Moisture Susceptible Asphaltic Mixtures. Civil Engineering Studies. Illinois Center for Transportation Series No. 14–004. ISSN: 0197–9191. UILU-ENG-2014–2004

[22] Zhu J, Kringos N. Towards the development of a viscoelastic model for phase separation in polymer-modified bitumen, Road Mater. Pavement Design. 2015;**16**:39-49

[23] de Carcer ÍA, Masegosa RM, Viñas MT, Sanchez-Cabezudo M, Salom C, Prolongo MG, Contreras V, Barceló F, Páez A. Storage stability of SBS/sulfur modified bitumens at high temperature: Influence of bitumen composition and structure. Construction and Building Materials. 2014;**52**:245-252

[24] Larsen DO, Alessandrini JL, Bosch A, Cortizo MS. Micro-structural and rheological characteristics of SBS-asphalt blends during their manufacturing. Construction and Building Materials. 2009;**23**:2769-2774

[25] Fang H, Haddock JE, White TD, Hand AJ. On the characterization of flexible pavement rutting using creep model-based finite element analysis. Finite Elements in Analysis and Design. 2004;**41**(1):49-73

[26] Abed AH, Al-Azzawi AA. Evaluation of rutting depth in flexible pavements by using finite element analysis and local empirical model. American Journal of Engineering and Applied Sciences. 2012;**5**(2):163-169

[27] Whiteoak D, Read J. The Shell Bitumen Handbook. London: Thomas Telford Ltd; 2003

[28] Wu J. The Influence of Mineral Aggregates and Binder 1068 Volumetrics on Bitumen Ageing. England: The University of Nottingham; 2009

[29] Ilica M, Tayfur S, Ozen H. Asphalt and Application. Istanbul, Turkey: ISFALT; 2001

[30] Iskender E. Evaluation of permanent deformation problem in asphalt concrete [Master Science Thesis]. Trabzon, Turkey: Blacksea Technical University; 2004

[31] Dogan M. Effect of Polymer Additives on the Physical Properties of Bitumen Based Composites, a Thesis Submitted to the Graduated School of Natural and Applied Science. Ankara: Middle East Technical University; 2006

[32] Yildirim Z. Use of waste plastics in the production of polymer modified bitumen materials [Master Science Thesis]. Institute of Science and Technology, Aegean University; 2006

[33] Karakas AS, Sayin B, Kuloglu N. The changes in the mechanical properties of neat and SBS-modified HMA pavements due to traffic loads and environmental effects over a one-year period. Construction and Building Materials. 2014;**71**:406-415

[34] Karakas AS, Ortes F. Comparative assessment of the mechanical properties of asphalt layers under the traffic and environmental conditions. Construction and Building Materials. 2017;**131**:278-290

[35] Karakas AS, Kuloglu N, Kok BV, Yilmaz M. The evaluation of the field performance of the neat and SBS modified hot mixture asphalt. Construction and Building Materials. 2015; **98**:678-684

[36] Brinkgreve RBJ et al. Plaxis Finite Element Code for Soil and Rock Analyses. Netherlands: Delft University of Technologhy & Plaxis b.v; 2002

[37] Tunc A. Flexible Coating Materials Handbook. Ankara: Asil publication distribution; 2004

[38] Tunc A. Road Materials and Applications. Istanbul: Atlas publisher; 2001

Chapter 3

Novel Applications with Asphaltene Electronic Structure

Eva M. Deemer and Russell R. Chianelli

Additional information is available at the end of the chapter

http://dx.doi.org/10.5772/intechopen.78379

Abstract

Asphaltenes are the molecular components of Asphalts and have polyaromatic hydrocarbon (PAH) structures similar to nanographenes. Thus, organic-based dye sensitized solar cells can be produced from asphaltenes. In addition, graphene based structures doped with transition metals can be synthesized from asphaltenes. These materials are simple to synthesize and inexpensive relative to other methods for doping graphene. Thus, what is considered a "Waste Material - Tar" can now be utilized in several important applications. These novel materials from asphaltene are also termed Discotic Liquid Crystals (DLC) and now have great potential in many areas, because of novel and valuable properties, easy synthesis and low cost.

Keywords: synthetic asphaltene, organic photovoltaics (OPVs), polyaromatic hydrocarbons (PAHs), discotic liquid crystals (DLCs), dye sensitized solar cells (DSSC), light harvesting molecules, nanographene, doped graphene

1. Introduction

Carbon-based systems including polymers, nanotubes, graphene and quantum dots are active materials in electronic, photonic or magnetic devices. Their properties depend on chemical structure and size and thus they can be chemically or physically tuned. Extended π-conjugated scaffolds that can be decorated with functional groups are the main feature related in these structures. Their functionalization can be optimized in order to facilitate their self-assembly into highly ordered supramolecular architectures, that are driven by non-covalent $\pi - \pi$ stacking interaction, hydrogen bonding, etc. Small molecules which can be characterized by their π-conjugated networks (pyrenes, pentacenes, coronenes, polythiophenes, etc.) possess

Device	Area Cross sectional (nm^2)	Current density (electrons/nm^2-sec)
1 mm copper wire	3×10^{12}	2×10^{6}
Polyphenylene wire	0.05	4×10^{12}
Carbon nanotube	3	2×10^{11}

Table 1. Current density of molecular wires expressed in nanoscale units compared to current density of macroscopic copper [14].

electronic bandgaps that are well defined and shapes such as fibers, nanocrystals or uniform monolayers which enable molecular self-assembly into highly ordered low-dimensional architectures. Conjugated molecules have been explored for use in organic electronics and vary widely, however conjugated discotic materials and their self-assembly have been of interest to researchers due to their unique liquid crystalline properties [1, 2].

Experiments done in the mid and late 1990s demonstrated individual molecules can possess physical phenomena which previously thought to have been limited to semiconductors and revolutionized the material science. In 1996, it was still questionable whether or not individual molecules could actually conduct electricity but experiments performed from 1995 to 1997 [3–8] determined that individual molecules can conduct and also switch small electrical currents [9–13]. These revolutionary works demonstrated the use and assembly of molecular electronic devices using aromatic organic molecules, nanotubes, biomolecules or nanowires (**Table 1**) but more importantly, they gave the promise of low cost, carbon-based electronics at the smallest of scales which could be printed onto plastic.

2. Asphaltene and synthetic asphaltene: the theoretical platform

Asphaltenes are a relatively exotic class of hydrocarbon component in crude oils [15, 51]. Naturally occurring crude oil contains an enormous range of compounds that spans hydrocarbon compositions from dry natural gas to tar. The density and viscosity increases dramatically and color changes from clear to deep brown as asphaltene content increases from 0 to nearly 20% across that range. Researchers agree that the asphaltene structure is comprised of some carbon and hydrogen atoms which are bound in ring-like, aromatic groups, and also contains the heteroatoms. Alkane chains and cyclic alkanes include the rest of the carbon and hydrogen atoms, linked to ring groups. Within this arrangement, asphaltenes exhibit a range of molecular weight and composition. These characteristics of asphaltenes are acceptable to nearly all researchers and specialists, but leaves sufficient room for discussion regarding the structure or size of individual asphaltene molecules.

Extensively studied by Chianelli et al., asphaltene structure has been shown to have a structure similar to that of the synthetic compound tetraoctyl carboxylate perylene (TOPC) [16]. X-ray diffraction (XRD) studies performed on TOPC (shown in **Figure 1**) differentiate two peaks

http://dx.doi.org/10.5772/intechopen.78379

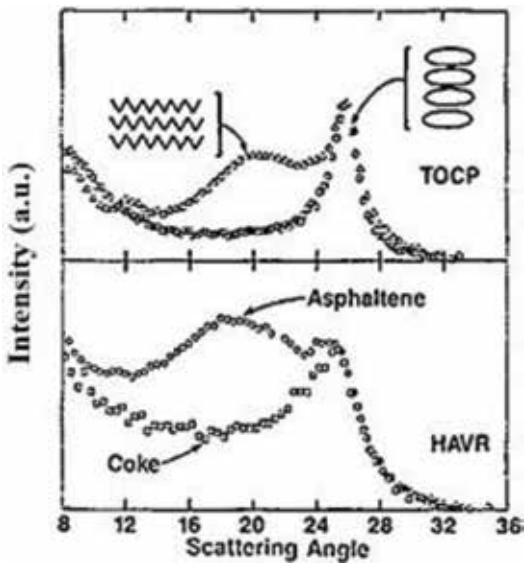

Figure 1. X-ray diffraction of asphaltene –high aromatic vacuum residue (HAVR) compared to synthetic molecule tetraoctyl carboxylate perylene (TOPC) [16].

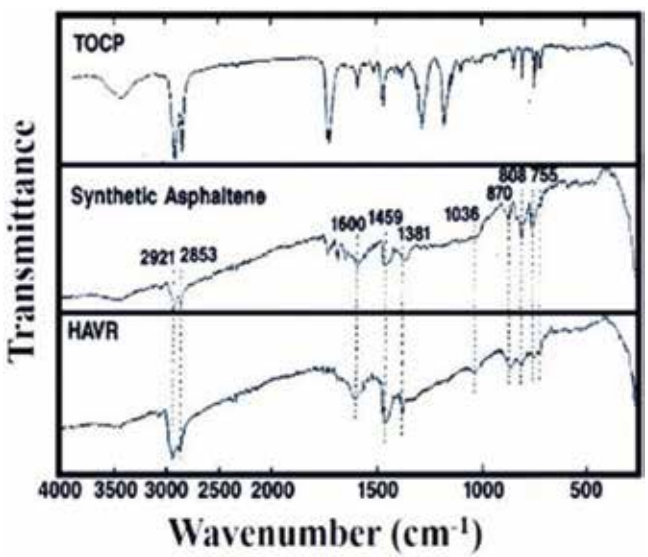

Figure 2. Infrared spectra of the TOCP precursor, synthetic asphaltene and HAVR (heavy Arab vacuum reside) asphaltene showing the significant similarity between the synthetic and the HAVR asphaltene [16].

that can determine distinction between alkane chains and stacked aromatic cores. Using these synthetic structures as a model, the structure of asphaltene before and after thermal processing was explored using XRD and the results show that the production of coke is actually

Chemical properties of synthetic asphaltene and HVAR				
	H/C	% C Aromatic	% C Aliphatic	MW
Synthetic asphaltene	1.06	58	42	2750
HVAR asphaltene	1.10	33–45	55–65	1.000–10.00

Table 2. Comparison of some chemical properties of synthetic asphaltene and HVAR [16].

the self-assembly of stacked aromatic cores. This work helped researchers understand the fundamental physical characteristics and the process of coke formation through self-assembly using of synthetic asphaltene.

When the temperatures increased above 350°C during thermal processing, the aliphatic ester of TOCP becomes the weakest region for thermal cleavage. When temperature reaches above 420°C in the absence of oxygen, TOCP completely thermally converts into a sea of free radicals containing aromatic cores and long-chain alkyl fragments. After Chianelli et al. successfully prepared synthetic asphaltene, the Infrared (IR) spectrum of TOCP, synthetic asphaltene, and HVAR (Heavy Arab Vacuum Residuum) were compared (**Figure 2**) and it is clear that absorption bands of synthetic asphaltene match well with band position and intensity of the IR spectrum of HVAR [17]. The comparison in chemical properties between synthetic asphaltene and HVAR illustrated in **Table 2**.

3. Organic photovoltaics using asphaltenes

3.1. Introduction to organic photovoltaics

The photovoltaic effect represents the generation of a potential difference at the junction of two different materials in response to various forms of radiation. The whole field of converting solar energy into electricity is the field of "photovoltaics" [18]. The photovoltaic process combines four stages which comprise the following: (1) light absorption, (2) charge generation, (3) charge transport, and (4) charge collection [19]. When the material has a semiconducting property that responds to incident waves, the first stage light absorption occurs. The absorption characteristic of the material is based on the intrinsic extinction coefficient and the band gap of the semiconducting material. Once light has absorbed by a material, the second stage occurs. As the incident photon hits electrons at the ground state, inorganic semiconductors generate free carriers (i.e. holes and electrons) and charge generation ensues. However, in organic semiconductors, excited electrons form an exciton, which is a bounded electron and hole pair. To make an efficient organic photovoltaic cell, the dissociation of excitons is an important matter as the binding energy of the exciton is relatively large (0.3 eV) [20].

Dye sensitized solar cells (DSSC) are low cost alternatives for the conventional solar cells, and commercially promising because of the promise of low-cost materials and roll-to-roll manufacturing. The DSSC can be classified as a photo electrochemical (PEC) solar cell because of its utilization of photons, charges, and electrolyte for its basic operation [21]. O'Regan and Grätzel built and demonstrated the first DSSC by 1991, [22] and attracted widespread academic and

industrial interest. Compared to conventional solar cells, DSSCs had the promise of easy fabrication at a low-cost in environment friendly and have high-energy conversion efficiency [23]. One more advantage of DSSCs is that changes in temperature do not affect the performance, while temperature changes can affect the performance of conventional silicon solar cells [24].

Ooyama and Harima [30] have done an extensive literature review on the main requirements for efficient organic molecule (dye) used so far for DSSCs. Their conclusions are summarized in the following four statements:

1. The organic molecule (dye) should have a minimum of one anchoring group like COOH, $–SO_3H$, $–PO_3H_2$, –OH for adsorption onto the TiO_2 surface to provide a tightly held dye and suitable electron interaction between them.
2. To achieve efficient electron injection from the excited dye to the conduction band of the TiO_2, the dye has to have an energy level of the lowest unoccupied molecular orbital (LUMO) which is higher (more negative) than that of the conduction band of the TiO_2 electrode. However, the energy level of the highest occupied molecular orbital (HOMO) of the dye must be lower (more positive) than the I_3^-/I^- redox potential in the electrolyte to achieve efficient regeneration of the oxidized state by electron transfer from I_3^-/I^- redox couple.
3. The organic molecule should have high molar absorption coefficients over the wide region of sunlight extending into near infra-red, to provide a large photocurrent to give the high light harvesting efficiency.
4. To achieve a stable DSSC, the organic molecule should have chemical stability in its photo excited state and the redox reactions throughout the reaction cycle.

Dye molecules (sensitizers) are the key component of a DSSC that increase efficiency through their abilities to absorb visible light photons Despite the fact that the highest efficiency of a dye sensitized solar cells is achieved from a combined effect of numerous physiochemical nanoscale properties, the main focus in these studies is the dye sensitization of large band-gap semiconductor electrodes. In DSSCs, this is accomplished by coating the internal surfaces of porous TiO_2 electrodes with dye molecules specifically tuned to absorb the incoming photons [23]. The dye is the light absorber and the photoreceptor sensitizing the semiconductor and so some conditions must be fulfilled. Without a doubt, a dye that absorbs nearly all the sunlight radiation incident on earth, like a black-body absorber, is highly desirable. Organic dyes consisting of natural pigments and synthetic organic dyes have a donor-acceptor structure called push-pull design, which improves the absorption in red and infrared region by increasing short circuit current density. Natural pigments, like chlorophyll, carotene, and anthocyanin, are available in plant leaves, flowers, and fruits and fulfill these requirements. Experimental results showing that natural-dye sensitized solar cells achieved the efficiency of 7.1% and high stability [24].

Co-sensitization, the use of two dyes combination that complements each other in their spectral features is another strategy to get a broad optical absorption expanding throughout the visible and near IR region. This strategy enhances photo-absorption through optical effects which allow the two sensitizers to be additive. In particular, there was no negative interference between co-adsorbed chromophores, making way for testing a multitude of other dye combinations [25].

To increase improvement of the performance of DSSC, different kinds of additives have been added into dye solutions. For example, Kay and Grätzel found that the addition of cholic acid (CA) with porphyrin derivatives improved both the photocurrent and photovoltage of the solar cell [26]. Additionally, other co-adsorbents such as hexadecylmalonic acid (HDMA) [27], deoxycholic acid (DCA) [28], and chenodeoxycholic acid (CDCA) [29] were also used in the dye solution when fabricating sensitized TiO2 films into devices, among which CDCA is the most popular co-adsorbent.

Dye aggregation on the TiO_2 surface should be avoided. This aggregation leads to reduction in electron-injection yield from the dyes to the CB of the TiO_2 due to intermolecular energy transfer causing low conversion efficiency of the DSSC [30]. The main parts of the dye sensitized solar cell are illustrated schematically in **Figure 3**. The transparent and counter conducting electrodes, wide bandgap semiconducting nanostructured layer, the sensitizer, and the electrolyte are the main four elements of the cell. The transparent conducting electrode and counter-electrode are coated with a conductive and transparent thin film such as fluorine doped tin dioxide (SnO_2) [31].

The photocurrent density calculated at short circuit (J_{SC}) the open-circuit photovoltage (V_{oc}) the fill factor (FF), and the power of the incident light (P_{in}) are used to determine the total conversion efficiency (%η) of the dye-sensitized solar cell. These values can be taken from the photocurrent density-voltage characteristics (IV curves) under full sunlight (P_{in} = 100 $mWcm^{-2}$). The relationship between voltage (V) and current (I) is determined by varying the resistance of the outer circuit and considered J_{SC} when resistance of the outer circuit is zero (thus voltage is zero) and Voc when resistance is maximum (thus photocurrent is zero). The power output of the device equals the product of J and V, and the fill factor states the efficiency of the device compared to that of an ideal cell. P_{max} relates to the maximum value that can reach the output power and is usually reported as the output power of the commercial device. The performance of DSSC can be projected using the following Equations [32]: (101)

$$\eta\,(\%) \;=\; \frac{Jsc * Voc * FF}{Pin} \tag{1}$$

where:

$$FF \;=\; \frac{Jm\,Vm}{Jsc\,Voc} \tag{2}$$

3.2. Results: The resurrection of an ancient leaf

Dr. Rajab E. Abujnah built the first ever asphaltene DSSC (dye-sensitized solar cell) as a graduate student in the lab of Dr. Chianelli, which demonstrated a photo-conversion efficiency (PCE) of 1.8%. Four natural organic asphaltene fractions were extracted and tested as dyes using various parameters with TiO_2 based dye-sensitized solar cell DSSC. The photovoltaic performance of the cells was determined by parameters such as open-circuit voltage (V_{oc}), short-circuit current (I_{sc}), fill factor (FF), and series resistance. The overall energy conversion efficiency was also measured to correlate the different effects of asphaltene fraction as well as concentration and influence on the improvement of the solar cell parameters.

http://dx.doi.org/10.5772/intechopen.78379

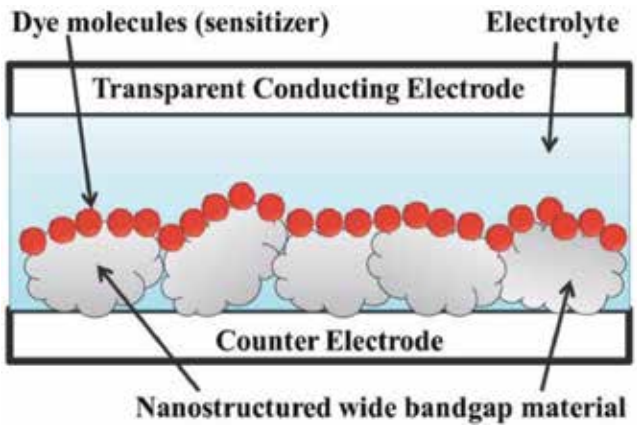

Figure 3. Schematic of the structure of the dye sensitized solar cell.

The sensitization of TiO_2 electrode using asphaltene obtained with a 90/10 ratio of toluene to pentane ratio resulted in an energy conversion efficiency of 1.8%. Un-fractionated asphaltene was shown to produce comparable results as Fraction 3 as sensitizer in DSSC. A strategy to minimize series resistance, improve photo current and open circuit voltage was also studied. Purifying asphaltene using the RTV mask, employing the TiO_2 compact layer, in addition to UV-Ozone cleaning treatment of the transparent electrode have been shown to improve the performance of asphaltene DSSCs [33].

The asphaltene dye covered TiO_2 electrode and Pt-counter electrode were assembled into a sandwich type and assembled with using a binder clamps as shown in **Figure 4**. The clamps used to attach the two electrodes and to provide space for the electrolyte between two electrodes. Sealant also can be used to assemble the sandwich of electrodes. It is can be used to prevent leakage of electrolyte. For good results, sealant was put between two electrodes and put under the hot press machine. Temperature and pressure were adjusted and then the hot press was heated up to join both electrodes by using the sealant. A drop of the electrolyte solution was

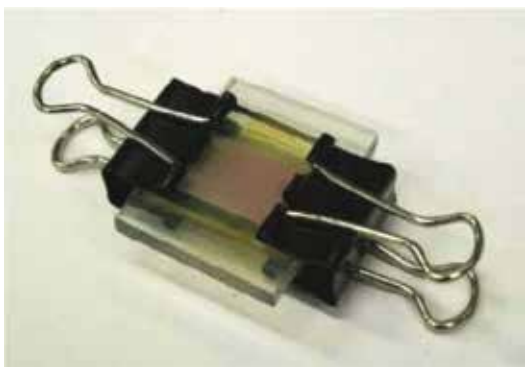

Figure 4. Completed synthetic asphaltene DSSC.

injected into the hole in the back of the counter electrode and to prevent leakage of electrolyte, the hole was covered by tape. The electrolyte was introduced into the cell by using vacuum.

Synthetic asphaltene has shown experimental evidence and preliminary results to suggest it can fulfill the requirements of organic semiconductors due its ability to absorb visible light. It was also found that this material can be adsorbed easily on the surface of the nano-crystalline particles TiO_2, therefore synthetic asphaltene is an excellent candidate for use in DSSC. Dr. Hassan Sharif experimented with synthetic asphaltene samples subsequently to Dr. Abujnah and applied as-synthesized asphaltenes into various solar cells with different parameters in the TiO_2 layer of the DSSC. DSSCs were fabricated using the synthetic asphaltene as dye.

To further research and optimize the cells, Porphyrin was added to the synthetic asphaltene to improve the efficiency of the cell. Porphyrin is already used as organic dye in DSSC. The new compound is prepared in the lab by dissolving the same ratio of synthetic asphaltene with free metal Porphyrin in Toluene for 24 hrs under heating; the mixture was kept under the hood to evaporate the Toluene. The final product was collected and used in this experiment. The table below shows the effects of mixing Porphyrin with synthetic asphaltene on the conversion efficiency of synthetic asphaltene dye. From the table it is clear that the new dye is increasing both current density J_{SC} and V_{OC}, and then increasing the performance efficiency.

Asphaltene has shown to be able to produce voltage, and according to the results outlined in **Table 3**, could be considered a good candidate in photovoltaic in part, due to its low cost [34]. New material was prepared by dissolving synthetic asphaltene and crude oil asphaltene. This asphaltene was extracted from crude oil asphaltene and purified by using Toluene. Real asphaltene was dissolved with synthetic asphaltene in Toluene in the ration of 1:1 and kept for 24 hours for dissolving under heating. The solvent kept under the hood until the Toluene completely evaporated, and the solid product was collected and used for the experiment.

During his work with synthetic asphaltene as new dye in the fabrication of DSSC, Dr. Sharif noticed some precipitates when synthetic asphaltene dissolved in Toluene. These precipitates prevent the good absorbance of synthetic asphaltene dye into the surface of TiO2. So, synthetic asphaltene was filtrated to remove any impurities. The table below compares the

Experiment	Open current Voltage	Short Circuit Current (mA/cm^2)	Fill Factor %	PCE (%)
Synthetic asphaltene mixed with porphyrin and dissolved in toluene	0.429	6.57	54	1.85
Real Asph. mixed with synthetic asphaltene	0.435	7.28	46	1.40
Unpurified synthetic asphaltene	0.445	4.19	56	1.0
Purified synthetic asphaltene	0.455	7.05	61	1.83
Purified synthetic asphaltene with chenodeoxycholic acid (CDCA)	0.506	7.00	0.61	2.08

Table 3. The performance of synthetic asphaltenes in DSSCs using different parameters.

results before and after purifying the synthetic asphaltene. There is a high increase in the current density and also fill factor, but the small increase in the voltage. The efficiency was improved from 1.0 to 1.83% which illustrates the importance of processing parameters on devices performance and optimization.

The effects of chenodeoxycholic acid (CDCA) in a dye solution as a co-adsorbent on the photovoltaic performance of dye-sensitized solar cells (DSSCs) based organic dye containing purified synthetic asphaltene dye was also studied. It was observed that the co-adsorption of CDCA can eliminate and reduce the formation of dye aggregates and improve electron injection yield and thus, the short-circuit current (*J*sc). This has also led to a rise in photovoltage, which is attributed to the decrease of charge recombination. The DSSC, based on synthetic asphaltene dye with CDCA, overall conversion efficiency was further improved to 2.0% (*J*sc = 7.00 mA/cm^2, *V*oc = 0.506 V, *FF* = 0.61) upon addition of 1:1 ratio of CDCA to the dye solution.

3.3. Summary and discussion

In general, we can conclude from these studies that asphaltene was successfully prepared in the lab and the characterization results were similar as in the literatures. Even primary results show that synthetic asphaltene has good ability to absorb sunlight, but the results of the first use of synthetic asphaltene in DSSC were not satisfied. More work was carried during the study to increase the performance efficiency from 0.4 to 2.0%. We conclude also synthetic asphaltene can give good results by adding some additives, but it also can improve the conversion efficiency just by purifying process which increase efficiency from 1.0 up to 1.83%. Instead of additives, there is another parameters can increase the efficiency of synthetic asphaltene as dye in DSSC for example, the number of layers of the paste and using UV-O treatment. Therefore, a total overall efficiency of 3.5–5.0% could be easily attained with good engineering design and material process.

The first result obtained with using synthetic asphaltene as dye was 0.4%. The maximum PCE obtained using synthetic asphaltene as dye after adjusting some variables and adding some additives reached 2.0%. The benefit to this study and in using synthetic material will help researchers to find new and inexpensive dyes as well as to understand better the characterization of crude oil asphaltene [35].

4. Doped graphene from asphaltene

4.1. Introduction to doped graphene applications

The electronic and magnetic properties of graphene can be modified through combined transition-metal (TM) and nitrogen decoration of vacancies. Additional modes of functionalization that are currently being explored for a wide range of applications in nanoelectronics [36–38], spintronics [39] and electrocatalysts [40]. Researchers previously discovered that TMs bind to graphene strongly in a porphyrin ring coordinated by four nitrogens [41]. The stability in the presence of the defects associated with TMs can be attributed to the reduced

electrostatic repulsion between nitrogen lone-pair electrons due to the hybridization between N and TM. Results from DTF studies have predicted these types of structures to be particularly promising candidates for graphene-based ferromagnets, which could find applications in nanoelectronics and nanomagnetism.

Graphene-type molecules, typically large polycyclic aromatic hydrocarbons (PAHs), have gained enormous interest because of their unique self-organization behavior and promising electronic properties for applications in organic electronics [42]. Asphaltene is a part of crude oils that contain a large number of structures, specifically high molecular weight bonded aromatic hydrocarbons components with hetero-atoms. Several metals (e.g., Ni, V, Fe, Al, Na, Ca, and Mg) shown to accumulate in the asphaltenes fraction of crude oil, typically in concentrations less than 1% w/w [43–45]. Vanadium and nickel, the most abundant of the trace metals, present mainly as chelated porphyrin compounds, and they linked to catalyst poisoning during upgrading of heavy oils [46, 47]. The concentrations of other trace metals not bound in porphyrin structures (e.g., Fe, Al, Na, Ca, and Mg) indicated to change in deposits as a function of well depth [48], and among sub fractions of asphaltene.

Graphene produced from chemical vapor deposition is viable for use in technologies such as touch screens, sensors, transistors, novel optical/electronic/photonic devices such as IR cameras, radiation shielding and camera lenses. Because they are expected to induce novel magnetic and superconducting behavior, TM adatoms and graphene are a topic of great interest are expected to induce novel magnetic and superconducting behavior. Because of this interest, there have been extensive theoretical studies but the experimental exploration of TM/graphene systems is very limited. Graphene with Boron and Nitrogen (BCN) is a sought after material due to the fact that graphene has no band gap [49]. Graphene in its single crystal form is a conductor, not a semi-conductor, so while it has amazing properties sought after by so many researchers, it has yet to make a significant impact on electronic industries for this reason. BCN is currently the subject of doped graphene research because it can be introduced by vapor. In contrast, TMs cannot be introduced by vapor. Even if they could be introduced at high temperatures, it has been determined that they would not be stable in an in-plan configuration due to the high differences in energy between TMs and carbon. Boron and Nitrogen both neighbor carbon on the periodic table and do not have a large differences in electron structure. As a carbon source, asphaltene is generated from waste crude oils and remains unsuitable for hydrocracking because of the presence of TMs. This study attempts to utilize that waste as a valuable source of metalloporphyrins for placing TMs doping graphene materials.

Asphaltene materials were extracted from crude using different n-alkanes and dissolved in toluene for deposition. Asphaltene/toluene (1 mg/ml) solutions were then deposited using drop coating onto previously prepared copper foil and experiments proceeded according to **Table 4**. Experiment 1 deposited asphaltene onto copper using spin coating. A 4 inch tube furnace was used to anneal the material under a reducing environment (H_2). The system was equipped with a turbo pump with a direct line-of-sight to the sample and the substrate and allowed for base pressures below 10^{-8} Torr. A turbo pump was used and all the flanges on the high vacuum side of the system were constructed with conflat flanges; capable of achieving ultra-high vacuum (UHV). Reaching low background pressures allowed the removal of residual gasses like water

Experiment	Temperature [°C]	Time [min]	Material	Gas
1	1050	5	C7-spin coated	H (10 ccm)
2	1050	5	C7-drop coated	H (10 ccm)
3	1050	5	Synthetic	H (10 ccm)

Table 4. Experimental conditions and parameters and (above) figure of furnace used in experiment.

and oxygen from the system before growth. The use of a turbo pump also allowed for the system to reach pressures low enough (below 10^{-5} Torr) to operate a residual gas analyzer (RGA) instrument. In a typical growth, the sample was loaded into the furnace and allowed to pump down using the turbo pump for 2 hours prior to heating and gas flow (**Figure 5**).

Raman was taken using Witec Alpha 300 micro-Raman confocal microscope after graphene had been transferred to SiO_2/Si wafers. Scanning Electron Microscope (SEM) Images were taken using a FEI Quanta 650 SEM equipped with Bruker EDX system for chemical analysis. Optical Microscope images of asphaltenes were taken on copper foils before and after growth. Transfers were performed by spin coating polymer, dissolving copper foil and transferring graphene to SiO_2/Si wafers. Zeiss Axiovert 100A Light Microscope was used to take images of asphaltenes before and after growth.

4.2. Single-layer asphaltene

Conditions for graphene growth were applied for all experiments. The resulting averaged Raman from all experiments show heavy carbonization and some graphitization of the solid carbon source. We were able to find metals in more than one sample of the post growth heptane extracted asphaltene. When drop coating was used for application before the growth process, the Raman from **Figure 6** indicates mostly carbon with some graphitization. Only

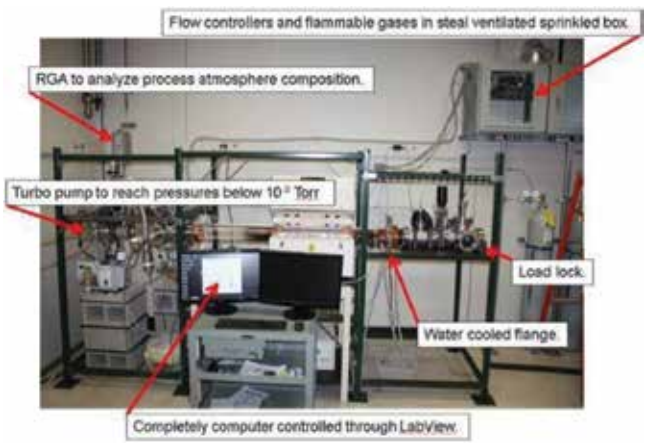

Figure 5. CVD set-up at the J.J. Pickle Research Center Austin, TX [50].

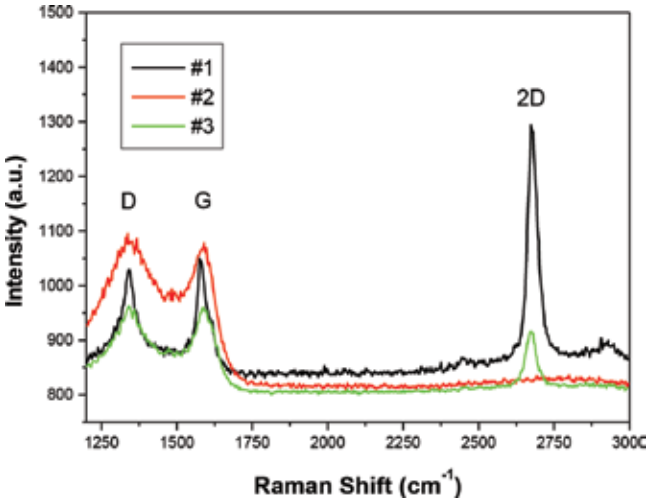

Figure 6. Raman summary of experiment 1, 2 & 3.

experiment 1 exhibited the ratio of (> 2:1) 2D to G and D peaks that would indicate the presence of quality graphene rather than sp^2 hybridized carbon.

Metals identified in post growth samples from experiment 1 and 2 included Al, Fe, Zr and adatoms included sulfur. Electron Diffraction X-ray (EDX) analysis was taken of the copper foil before any etching in **Figure 7** and foil which had been sonicated in acetone before applying asphaltenes shows no metals or adatoms present before growth indicating that metals and adatoms indeed came from asphaltene samples. After growth, EDX spectra taken of sample from Experiment 1 show the presence of Aluminum and Iron.

To further study asphaltene adatoms, EDX elemental analysis was taken of synthetic asphaltene containing no metals applied to copper foil. Needless to say from data in **Figure 8** no TM or adatoms could be found present after growth.

Images taken using optical microscope **Figure 9** show copper coated with heptane extracted asphaltenes before and after Experiment 1 growth. There are clustered discotic structures before growth and curiously there are areas after growth that show clearly more than a few layers graphitized **Figure 10**. There are areas that can be seen where copper can be seen as clear orange from underneath sheets of graphitized carbon in **Figure 9(c)** and **(d)**.

4.3. Summary

Because they are expected to induce novel magnetic and superconducting behavior, TM adatoms and graphene are a topic of great interest. There have been extensive theoretical studies because of these interesting properties but the experimental exploration of TM/graphene systems is very limited. Graphene with Boron and Nitrogen (BCN) is a sought after material due to the fact that graphene has no band gap. Graphene in its single crystal

http://dx.doi.org/10.5772/intechopen.78379

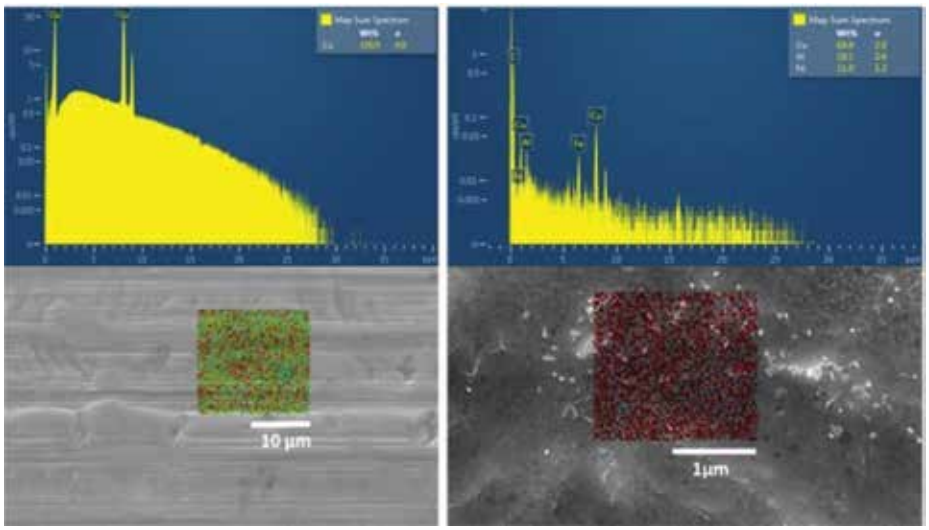

Figure 7. EDX analysis (top left) of copper foil sonicated in acetone before application of solid carbon source with corresponding SEM image (bottom left) EDX elemental analysis respectively (top right) from SEM section (bottom right) from asphaltene extracted using heptane in Experiment 1.

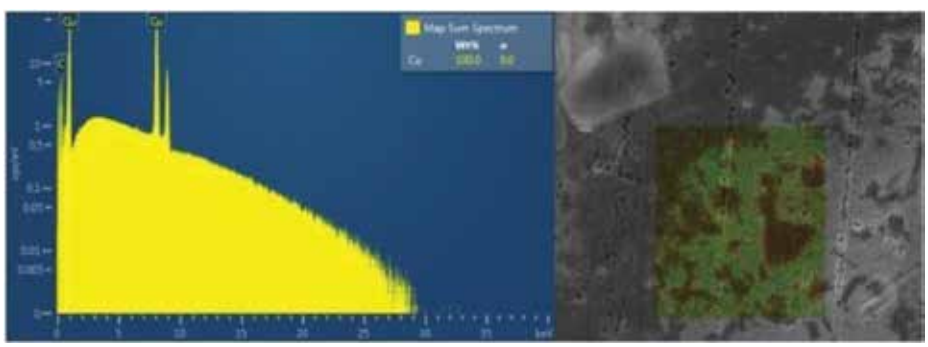

Figure 8. EDX (left) copper with drop coated synthetic asphaltene (right) after growth.

form is a conductor, not a semi-conductor, so while it has amazing properties sought after by so many researchers, it has yet to make a significant impact on electronic industries for this reason. BCN is currently being researched because it can be introduced by vapor. In contrast, TMs cannot be introduced by vapor. Even if they could be introduced at high temperatures, it has been determined that they would not be stable in an in-plan configuration due to the high differences in energy between TMs and carbon. Boron and Nitrogen both neighbor carbon on the periodic table and do not have a large difference in electron structure. Our carbon source generated from waste crude oils is unsuitable for hydrocracking because of the presence of TMs. We were able to utilize that waste as a valuable source of metalloporphyrins for placing TMs directly inside the graphene lattice.

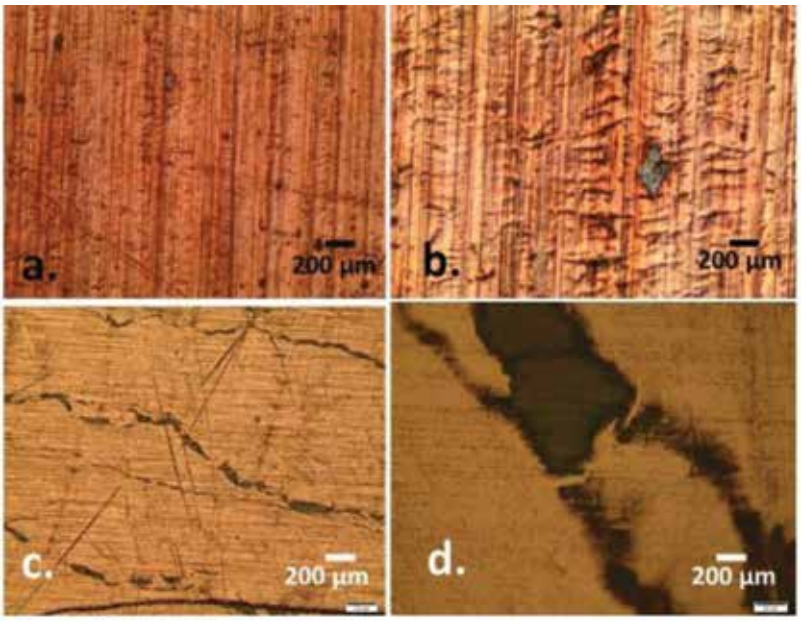

Figure 9. Optical microscope images of heptane asphaltene on copper foil from experiments before (a,b) and after growth (c,d).

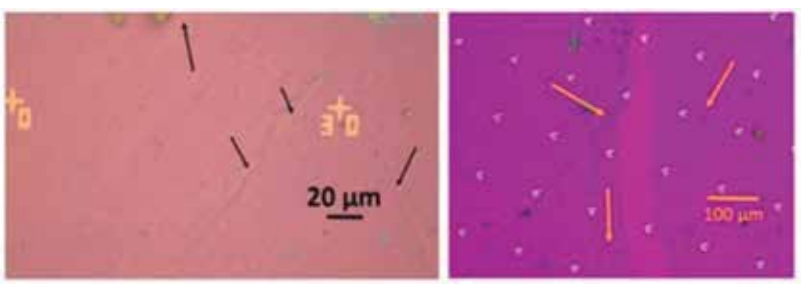

Figure 10. Optical microscope image of experiment 1 transferred to SiO2/Si wafer with rips and wrinkles (left) compared to OM image of a graphene sheet (purple) on SiO_2/Si wafer (pink). Arrows show wrinkles and tears in the material (right). (graphene provided courtesy Ruoff group at UT).

5. Conclusions

All electronic processes in nature occur using carbon-based molecular structures; from signal transduction in the brain all the way to photosynthesis in a leaf. Carbon Molecular Electronics (CMEs) as a field is the result of developments in an interdisciplinary field with increasing numbers of synthetic and quantum chemists, physicists and engineers. New devices have been designed and investigated for the exciting realization of CMEs for photovoltaics, transistors, switches and other non-linear electronic components.

The results demonstrated in these works illustrate the use of asphaltene as a light-harvesting active molecular dye effectively in dye sensitized solar cells for application in the field of organic photovoltaics. Higher-power conversion efficiencies can be achieved by further optimizing the device structure. In addition, they also show asphaltene as a promising candidate for doping multi-layer and potentially single layer graphene for future novel nanoscale magnetic or optoelectronic uses.

Acknowledgements

We would like to acknowledgeDr. Harry Chou's assistance with graphene growth and characterization in Section 4. Doped Graphene from asphaltene at The University of Texas (Austin, TX). Thanks To Dr. Carl Magnuson for assistance and instruction on tube furnace construction and apparatus.

Author details

Eva M. Deemer[1] and Russell R. Chianelli[1,2]*

*Address all correspondence to: chianell@utep.edu

1 Materials Research and Technology Institute, The University of Texas at El Paso, TX, USA

2 Department of Chemistry, The University of Texas at El Paso, El Paso, TX, USA

References

[1] Sergeyev S, Pisula W, Geerts YH. Discotic liquid crystals: A new generation of organic semiconductors. Chemical Society Reviews. 2007;**36**:1902. DOI: 10.1039/b417320c

[2] Laschat S, Baro A, Steinke N, Giesselmann F, Hägele C, Scalia G, Judele R, Kapatsina E, Sauer S, Schreivogel A, Tosoni M. Discotic liquid crystals: From tailor-made synthesis to plastic electronics. Angewandte Chemie International Edition. 2007;**46**:4832-4887. DOI: 10.1002/anie.200604203

[3] Bumm LA, Arnold JJ, Cygan MT, Dunbar TD, Burgin TP, Jones L, Allara DL, Tour JM, Weiss PS. Are single molecular wires conducting? Science (80). 1996;**271**:1705-1707. DOI: 10.1126/science.271.5256.1705

[4] Reed MA, Zhou C, Muller CJ, Burgin TP, Tour JM. Conductance of a molecular junction. Science. 1997;**278**:252-254. DOI: 10.1126/science.278.5336.252

[5] Joachim C, Gimzewski JK. Analysis of low-voltage I(V) characteristics of a single C60 molecule. Europhysics Letters. 1995;**30**:409-414. DOI: 10.1209/0295-5075/30/7/006

[6] Dorogi M, Gomez J, Osifchin R, Andres RP, Reifenberger R. Room-temperature Coulomb blockade from a self-assembled molecular nanostructure. Physical Review B. 1995;**52**:9071-9077. DOI: 10.1103/PhysRevB.52.9071

[7] Dai H, Wong EW, Lieber CM. Probing electrical transport in nanomaterials: Conductivity of individual carbon nanotubes. Science (80). 1996;**272**:523-526. DOI: 10.1126/science.272.5261.523

[8] Dekker C, Tans SJ, Verschueren ARM. Room-temperature transistor based on a single carbon nanotube. Nature. 1998;**393**:49-52. DOI: 10.1038/29954

[9] Zhou C, Deshpande MR, Reed MA, Jones Ii L, Tour JM. Nanoscale Metal/Self-Assembled Monolayer/Metal Heterostructures. Applied Physics Letters. 1997;**71**:611 DOI: org/10.1063/1.120195

[10] Reed MA. Molecular-Scale Electronics. In: Proceedings of the IEEE. April 1999;**87**(4): 0018-9219

[11] Joachim C, Gimzewski JK. An electromechanical amplifier using a single molecule. Chemical Physics Letters. 1997;**265**:353-357. DOI: 10.1016/S0009-2614(97)00014-6

[12] Metzger RM, Chen B, Höpfner U, Lakshmikantham MV, Vuillaume D, Kawai T, Wu X, Tachibana H, Hughes TV, Sakurai H, Baldwin JW, Hosch C, Cava MP, Brehmer L, Ashwell GJ. Unimolecular electrical rectification in hexadecylquinolinium tricyanoquinodimethanide. Journal of the American Chemical Society. 1997;**119**(43):10455-10466. DOI: 10.1021/JA971811E

[13] Chen R, Rawlett T. Large on-off ratios and negative differential resistance in a molecular electronic device. Science. 1999;**286**:1550-1552. http://www.ncbi.nlm.nih.gov/pubmed/10567259 [Accessed: March 24, 2017]

[14] Ellenbogen JC, Love JC. Architectures for molecular electronic computers. I. Logic structures and an adder designed from molecular electronic diodes. In: Proc. IEEE. 2000;**88**:386-426. DOI: 10.1109/5.838115

[15] Mullins OC, Sheu EY, Hammami A, Marshall AG, editors. Asphaltenes, Heavy Oils and Petroleomics. New York City: Springer; 2007

[16] Chianelli RR, Siadati M, Mehta A, Pople J, Ortega LC, Chiang LY. Self-assembly of asphaltene aggregates: Synchrotron, simulation and chemical modeling techniques applied to problems in the structure and reactivity of asphaltenes. In: Asphaltenes, Heavy Oils, and Petroleomics. New York, New York, NY: Springer; 2007. pp. 375-400. DOI: 10.1007/0-387-68903-6_15

[17] Zeman M. Introduction to photovoltaic solar energy. Solar Cells. Coll. 2003:1-139. http://paginas.fisica.uson.mx/horacio.munguia/aula_virtual/Cursos/Teoria de Control/Solar Cells Miro Zeman.pdf [Accessed: December 10, 2017]

[18] Knier G. How do Photovoltaics Work? | Science Mission Directorate, Scientific Beta. 2016. https://science.nasa.gov/science-news/science-at-nasa/2002/solarcells [Accessed: December 10, 2017]

[19] Knupfer M. Exciton binding energies in organic semiconductors. Applied Physics A: Materials Science & Processing. 2003;**77**:623-626. DOI: 10.1007/s00339-003-2182-9

[20] Yu K, Chen J. Enhancing solar cell efficiencies through 1-D nanostructures. Nanoscale Research Letters. 2009;**4**:1-10. DOI: 10.1007/s11671-008-9200-y

[21] O'Regan B, Grätzel M. A low-cost, high-efficiency solar cell based on dye-sensitized colloidal TiO_2 films. Nature. 1991;**353**:737-740. DOI: 10.1038/353737a0

[22] Grätzel M. Conversion of sunlight to electric power by nanocrystalline dye-sensitized solar cells. Journal of Photochemistry and Photobiology A: Chemistry. 2004;**164**:3-14. DOI: 10.1016/j.jphotochem.2004.02.023

[23] Grätzel M. Dye-sensitized solar cells. Journal of Photochemistry and Photobiology C:Photochemistry Reviews. 2003;**4**:145-153. DOI: 10.1016/S1389-5567(03)00026-1

[24] Campbell WM, Jolley KW, Wagner P, Wagner K, Walsh PJ, Gordon KC, Schmidt-Mende L, Nazeeruddin MK, Wang Q, Gra M, Officer DL. Highly efficient porphyrin sensitizers for dye-sensitized solar cells. Journal of Physical Chemistry C. 2007;**111**(32):11760-11762. DOI: 10.1021/jp0750598

[25] Sayama K, Tsukagoshi S, Mori T, Hara K, Ohga Y, Shinpou A, Abe Y, Suga S, Arakawa H. Efficient sensitization of nanocrystalline TiO_2 films with cyanine and merocyanine organic dyes. Solar Energy Materials & Solar Cells. 2003;**80**:47-71. DOI: 10.1016/S0927-0248(03)00113-2

[26] Kay A, Graetzel M. Artificial photosynthesis. 1. Photosensitization of titania solar cells with chlorophyll derivatives and related natural porphyrins. The Journal of Physical Chemistry. 1993;**97**:6272-6277. DOI: 10.1021/j100125a029

[27] Wang P, Zakeeruddin SM, Comte P, Charvet R, Humphry-Baker R, Grätzel M. Enhance the performance of dye-sensitized solar cells by co-grafting amphiphilic sensitizer and hexadecylmalonic acid on TiO_2 nanocrystals. Journal of Physical Chemistry B. 2003;**107**(51):14336-14341. DOI: 10.1021/JP0365965

[28] Wang Z-S, Cui Y, Dan-oh Y, Kasada C, Shinpo A, Hara K. Thiophene-functionalized coumarin dye for efficient dye-sensitized solar cells: Electron lifetime improved by coadsorption of deoxycholic acid. Journal of Physical Chemistry C. 2007;**111**(19):7224-7230. DOI: 10.1021/JP067872T

[29] Qu S, Wu W, Hua J, Kong C, Long Y, Tian H. New diketopyrrolopyrrole (DPP) dyes for efficient dye-sensitized solar cells. Journal of Physical Chemistry C. 2010;**114**:1343-1349. DOI: 10.1021/jp909786k

[30] Ooyama Y, Harima Y. Molecular designs and syntheses of organic dyes for dye-sensitized solar cells. European Journal of Organic Chemistry. 2009;**18**:2903-2934. DOI: 10.1002/ejoc.200900236

[31] Jasim KE. Dye sensitised solar cells-working principles, challenges and opportunities. Dye Sensitized Solar Cells - Working Principles, Challenges and Opportunities. 2007:171-204. http://cdn.intechopen.com/pdfs/23333.pdf [Accessed: December 10, 2017]

[32] Colodrero S, Calvo ME, Míguez H. Solar Energy, 2010. http://cdn.intechweb.org/pdfs/8565.pdf [Accessed: December 10, 2017]

[33] Abujnah RE. Asphaltene as Light Harvesting Material in Dye Sensitized Solar Cell. Texas, El Paso: ETD Collect. Univ; 2011. http://digitalcommons.utep.edu/dissertations/AAI10118135 [Accessed: December 10, 2017]

[34] RE A, H S, B T, K C, V G, RR C. Asphaltene as light harvesting material in dye-sensitized solar cell: Resurrection of ancient leaves. Journal of Environmental & Analytical Toxicology. 2016;**6**. DOI: 10.4172/2161-0525.1000345

[35] Sharif HM. Synthetic Asphaltene as a Novel Dye in Dye Sensitized Solar Cells DCCs. Texas, El Paso: ETD Collect. Univ; 2013. http://digitalcommons.utep.edu/dissertations/AAI3597255 [Accessed: December 10, 2017]

[36] Krasheninnikov AV, Nieminen RM. Attractive interaction between transition-metal atom impurities and vacancies in graphene: A first-principles study. Theoretical Chemistry Accounts. 2011;**129**:625-630. DOI: 10.1007/s00214-011-0910-3

[37] Wei D, Liu Y, Wang Y, Zhang H, Huang L, Yu G. Synthesis of N-doped graphene by chemical vapor deposition and its electrical properties. Nano Letters. 2009;**9**:1752-1758. DOI: 10.1021/nl803279t

[38] Wu M, Cao C, Jiang JZ. Light non-metallic atom (B, N, O and F)-doped graphene: A first-principles study. Nanotechnology. 2010;**21**:505202. DOI: 10.1088/0957-4484/21/50/505202

[39] Krasheninnikov AV, Lehtinen PO, Foster AS, Pyykkö P, Nieminen RM. Embedding transition-metal atoms in graphene: Structure, bonding, and magnetism. Physical Review Letters. 2009;**102**:126807. DOI: 10.1103/PhysRevLett.102.126807

[40] Tripkovic V, Vanin M, Karamad M, Björketun ME, Jacobsen KW, Thygesen KS, Rossmeisl J. Electrochemical CO_2 and CO reduction on metal-functionalized porphyrin-like graphene. Journal of Physical Chemistry C. 2013;**117**:9187-9195. DOI: 10.1021/jp306172k

[41] Kattel S, Atanassov P, Kiefer B. Stability, electronic and magnetic properties of in-plane defects in graphene: A first-principles study. Journal of Physical Chemistry C. 2012;**116**:8161-8166. DOI: 10.1021/jp2121609

[42] Pisula W, Feng X, Müllen K. Charge-carrier transporting graphene-type molecules. Chemistry of Materials. 2011;**23**:554-567. DOI: 10.1021/cm102252w

[43] Spiecker PM, Gawrys KL, Kilpatrick PK. Aggregation and solubility behavior of asphaltenes and their subfractions. Journal of Colloid and Interface Science. 2003;**267**:178-193. http://www.ncbi.nlm.nih.gov/pubmed/14554184 [Accessed: March 24, 2017]

[44] Pena ME, Manjarréz A, Campero A. Distribution of vanadyl porphyrins in a Mexican offshore heavy crude oil. Fuel Processing Technology. 1996;**46**:171-182. DOI: 10.1016/0378-3820(95)00053-4

[45] Thomas J, Kaminski HSF, Wolf N, Wattana P, Mairal A. Classification of Asphaltenes via fractionation and the effect of heteroatom content on dissolution kinetics. Energy Fuels. 1999;**14**(1):25-30. DOI: 10.1021/EF990111N

[46] Yang X, Hamza H, Czarnecki J. Investigation of subfractions of athabasca asphaltenes and their role in emulsion stability. Energy Fuels. 2004;**18**(3):770-777. DOI: 10.1021/EF0301654

[47] Ali MF, Perzanowski H, Bukhari A, Al-Haji AA. Nickel and vanadyl porphyrins in Saudi Arabian crude oils. Energy & Fuels. 1993;**7**:179-184. DOI: 10.1021/ef00038a003

[48] Chouparova E, Lanzirotti A, Feng H, Jones KW, Marinkovic N, Whitson C, Philp P. Characterization of petroleum deposits formed in a producing well by synchrotron radiation-based microanalyses. 2004. DOI: 10.1021/EF030108A

[49] Ozturk B, de-Luna-Bugallo A, Panaitescu E, Chiaramonti AN, Liu F, Vargas A. Atomically thin layers of B–N–C–O with tunable composition. Science Advances. 2015;**1**(6):1790-1798. DOI: 10.1126/sciadv.1500094

[50] Magnuson CW, Chemical vapor deposition graphene on polycrystalline copper foil, [thesis]. 2014. http://citeseerx.ist.psu.edu/viewdoc/download?doi=10.1.1.835.2607&rep=rep1&type=pdf [Accessed: December 11, 2017]

[51] Mullins OC, Sheu EY. Structures and dynamics of asphaltenes. New York City: Plenum, 1998. In: Chilingarian GV, Yen TF, editors. Bitumens, Asphalts, and Tar Sands. New York City: Elsevier Scientific Publishing Co; 1978

Chapter 4

Fatigue Destruction of Asphalt Concrete Pavement: Self-Organization and Mechanical Interpretation

Bagdat Teltayev

Additional information is available at the end of the chapter

http://dx.doi.org/10.5772/intechopen.75536

Abstract

This chapter analyzes the fatigue failure of the asphalt concrete pavement of the highway on a macroscopic level. Based on the actual data, obtained on the sections of the real highways, the principle was formulated for the staged fatigue failure of the asphalt concrete pavement. During the analysis of the existing classifications of the fatigue cracks, it was determined that in Kazakhstan, the stage behavior of the fatigue cracks was not considered, and in the USA, the relation between stages of failure was not established. Similarly to the known phenomena of self-organization in thermodynamics of irreversible processes and dynamics of nonlinear systems (synergetics)—Benar's effects and division of biological cell, it was proposed to consider the parts of the asphalt concrete pavement as the specific dissipative structures, occurring in critical conditions, and a new regularity of fatigue failure was formulated. The formulated regularity of the staged fatigue failure of the asphalt concrete pavement was explained based on the new proposed scheme of bifurcation with the use of the results of experimental determination of the occasional, cyclic, long-term and residual strength.

Keywords: asphalt concrete pavement, staged fatigue failure, consequential change of deformation types, asphalt concrete strength, self-organization, dissipative structures, bifurcation

1. Introduction

Fatigue is one of the main types of failure for the asphalt concrete pavement of a highway. As it determines, in association with other types of failure (rutting, low-temperature cracking), the service life of pavement in accordance with the requirements of standard document [1], all pavement structures of the highways of capital and lightweight types on the design stage

should be calculated for strength under the criterion of tensile bending strength of the cast-in-situ (asphalt concrete) layers.

It is considered that the fatigue cracking on the asphalt concrete pavement of highways occurs at frequently repeated load impact of the vehicles' wheels [2].

Hveem F.N. of the far abroad country has been one of the first researchers, who mentioned the phenomenon of fatigue in the asphalt concrete pavement of a highway [3]. The first investigations of the fatigue properties for the asphalt concretes in laboratory conditions were performed by Sall R.N.J., Pell P.S., Taylor I.F. in the UK [4, 5] and Monismith C.L. in the USA [6].

The study of the fatigue of the asphalt concretes in the former Soviet Union was started by the works of Sall A.O. (Leningrad), Radovskiy B.S. (Kiev), Zolotaryov V.A. (Kharkov), Rudenskiy A.V. and Kalashnikova T.N. (Moscow) [7–11].

It was found out that the phenomenon of fatigue failure for the asphalt concrete pavement of a highway was a complex one. In spite of the fact that the specialists of many countries of the world have been studying the phenomenon to the present day, the issue of the fatigue life for the asphalt concretes and asphalt concrete pavement remains actual.

2. Field observation

Figure 1 represents the photos showing fatigue failure of the asphalt concrete pavement of Karagandy-Shakhtinsk highway. These photos show clearly that the fatigue failure occurs by stage: first, parallel quasi-straight line longitudinal cracks occur on the patch line, between which quasi-straight line asphalt concrete strips have been formed, and then these quasi-straight line asphalt concrete strips are divided into cells of small sizes due to the occurrence of quasi-transversal cracks. Thus, in the considered case, the formation of a grid of alligator

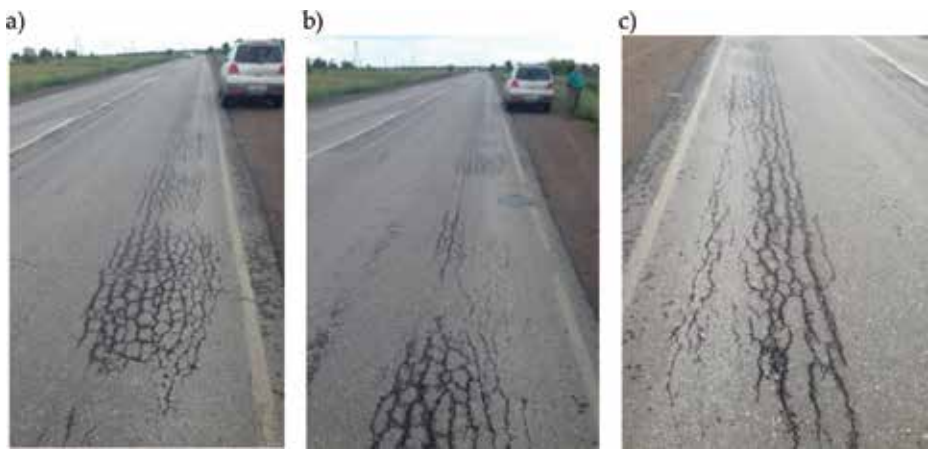

Figure 1. Fatigue failure of asphalt concrete pavement (860 km) of Karagandy-Shakhtinsk highway (Kazakhstan, Karagandy oblast, July, 2016).

http://dx.doi.org/10.5772/intechopen.75536

cracks on the asphalt concrete pavement represents by itself a two-staged process, each of which has been realized during less or more prolonged period.

The fragments of another sequence for crack occurrence in the staged process of fatigue failure of alligator type on the asphalt concrete pavement are shown in **Figures 2** and **3**. As it is seen from **Figure 2**, there are only specific (separated from each other) quasi-parallel transverse cracks on the asphalt concrete pavement within the patch line. At first sight, they are similar to the low-temperature cracks. But that is not the case. The considered highway is located in Sharjah city (United Arab Emirates), where there is actually no winter. But, **Figure 3** shows the patterns of fatigue cracks of alligator type, which are formed at the further occurring of longitudinal cracks, connecting the existing transverse ones. During the period of observation, it has been determined that a large number of multiaxle heavy vehicles run along the highway, and it suggests that this type of staged fatigue failure has been connected with dense traffic of multiaxle heavy vehicles. Based on the abovementioned types of the staged failure for asphalt concrete pavements of the highways, we can formulate the following principle: "The process of fatigue failure for the asphalt concrete pavements of the highways occurs stage by stage and according to various types of stages. Type 1: stage I—quasi-linear parallel longitudinal cracks occur on the patch lines, between which quasi-straight line asphalt concrete strips are formed; stage II—formation of patterns of fatigue cracks of the alligator type by division of quasi-straight line strips of the asphalt concrete into the cells with small sizes by quasi-transverse cracks. Type 2: stage I—occurrence of insulated quasi-parallel transverse cracks; stage II—formation of alligator type cracks with relatively large dimensions of cells due to the occurrence of longitudinal cracks, connecting the existing transverse ones; stage III—decrease of dimensions for the cells of crack patterns due to the sequential occurrence of transverse and longitudinal cracks within each cell".

We suppose that the staged progressing of the fatigue failure is mechanically and thermodynamically "of benefit" to the system—to the asphalt concrete pavement, and which type of the stage is progressed—"the system will choose itself" depending on specific conditions: volume and type of traffic, regime and speed of traffic, weather and climatic conditions, design features, properties of the materials, including asphalt concretes, and so on.

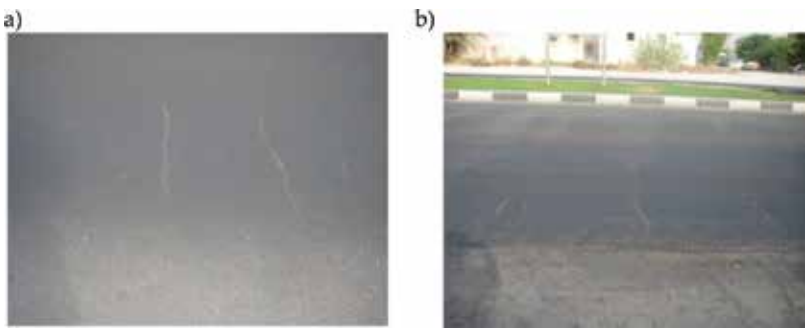

Figure 2. Fatigue failure of asphalt concrete pavement: transverse fatigue cracks (Sharjah city, United Arab Emirates, August, 2010).

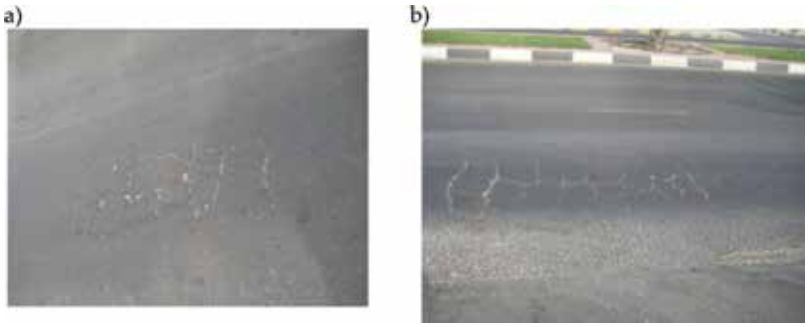

Figure 3. Fatigue failure of asphalt concrete pavement: alligator cracks (Sharjah city, United Arab Emirates, August, 2010).

3. Fatigue cracks classification

In Kazakhstan, the fatigue and other types of cracks on an asphalt concrete pavement for diagnostics and evaluation of road condition are considered in the standard [12], in which all defects on the pavements are divided into two groups: the defects, certifying inadequate strength and the defects, which do not certify inadequate strength in explicit form. Analysis of these defects shows that:

- in spite of the fact that they have different causes for their occurrence and progress character, cracks of various types (fatigue, thermal, reflected, sagging) are not identified separately;
- the staged development nature is not reflected for fatigue cracks;
- the maximum allowable measures are not contained for the cracks, including the fatigue ones.

The largest and wide scale program on investigation of performance for road structures (highway pavements) was started within the so-called Strategic Highway Research Program (SHRP) in the USA in 1987. The road agencies of the American States and 15 other countries have been collecting the data for 20 years for state of repair of pavements, climate, volume and density of traffic on more than 1000 experimental sections of the highways.

A special guide has been developed to perform data collection under the unique method, which was published three more times in the following years [13]. This Guide gives the following definition for the fatigue cracks in asphalt concrete pavement: "They occur in the areas subjected to repeated traffic loadings (wheel paths). They can be a series of interconnected cracks in early stages of development. They develop into many-sided, sharp-angled pieces, usually less than 0.3 m on the longest side, characteristically with a chicken wire/alligator pattern, in later stages. The fatigue cracks are divided into three levels. Low level: an area of cracks with no or only a few connecting cracks; cracks are not spalled or sealed; pumping is not evident. Moderate level: an area of interconnected cracks forming a complete pattern; cracks may be slightly spalled; cracks may be sealed; pumping is not evident. High level: an area of moderately or severely spalled interconnected cracks forming a complete pattern; pieces may move when subjected to traffic; cracks may be sealed; pumping may be evident."

http://dx.doi.org/10.5772/intechopen.75536

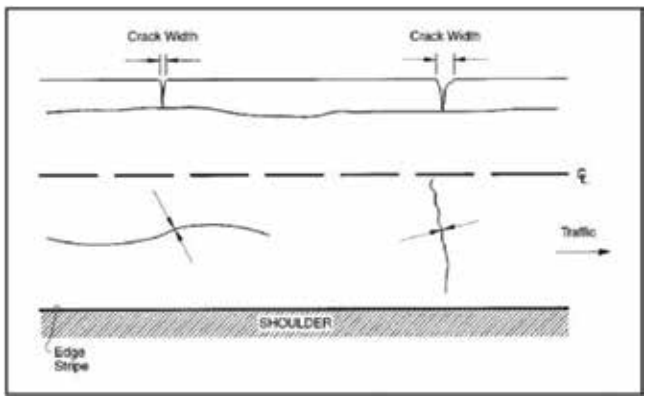

Figure 4. All levels of fatigue failure of asphalt concrete pavement for the highway according to the Guide [13].

Figure 5. Fatigue failure of asphalt concrete pavement for the highway according to the Guide [13]: (a) low level; (b) middle level and (c) high level.

Figures 4 and **5** show the photos from the Guide [13], which demonstrate visually the levels of the fatigue failure for the asphalt concrete pavement under the adopted classification.

As it is seen, contrary to the Kazakhstan Guide, the American Guide identifies the fatigue cracks separately from other types of cracks and three levels have been established for their development. Another American standard document [14] subdivides the fatigue cracks into two types: surface-down fatigue cracking and bottom-up fatigue cracking; admissible limit values have been shown for these types of cracks for surface-down—1000 ft./mile = 190 m/km and for bottom-up—25–50% of the lane area.

4. Self-organization

The works [15–17] based on provisions of thermodynamics of irreversible processes and nonlinear dynamics (synergetics) show that the asphalt concrete pavement with low-temperature cracks is a specific dissipative structure, which is the form of adaptation for a thermodynamic system to the external conditions and each time, when air temperature reaches the critical temperature of pavement, the crack occurs. This is regularity, determined by collective behavior (self-organization) of structural elements of the asphalt concrete pavement in critical conditions.

In thermodynamics [18, 19], the systems, which exchange their energy and mass with the environment, are considered as open ones, and they are structurally complex. Due to the complexity of open systems, the various forms of structure occur in them in critical conditions. Energy dissipation plays the constructive role in the formation of these structures. To emphasize that I. Prigozhin introduced the term "dissipative structures" [20–23], and H. Haken introduced the term "synergetics" to stress the role of collective behavior for substructural elements in formation of dissipative structures [24, 25].

Prigozhin I. showed that the entropy variation ds for open thermodynamics system can be considered as the sum of two summands [19–21]:

$$ds = ds_e + ds_i, \tag{1}$$

where ds_e is entropy variation, connected with its inflow or outflow; ds_i is an amount of entropy, produced inside a system.

For short, ds_i is simply called "entropy production."

Component ds_e can have as positive sign, as well as negative one depending on the fact if the system receives or give energy as the result of interaction with environment. According to the second law of thermodynamics, entropy production ds_i is positive or equal to zero:

$$ds_i \geq 0, \tag{2}$$

Equal-zero entropy production, that is, $ds_i = 0$ will occur only under condition of balance.

4.1. Benar's effect

It is known that Benar's effect [26–28] is one of the famous examples for formation of dissipative structures in an open thermodynamic system. It occurs at critical difference of temperatures ΔT_{cr} of bottom and upper surfaces of the thin layer of the viscous liquid (for example, in silicon oil) in a dish, heated from below. When reaching T_{cr}, the behavior of the liquid varies dramatically—convection occurs, and the liquid is divided into hexagonal cells (**Figure 6**). The new structure is created by joint cooperative molecular motion of the liquid. As it is seen from **Figure 7**, the sharp break occurs for a dependence of heat transport rate dQ/dt on temperature difference ΔT at ΔT_{cr} and formation of a new structure occurs. The outflow (export) of entropy is precisely compensated by entropy production inside the liquid up to ΔT_{cr}, and when reaching ΔT_{cr}, the heat transport rate increases due to the convective mechanism of the heat exchange.

4.2. Cell separation

The work of M.V. Volkenstein [26] showed one more example of the formation for the dissipative structure in the open thermodynamics system. This is a cell separation of the living organism.

http://dx.doi.org/10.5772/intechopen.75536

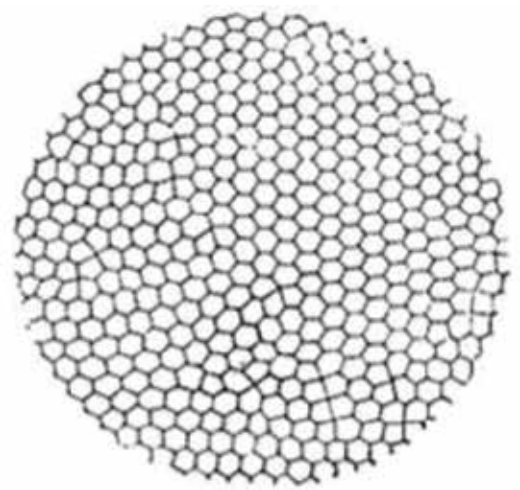

Figure 6. Benar's effect.

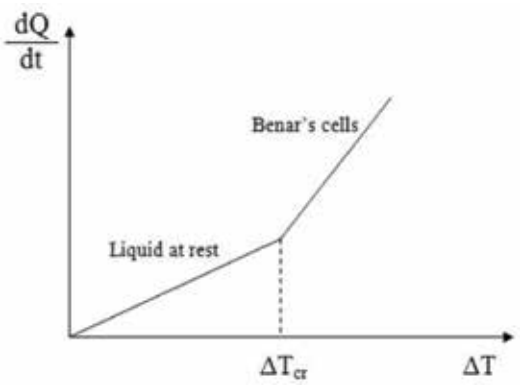

Figure 7. Dependence of heat transport rate on temperature difference.

For the simplicity, the cell is considered as a sphere with radius R. Entropy production inside the cell ds_i is proportional to its volume $V = \frac{4}{3}\pi R^3$, and entropy outflow from the cell ds_e is proportional to the area of its surface $S_{пов.} = 4\pi R^2$. Then, according to the expression (Eq. (1)), we have:

$$ds = A \cdot \frac{4}{3}\pi R^3 - B \cdot 4\pi R^2, \tag{3}$$

where A and B are the parameters of proportionality, which have appropriate dimensions.

The cell grows with the growth of the organism, and radius of the sphere R increases. The cell under the mechanism of self-organization tries to remove the excess of the accumulated entropy. As the entropy production ds_i increases proportionally to the cube of the radius R, that is, R^3, and the entropy outflow increases proportionally to the square of the radius R, that is, R^2, then the gradual accumulation of entropy occurs under the expression (Eq. (3)).

Stationary state is achieved at $R = \frac{3B}{A}$, that is, $ds = 0$. And at $R > \frac{3B}{A}$, that is, $ds > 0$, therefore, at $R_{cr} > \frac{3B}{A}$ (R_{cr}: critical size of the cell) the cell should be separated, otherwise, it will die. The volumes of the mother cell and two daughter cells are similar, and the total area of the surfaces of new cells is bigger.

The abovementioned examples for self-organization in thermodynamics systems—Benar's cells and cell separation can be used further for the explanation of the fatigue failure phenomenon for the asphalt concrete pavement.

Fatigue failure of the asphalt concrete pavement, of course, has been directly connected with the asphalt concrete strength.

5. Asphalt concrete strength

5.1. Bitumen

Bitumen of grade BND 100/130, produced by Pavlodar Petrochemical Plant (PPCP), was used for the preparation of fine-grained dense asphalt concrete in laboratory conditions in this work. Bitumen complies with the requirements of Kazakhstan standard ST RK 1373-2013 [29]. Standard indicators for bitumen are represented in **Table 1**. Content of bitumen in the asphalt concrete was 4.8% by the mass of the dry filler.

5.2. Asphalt concrete

Hot dense fine-grained asphalt concrete of Type B was adopted for test, which satisfies the requirements of the Kazakhstan standard ST RK 1225-2013 [30], and it was prepared with the use of aggregate of fractions 5–10 mm (20%), 10–15 mm (13%), 15–20 mm (10%) from Novo-Alekseevsk rock pit (Almaty oblast), sand fraction 0–5 mm (50%) from the plant "Asphaltconcrete-1" (Almaty city) and mineral powder (7%) from Kordai rock pit (Zhambyl oblast). The main standard indicators for asphalt concrete are represented in **Table 2**. The grading curve of mineral part of hot mix asphalt concrete is shown in **Figure 8**.

5.3. Test methods

In this study, asphalt sample tests have been performed according to the following methods:

1. Determination of asphalt concrete strength at direct tension at various temperatures has been performed in thermal chamber of TRAVIS, manufactured by Infratest GmbH (Germany). Sample tests have been performed at deformation with constant rate 1 mm/min in accordance with European standard pr EN 12697-46 [31]. Samples had dimensions of 5 × 5 × 16 cm.
2. Cyclic (fatigue) asphalt concrete strength at various temperatures has been determined by sample testing with dimensions 5 × 5 × 38 cm in thermal chamber of four-point bending device under European standard EN 12697-24 [32]. Loading frequency was f = 10 Hz. The stress, equal to σ = 1400 kPa, was kept as constant prior to the sample failure.

3. Asphalt concrete samples in the form of beam with dimensions 4 × 4 × 16 cm have been tested at various temperatures on mechanical press with the use of special device under transverse bending scheme according to standard ST RK 1218-2003 [33]. The deformation rate was 3 mm/min.

4. Asphalt concrete sample strength of various shapes (cylindrical and rectangular), various dimensions and at various temperatures at direct compression has been determined by their testing on the mechanical press under standard ST RK 1218-2003 [33]. The deformation rate was 3 mm/min.

Indicators	Unit	Requirement of ST RK 1373-2013	Value of indicators
Depth of needle penetration			
25°C	0.1 mm	101–130	110
0°C		30	37
Penetration index	—	−1.0… + 1.0	−0.82
Ductility			
25°C	cm	≥90	135
0°C		≥4.0	6.6
Softening point	°C	≥43	44.0
Fraas point	°C	≤−22	−30.2
Dynamic viscosity, 60°C	Pa·s	≥120	121.0
Kinematic viscosity, 135°C	mm^2/s	≥180	329.0

Table 1. Main standard indicators for bitumen.

Indicators	Unit	Requirements of ST RK 1225-2013	Value of indicators
Average density	g/cm^3	—	2.38
Water saturation	%	1.5–4.0	3.4
Air voids of mineral filler	%	≤19	15.1
Air voids of asphalt concrete	%	2.5–5.0	3.8
Compression strength			
0°C	MPa	≤13	7.4
20°C		≥2.5	3.5
50°C		≥1.3	1.38
Water resistance	—	≥0.83	0.80
Shear resistance	MPa	≥0.38	0.39
Crack resistance	MPa	4.0–6.5	4.5

Table 2. Main standard indicators for asphalt concrete.

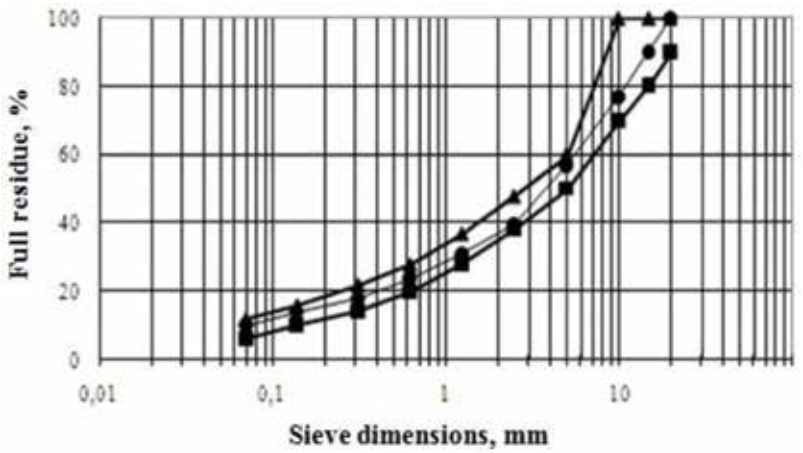

Figure 8. Asphalt mixture grading curve.

5.4. Sample preparation

Asphalt concrete samples of cylindrical shape, designed for direct compression, were prepared under Kazakhstan standard ST RK 1218-2003 [33] by compaction of the asphalt concrete mix in special mold. The samples of rectangular shape and in the shape of beam of various dimensions were prepared in the following way. First, the asphalt concrete samples in the shape of square slab with dimensions 5 × 30.5 × 30.5 cm were prepared by roller compactor (model CRT-RC2S, company Cooper, UK) in accordance with European standard EN 12697-33 [34]. Then, the samples with the shape of rectangular prism of various dimensions were obtained from square slabs.

5.5. Single loading, cyclic and long-term strength of asphalt concrete

Figure 9 represents the graphs, showing the dependence of the asphalt concrete strength at various types of loading—tension, compression and bending. As it is seen, in the considered temperature interval (0–50°C), the asphalt concrete has the least tensile strength, and the largest—at compression. Bending strength occupies the intermediate location between tension and compression. Meanwhile, compression and bending strength of the asphalt concrete with the temperature increase decreases nearly with the similar rate within the whole temperature interval considered, and at tension, the rate of decrease is higher than two times compared with compression and bending strength. It is also seen that the difference between temperature curves of bending strength and compression strength is kept as constant in the whole temperature interval considered and it is equal to, at average, 1.0 MPa. The maximum difference between temperature curves of tensile strength and bending (compression) strength occurs at low temperatures (0–10°C), which is equal to 2.5 MPa (3.5 MPa) and decreases with the temperature increase; these differences at temperature 50°C are equal to 0.8 and 1.6 MPa, respectively.

It is generally accepted that the fatigue cracks occur due to the repeated impact of the tensile stress in the bottom surface of the asphalt concrete pavement [2, 35–39], the more the value of

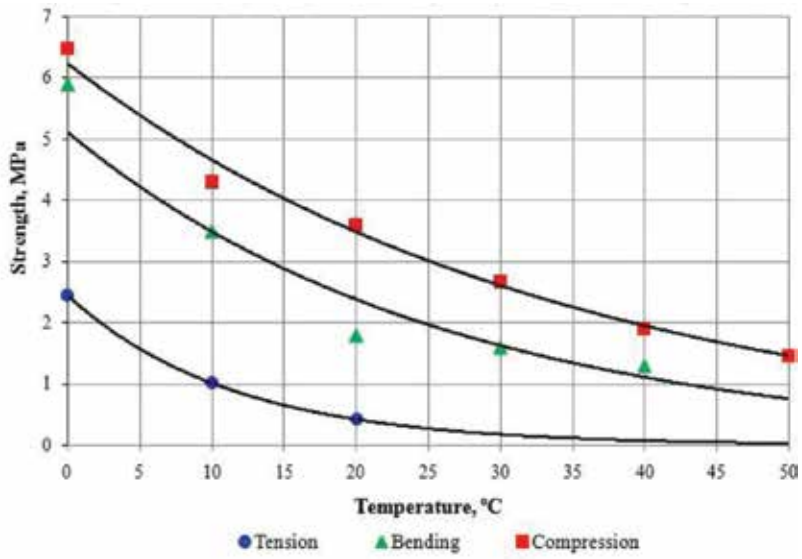

Figure 9. Strength of fine-grained asphalt concrete (BND 100/130, PPCP) at various types of stressed condition.

which at any other equal conditions, the more is the ratio of elasticity modulus of the asphalt concrete layers to the elasticity modulus of the under layers of the pavement base and subgrade soil [10, 40]. It is considered that the abovementioned ratio of elasticity moduli in pavement structure is the biggest one in the spring season, when the upper part of subgrade has been defrosted and loosened, and the asphalt concrete pavement has a big stiffness due to the relatively low air temperature, which is within 0 and +10°C [2, 41–43].

As it is seen from **Figure 10**, namely within the temperature interval 0 and +10°C, the difference in the asphalt concrete tensile strength and bending strength (compression) is the biggest one!

Figure 10 shows the graphs of cyclic strength for fine-grained dense asphalt concretes at bending and tension at the temperature of 20°C. The upper graph has been constructed at testing of asphalt concrete samples under scheme of bending on the four-point bending device in Kazakhstan Highway Research Institute, and the bottom one has been constructed according to the experimental data, obtained in the University of North Carolina State (USA) at direct tension [44]. It is clearly seen that the cyclic strength of the asphalt concrete at bending is considerably higher than at tension. Similar regularity can be seen on the curves of the long-term strength of the asphalt concrete, as shown in **Figure 11** [45, 46].

Thus, single loading, cyclic and long-term strength of the asphalt concretes at tension is considerably less, than at bending and compression.

To answer the question: "Does the asphalt concrete strength depend on the tested sample dimensions at compression?", the test of samples for the fine-grained dense asphalt concrete of type B (BND 100/130) has been performed for direct compression. The thickness of all the samples was similar and equal to 5 cm, and the length and the width of the samples had the values

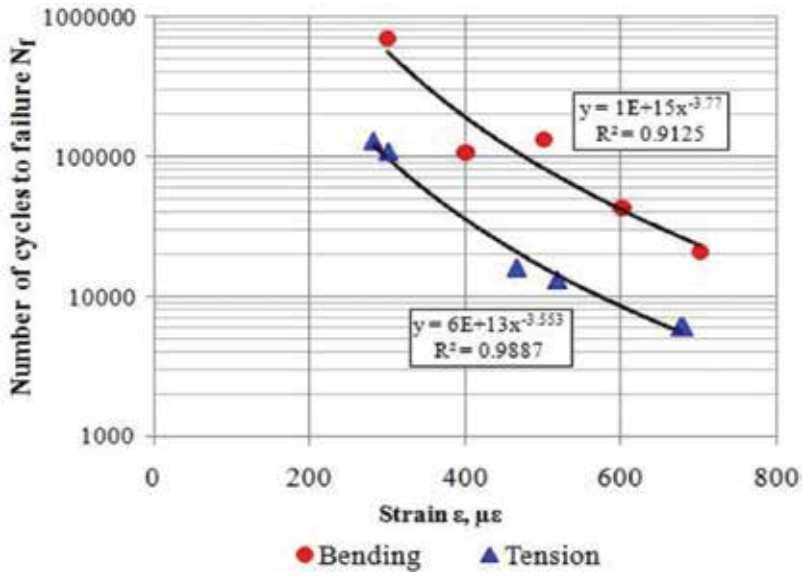

Figure 10. Cyclic strength of the asphalt concrete at bending and direct tension at the temperature of 20°C.

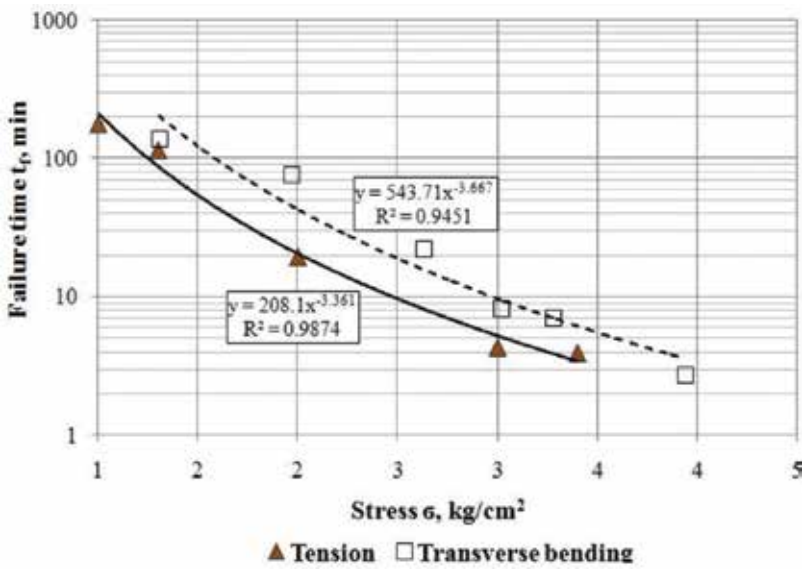

Figure 11. Long-term strength of the fine-grained asphalt concrete of type B (BND 60/90) at transverse bending and direct tension.

equal to 2, 5, 7, 10, 12 and 15 cm. The test has been performed at the temperatures of 0, 10 and 20°C. Three parallel tests have been performed at each temperature and dimensions of samples.

As it is seen from **Figure 12**, the asphalt concrete strength at compression depends considerably on sample dimensions. The biggest strength occurs at the temperatures of 10 and 20°C

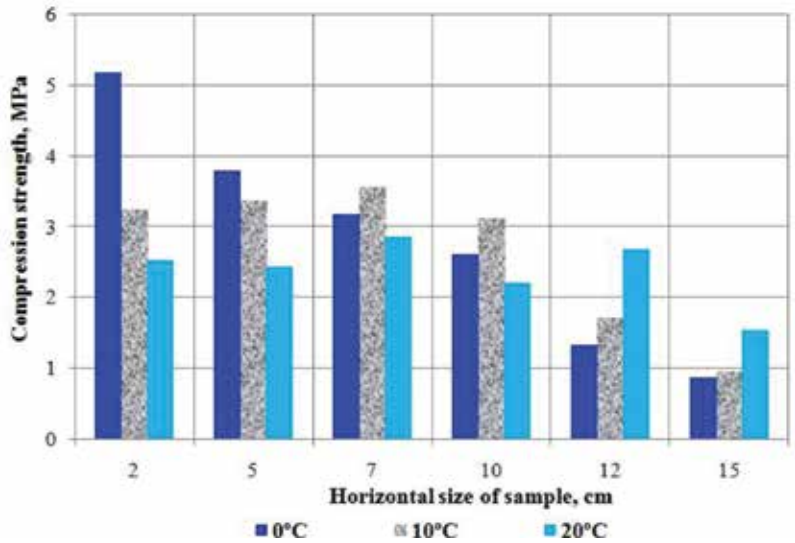

Figure 12. Compression strength of the fine-grained asphalt concrete samples of type B (BND 100/130, PPCP) of various dimensions at different temperatures.

with the length of sample side equal to 7 cm, and the strength increases almost linearly at the temperature of 0°C with the decrease of sample dimensions.

These results serve as the reliable explanation for gradual decrease of the horizontal dimensions of the asphalt concrete pavement cells with progressing of its fatigue failure.

5.6. Residual strength of asphalt concrete

The fatigue crack on the asphalt concrete pavement occurs when it almost completely lost its tensile strength (tension at bending). Let us raise the question: can such asphalt concrete have residual compression strength? To clarify the issue, we have carried out a special experiment. The same fine-grained dense asphalt concrete of type B (bitumen grade BND 100/130) has been adopted. First, the asphalt concrete samples with dimensions 5 × 5 × 38 cm have been tested on the four-point bending device for bending fatigue to failure (stiffness reduction to 10% of the initial one) at the temperatures of 10, 20 and 30°C. Then, the samples with dimensions

T, °C	Number of cycles to failure N_f			
	Parallel 1	Parallel 2	Parallel 3	Average
+10	5187	4965	10,180	6777
+20	568	512	534	538
+30	565	219	222	335

Table 3. Test results of the fine-grained dense asphalt concrete of type B (BND 100/130, PPCP, f = 10 Hz, σ = 1400 kPa) at fatigue on the four-point bending device.

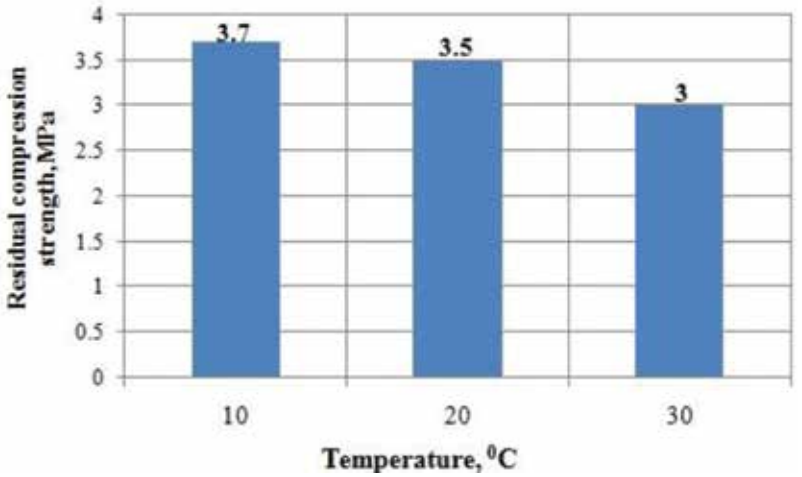

Figure 13. Residual strength of the asphalt concrete at compression after cyclic bending at various temperatures.

5 × 5 × 5 cm have been prepared from these samples, and they have been tested for direct compression at the same temperatures. Three asphalt concrete samples have been tested at each temperature. The results of the initial tests of the asphalt concrete samples at cyclic bending have been represented in **Table 3**, and their further test at direct compression—in **Figure 13**. As it is seen, the asphalt concrete has a high residual compression strength after the cyclic bending to failure, comparable with the strength of a new asphalt concrete (**Figures 9** and **12**).

6. Principle of consequential change of deformation types

As it is known, the self-organization phenomenon occurs in complicated open thermodynamics systems and new structures occur in them in critical conditions such as Benar's cells, separated cells of living organisms, laser ray, and so on. Occurrence of specific dissipative structures in critical low-temperature conditions on the asphalt concrete pavement has been shown in the works [15–17, 47]. The provided above staging of the fatigue failure for the asphalt concrete pavement, possibility in principle for occurrence of dissipative structures in it at critical conditions as a result of self-organization of its structural elements, significant dependence of single loading, cyclic and long-term strength of the asphalt concrete on deformation type (stressed condition) and existence of residual strength at another deformation type after failure allow formulating of a new regularity for the fatigue failure:

Fatigue failure of an asphalt concrete pavement under repeated load impact is realized according to the consequently changing stages in every of which pavement parts function as specific dissipative structures with characteristic deformation type, which interchange in the sequence of: tension-bending-compression.

http://dx.doi.org/10.5772/intechopen.75536

7. Bifurcation

The principle of consequential change of deformation types at fatigue failure for an asphalt concrete pavement formulated earlier can be explained on the basis of provisions for thermodynamics of irreversible processes and nonlinear dynamics (synergetics).

In short description of the examples for dissipative structure occurrence—Benar's cells and cell separation, it has been mentioned earlier that the action of systems in critical conditions in both cases is a benefit for them: liquid flow along the hexagonal cells allows including additional convective mechanism of heat exchange with environment; separation of the cell into two saves it from "death."

We also consider that the realization of the fatigue failure according to the consequent stages, changing deformation type from "tension" into "bending" and from "bending" into "compression" at the continuous mechanical impact is a benefit to the asphalt concrete pavement, as:

1. The asphalt concrete strength at bending is bigger than at tension, and at compression, it is bigger than at bending.
2. Residual strength of asphalt concrete at compression is relevant after its failure at deformation under the scheme of bending (tension).

Such staged failure with consequential change of deformation type prolongs the existence time ("life cycle") of separate parts of the asphalt concrete pavement.

The formulated principle can be visually demonstrated by the bifurcation scheme proposed (**Figure 14**).

In thermodynamics and synergetics, it is accepted to consider that the system away from the equilibrium condition acquires new properties. The system in the strong nonequilibrium condition becomes more active and all substructural elements of the system work jointly, consistently, fluctuations are synergized and new structures occur at the critical moment [18–26, 48]. In addition, the system has a choice in critical conditions—what scenario of evolution to follow further.

In accordance with the proposed bifurcation scheme, the asphalt concrete pavement works as continuous medium under scheme of volumetric stressed-deformed condition since the moment of starting of operation to the moment of losing of the tension resistance (0–1). At the time moment of the complete losing of the tension resistance (point 1), the thermodynamics system (substructural elements of the asphalt concrete pavement) has a choice—which thermodynamics branch (branch A and branch B)—to function further. If the system in point of bifurcation chooses the thermodynamics branch A, the parallel cracks occur on the patch lines in point 1, and the asphalt concrete strips work as a long beam between points 1 and 2, and they are deformed under the scheme of bending. The transverse cracks occur in point 2, long asphalt concrete strips are divided into more short parts, each of the obtained parts for the period of

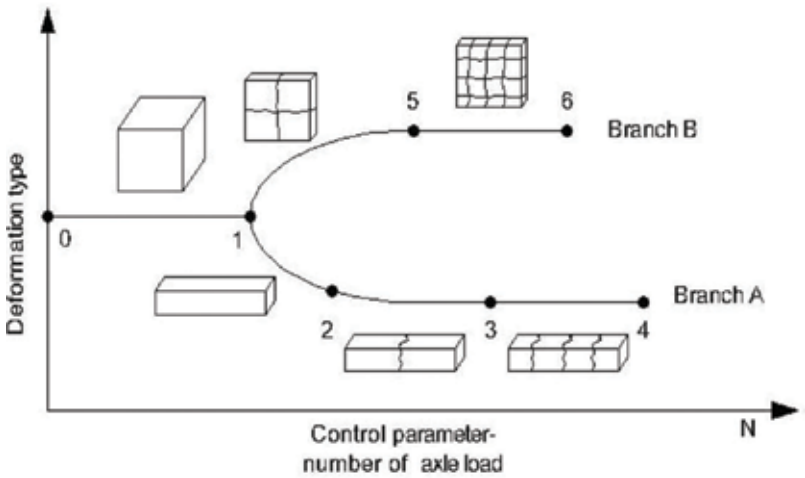

Figure 14. Bifurcation scheme at fatigue failure of an asphalt concrete pavement.

2–3, work as a short beam, and it is also deformed under the scheme of bending. In point 3, the number of the occurred cracks increases and for the period of 3–4, separate failure fragments of pavement work under scheme of direct compression. Complete failure of the asphalt concrete pavement occurs at the time moment 4. The road section of the highway "Karagandy-Shakhtinsk," described earlier can serve as an example of the practical realization for the fatigue failure of the asphalt concrete pavement according to the thermodynamics branch A.

If the system in point of bifurcation 1 chooses the thermodynamics branch B, then, first, the transverse cracks occur on pavement, then longitudinal fatigue cracks occur between them, and for the period of time 1–5, separate pavement blocks function as big and short slabs, and they are deformed under scheme of bending. Additional transverse and longitudinal cracks occur in point 5, grids of cracks become more intensive until each of the pavement fragments is not deformed under scheme of direct compression (time period 5–6). Complete failure of the asphalt concrete pavement occurs in time moment 6. The road section of the highway located in Sharjah city (UAE) can serve as an example of the practical realization for the fatigue failure of the asphalt concrete pavement under the thermodynamics branch B.

8. Conclusion

The results of this study allow drawing the following conclusions for the fatigue failure of the asphalt concrete pavement of a highway:

1. In Kazakhstan, the cracks of various types on the asphalt concrete pavements (fatigue, thermal, reflected and sagging) are not identified separately. The staged character of the fatigue failure was not considered. Maximum allowable characteristics, including the fatigue ones, were not determined as well. In the USA, the fatigue cracks are identified separately

from other types of cracks, three levels for their development have been determined, but the relation is not considered between these levels.

2. Fatigue failure of the asphalt concrete pavement is realized stage by stage. Change of stages for failure occurs under mechanism of self-organization for the substructural elements of the pavement material—asphalt concrete in critical conditions. Similar to the known phenomena of self-organization—Benar's effect and biological cell separation, it is proposed to consider the parts of the asphalt concrete pavement as specific dissipative structures. They work as specific dissipative structures on each stage of the fatigue failure.

3. Comparison of the results for the performed and known tests of the asphalt concretes for determination of single loading, cyclic, long-term and residual strength for tension, bending and compression has shown that the strength at bending is always more than at tension; and it is more at compression than at bending.

4. The determined staged character of the fatigue failure for the asphalt concrete pavement, possibility in principle for occurrence of dissipative structures in it, dependence of asphalt concrete strength on deformation type (stressed condition), moreover, its increase in the sequence of "tension-bending-compression," and also the existence of residual strength for the asphalt concrete at compression after failure at tension have served as a basis for formulating of a new regularity for the fatigue failure: *fatigue failure of an asphalt concrete pavement under repeated load impact is realized according to the consequently changing stages in every of which pavement parts function as specific dissipative structures with characteristic deformation type, which interchange in the sequence of tension-bending-compression.*

Author details

Bagdat Teltayev

Address all correspondence to: bagdatbt@yahoo.com

Kazakhstan Highway Research Institute, Almaty, Kazakhstan

References

[1] CN RK 3.03-19-2006. Design of flexible pavements. Astana; 2007. 87 p

[2] Ivanov NN, editor. Design and Calculation of Flexible Pavements. Moscow: Transport; 1973. 328 p

[3] Hveem FN. Pavement defections and fatigue failures. Highway Research Board. Bulletin 114

[4] Saal RNJ, Pell PS. Fatigue of bituminous road mixes. Kolloid-Zeitschrift. 1960;**171**:61-71

[5] Taylor IF, Pell PS. Could fatigue be a problem in flexible pavements? Roads and road Construction. 1969;**47**(560):236-243

[6] Monismith CL, Secor KE, Blackmer W. Asphalt mixture behavior in repeated flexure. Proceedings of Association of Asphalt Paving Technologists. 1961;**30**:188-222

[7] Sall AO. Peculiarities of asphalt concrete pavement bending at short-term load. Transactions of SoyuzdorNII. 1965;**3**:19-26

[8] Sall AJ, Zolotaryov VA, Radovskiy BS, Iliyev EB. Design parameters of asphalt concretes as applied to VSN 46-72. Automobile Roads. 1977;**5**:28-30

[9] Radovskiy BS, Rudenskiy AV. Regarding impact of characteristics of the materials structure on their fatigue and long-term strength. Transactions of SoyuzdorNII. 1975;**79**:43-48

[10] Radovskiy BS, Suprun AS, Kozakov II. Pavement Design for Trucks Traffic. Budivelnyk: Kiev; 1989. 168 p

[11] Rudenskiy AV, Kalashnikova TN. Analysis of asphalt concrete fatigue. Transactions of GiprodorNII. Road Construction Materials. 1973;**7**:3-15

[12] PR RK 218-27-2014. Instruction on diagnostics and evaluation of transport maintenance condition of the automobile roads. Astana; 2014

[13] Distress identification manual for the long-term pavement performance program. Report No. FHWA-RD-03-031. Federal highway administration. Georgetown Pike McLean; 2003

[14] Guide for mechanistic-empirical design of new and rehabilitated structures. Final report. Part 3. Design analysis. Chapter 3. Design of new and reconstructed flexible pavements. ARA, Inc., ERES Consulting division; 2004

[15] Teltayev BB. Regularities of self-organization of the low temperature cracking of asphalt concrete pavement. Reports of National Academy of Science of Republic of Kazakhstan. 2015;**4**:40-65

[16] Teltayev BB. Regularities of the increase for the number of cracks on the road asphalt concrete pavement. Report of National Academy of Science of Republic of Kazakhstan. 2015;**5**:35-57

[17] Teltayev BB. Road asphalt concrete pavement as dissipative structure. Report of National Academy of Science of Republic of Kazakhstan. 2016;**2**:11-37

[18] Bazarov IP. Thermodynamics. Saint-Petersburg: Publisher "Lan"; 2010. p. 384

[19] Prigozhin I. Introduction to Thermodynamics of Irreversible Processes. Moscow: Foreign Literature; 1960. 128 p

[20] Glansdorff P, Prigozhin I. Thermodynamic Theory of Structure, Stability and Fluctuations. Moscow: Mir; 1973. 281 p

[21] Prigozhin I. Time, structure and fluctuations (Nobel lecture in chemistry of 1977 year). Successes of Physical Sciences 1980;**131**(2):185-207

[22] Prigozhin I. From being to becoming. Moscow: Science; 1985

[23] Prigozhin I, Stengers I. Order out of Chaos: Man's New Dialogue with Nature. Moscow: Progress; 1986. 432 p

[24] Haken H. Synergetics. Moscow: Mir; 1980. 405 p

[25] Haken H. Synergetics: The Hierarchy of Instabilities in Self-organizing Systems and Devices. Moscow: Mir; 1985

[26] Wolkenstein MV. Entropy and Information. Moscow: Nauka; 1986. 192 p

[27] Klimontovich YuL. Introduction to physics of open systems. Soros Education Journal. 1996;**8**:109-116

[28] Osipov AI. Thermodynamics yesterday, today and tomorrow. Part 2. Nonequilibrium thermodynamics. Soros Education Journal. 1999;**5**:91-97

[29] ST RK 1373-2013. Bitumens and bitumen binders. Oil road viscous bitumens. Technical specifications. Astana; 2005

[30] ST RK 1225-2003. Hot mix asphalt for roads and airfields. Technical specifications. Astana; 2003

[31] PR EN 12697-46. Bituminous mixtures. Test methods for hot mix asphalt. Part 46: Low temperature cracking and properties by uniaxial tension tests. 2004

[32] EN 12697-24. Bituminous mixtures. Test methods for hot mix asphalt. Part 24: Resistance to fatigue. 2004

[33] ST RK 1218-2003. Materials based on the organic binders for road and airfield construction. Test methods. Astana; 2003

[34] EN 12697-33. Bituminous mixtures. Test methods for hot mix asphalt. Part 33: Specimen prepared by roller compactor. 2003

[35] Yoder EJ. Principles of Pavement Design. New York: John Wiley & Sons, Inc.; 1959

[36] Yoder EJ, Witczak MW. Principles of Pavement Design. New Jersey: John Wiley & Sons, Inc.; 1975. 736 p

[37] Birulya AK. Design and Calculation of Flexible Pavements. Transport: Moscow; 1964. 168 p

[38] Batrakov OT, editor. Strengthening of Flexible Pavements. Moscow: Transport; 1985. 144 p

[39] Privarnikov AK. Polydimensional deformation of multilayer base course. In: Stability and Strength of Structural Elements. Dnepropetrovsk. 1973. pp. 27-45

[40] Radovskiy BS. Experimental research of the stress strain behavior of road pavements as the layerwise visco-elastic base course at flexible loading. Applied Mechanics. 1980; **16**(4):131-135

[41] Krasikov OA. Evaluation of Strength and Calculation of Strengthening for Flexible Pavements. Almaty: KazgosINTI; 2006. 308 p

[42] Krasikov OA. Regularities for deforming of flexible pavements. Causes for occurring of deformations and failures. Transport and Roads of Kazakhstan. 2007;**1**:17-21

[43] Vasiliyev AP, Sidenko VM. Maintenance of Automobile Roads and Traffic Management. Transport: Moscow; 1990. 304 p

[44] Zhang J, Sabouri M, Guddati MN, Kim R. Development of a failure criterion for asphalt mixture under fatigue leading. Journal of the Association of Asphalt Paving Technologists. 2013;**82**:1-22

[45] Aitaliyev SM, Iskakbayev AI, Teltayev BB. Experimental research of regularities for creep and long-term strength of the asphalt concrete at cross bending. Bulletin of National Academy of Science of Republic of Kazakhstan. 1998;**1**:32-36

[46] Aitaliyev SM, Iskakbayev AI, Isayev D, Teltayev BB. Regularities of long-term strength for asphalt concrete samples at pure tension. Bulletin of National Academy of Science of Republic of Kazakhstan. 1998;**6**:23-25

[47] Teltayev BB. Regularity of self-organization for asphalt concrete pavement during low temperature cracking. Certificate No. 495 for scientific discovery. Moscow; 2016

[48] Prigozhin I. End of certainty. Time, Chaos and New Courses of Nature. Izhevsk: RDC "Regular and chaotic dynamics"; 2000. 208 p

Chapter 5

The Enhancement of Asphalt Concrete Surface Rigidity Based on Application of Shungite-Bitumen Binder

Podolsky Vladislav Petrovich,
Lukashuk Alexandr Gennadievich,
Tyukov Evgeny Borisovich and
Chernousov Dmitry Ivanovich

Additional information is available at the end of the chapter

http://dx.doi.org/10.5772/intechopen.76877

Abstract

Physical interaction of organic binder depends on bituminous film ability to absorb the mineral particles on the surface. The thick film formation begins with the bitumen amalgamation with mineral powder grains and finishes during the processes of application, seal arrangement and cooling down of asphalt concrete. Active surface centers are on every mineral material and they supply their reactive ability and interaction with bitumen. For proving experimentally and to study the physical and mechanical properties in real operation conditions that were arranged, the blanket was arranged from stone-mastic asphalt with shungite bituminous binder of 500 m long. The monitoring conducted during 3 years indicates that asphalt concrete with shungite binder is subjected to calibration to a lesser degree in comparison with asphalt concrete based on standard powder. For operation reliability of nonrigid road base, it is necessary to estimate and prognosticate asphalt concrete fatigue properties in a blanket. The characterized property appears in such a way that the effect of loads which is significantly smaller than the destructive ones leads to the gradual degradation of fatigue and destruction of the blanket. The results proved that asphalt concrete with shungite bituminous binders has higher operation characteristics.

Keywords: shungite, fullerenes, mineral powder, scan probe microscope, fatigue destruction

1. Introduction

The increase of interrepair period of life duration of road blanket from asphalt concrete is one of the important problems in the road industry. In the conditions of existing trend for the growth of intensity and traffic volume, it is necessary to find new materials and technologies to provide road integrity for the whole period of life cycle. The existing shortage stimulates the finding of the new materials and rock for dolomite and dolomitized limestone replacement during the process of asphalt concrete mixes replacement without their poorer operation quality. One of these rocks is shungite as a unique carbonaceous composite. That is why the research of fine dispersed powder, the substantiation of its application while fabricating asphalt concrete mixes, innovation technologies development of construction of blankets with better operation characteristics is an actual problem.

The high-cost of dolomite mineral powder and stable tendency to its rise stimulate the finding of new materials and technologies which can be used without asphalt concrete operation abilities deterioration.

Shungite is a black rock (flaky stone) from the field near Shunga. Strong strata of this mineral go out onto the shores of the lake Onega near the Tolvuya settlement. There are known five fields: Nizkoozyornoe, Shungskoe, Vikshozerskoe, Myagkozernoe and Krasnaya Selga, the raw materials of which were used for shungite production as a light filler for bitumen.

Shungite is a unique rock consisting of amorphous carbon. It is very active in redox reactions, silicon dioxide, ferric oxide, cobalt, vanadium, titanium and other elements.

Antimicrobial properties of shungite were known even in the seventeenth–eighteenth century that is why Russian tsar Peter I ordered the soldiers to drink water from the vessels with the piece of flaky stone in them.

American professor Semyon Tzipursky from Arizona University determined the uniqueness of carbon in Karelian shungite where it is evenly distributed as conglomerations of 200–300 angstrom. Therefore, they are able to migrate into water in appreciable volumes especially from powder shungite. According to the radiocarbon analysis, shungite age is about 2 billion years.

Carbon (C) from the fourth group of the periodic table is the only element for which valency and coordination number coincide. Thanks to this peculiarity, carbon is able to form the compounds practically with any atoms number in the chain in which there can be any numbers of multiple bonds at any combinations.

The work by Robert F. Curl and Richard Errett Smalley is of great importance. There, a hollow carbon molecule is described as cluster with 60 atoms in it [1]. Theoretically, the structure of 60 atoms (C_{60},) is calculated. The most stable structure of spherical shell is the combination of pentagons and hexagons. Under thermal graphite decomposition, there was synthesized a new substance, the molecules of which have spherical form. So there appeared fullerenes. Different compounds of fullerene molecules with hydroxyl groups were synthesized. Diagram of fullerene molecules is given in **Figure 1**. Fullerene is named by Buckminster Fuller who

http://dx.doi.org/10.5772/intechopen.76877

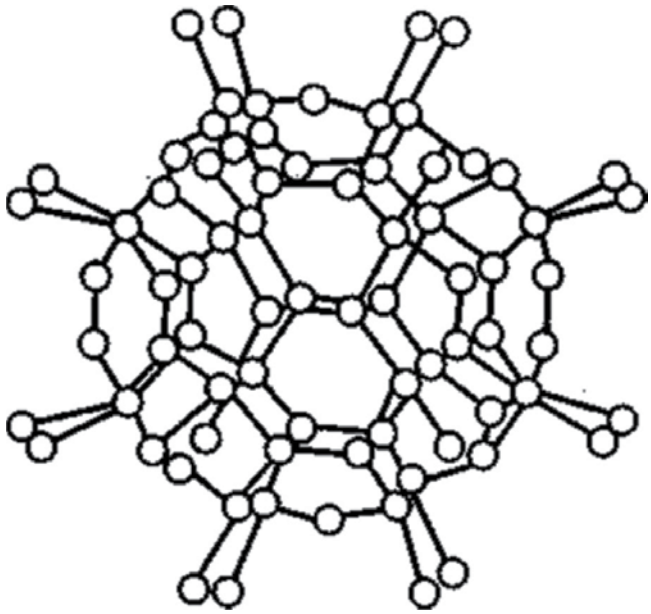

Figure 1. Schematic structure of fullerene is molecule C_{60} with affixed to it radicals (OH).

applied such forms while constructing dome-shaped structures [19]. Schematic structure of fullerene is molecule C_{60} with affixed to it radicals (OH). It is demonstrated in **Figure 1**.

There is a real possibility to obtain different organic compounds based on fullerenes in different spheres of man activity. Particularly, the researches of shungite affecting asphalt concrete surface operating performances are conducted in Voronezh State Technical University (Russia) [2–8].

The attention of the scientists from different countries to the new road construction materials can lead to the appearance of new carbon containing technologies based on fullerenes and graffenes and spreading our conceptions which will influence the civilization development.

2. Researches of materials surface on scanning tester microscope

The effect of shungite mineral powder particles surface nature on asphalt concrete binding agent performances is done by scanning tester microscope NanoEducator. It is for visualization, diagnosis and modification of substance with micro- and nanodimensional level of spatial resolution.

The complex of scanning tester microscope NanoEducator consists of measuring head of scanning tester microscope, electronic block, video camera, connecting cables, computer, eatching probes and also a set of test samples, expendable materials and toolwares. Software Mac OS X is used.

Main characteristics of C3M NanoEducator are presented in **Table 1**.

Characteristics	Quantitative characteristics
Scanning mode	ACM, CTM, lithography
Scanning area	70 × 70 × 10 mkm
Spatial resolution X-Y Z	~ 50 nm ~ 2 nm (depends on radius of probe curvature)
Minimal scanner step	10 nm
Scanning carrent	100–200 nm
Radius of probe curvature	10–100 nm
Time of scanning	30–40 min (depends on scanning area)
Time of set-up	Not more than 10 min
Tested sample size	12 × 12 mm
Sample height	Not more than 5 mm
Environment temperature температура	25 ± 5°C
relative humidity	Not more than 60%
Atmospheric pressure	760 ± 30 mm. of mercury column.
Electric network voltage	220 B
Frequency	50 Hz
	grounding

Table 1. Main characteristics of CZM (C3M) NanoEducator.

Fine powder from limestone, shungite and bitumen binding up to 70 μm was analyzed on the first stage [8].

Samples for scanning were prepared in the following way:

- dispersed powder-like material spreading on an adhesive tape. Before testing there were applied test metering lattices of the height from 21 to 500 nm ((± 1.2–2.5 nm) and the period of 3.0 ± 0.01 μm.

Then, the sample is fixed to the magnetic padding and placed on the magnetic table in the measuring head. After that, the area is chosen for investigation and the surface is scanned.

The state of mineral particles surface plays a great role as the chips, defects and microcracks promote the stronger internal frictions and consequently the better interaction of organic binding and mineral powder.

Mineral powder plays a role of asphalt concrete structure forming component which provides the transmission of voluminous bitumen into film state. Together with bitumen it forms asphalt concrete binding agent substance.

As a result of the analysis, it was determined that limestone powder (**Figure 2**) is characterized with compound surface relief by alternation of peaks and depressions with heights difference from −371 to +429 nm on the scanning area of 8.5 × 8.5 μm. Some evident peaks (light areas)

http://dx.doi.org/10.5772/intechopen.76877

and depression zones (dark areas) are observed on the surface under research. The surface unevenness is 0.43 μm. Fractal dimensionality of surface D is 1.73. The structure of shungite surface (**Figure 2** – limestone powder in 3D picture) has less compound relief on the area of 0.46 micromicrone and height difference from −342 to +457 nanomicrone. Shungite surface in 3D is shown in **Figure 3**.

Such structural nature indicates the more dense powder nature and its high value of specific surface and particles aggregation.

The structure of shungite surface has less compound relief on the area of 0.46 micromicrone and height difference from −342 to +457 nanomicrone. Surface fractal dimensionality D = 1.43.

Such nature of the structure indicated that the powder has more dense structure, its specific surface and particles aggregation is high.Bitumen has rather even uniform surface without any defects in structure (**Figure 4**). The scan sample size is 9.5 × 9.5μm, heights difference is from −821 to 820 nm. Fractal dimensionality of surface is D = 1.97. Bitumen surface in 3D is demonstrated in **Figure 4**.

Composite systems are studied on the second stage. The results of scanning show the interaction of shungite and organic binding agent (**Figure 5**). The results of the research by Chernousov D.I. testify the fact, that shungite with its high adsorptive activity relative to organic binding agent promotes its structurization. Bitumen particles penetrate into shungite porous space and fill it.

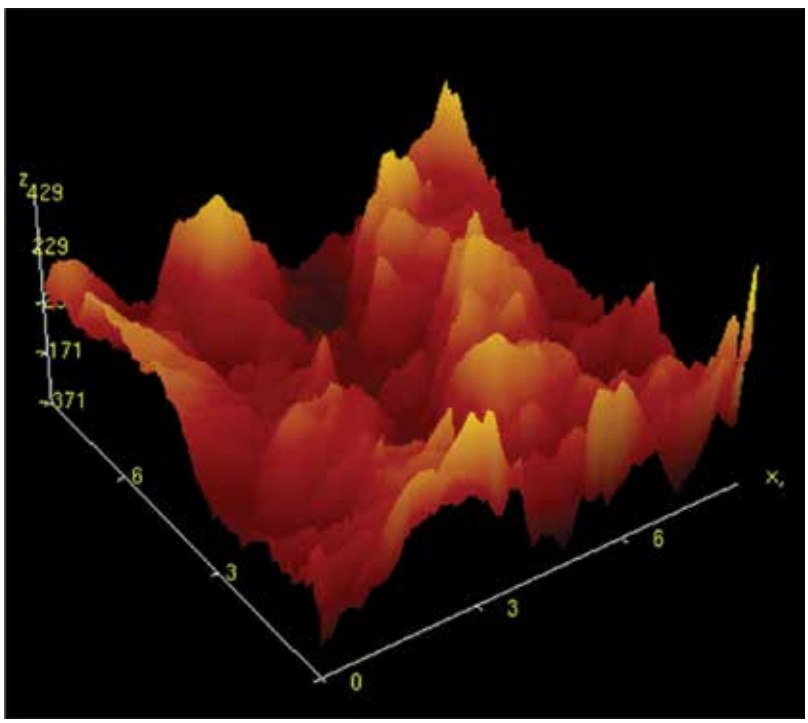

Figure 2. 3D picture of limestone powder. Surface fractal dimensionality D = 1.43.

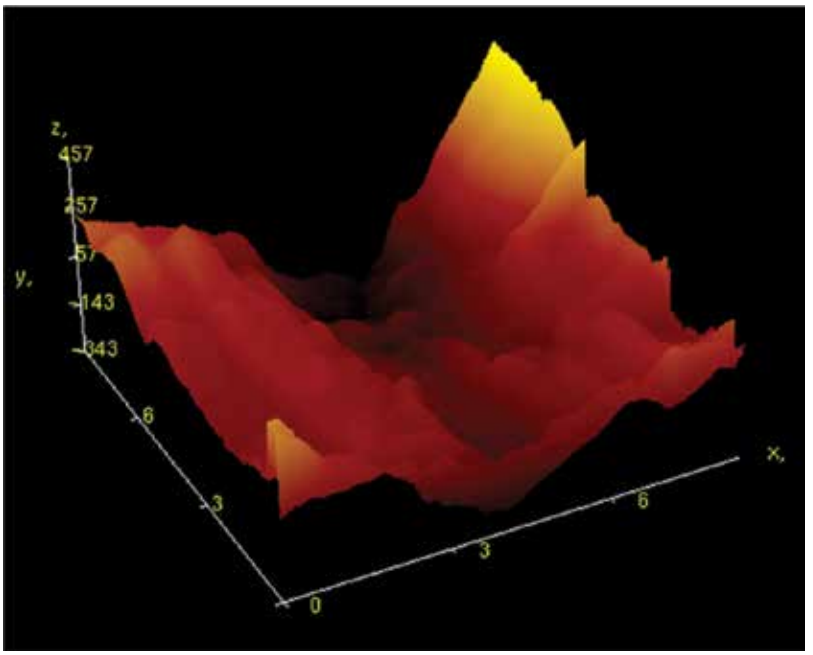

Figure 3. 3D picture of shungit surface.

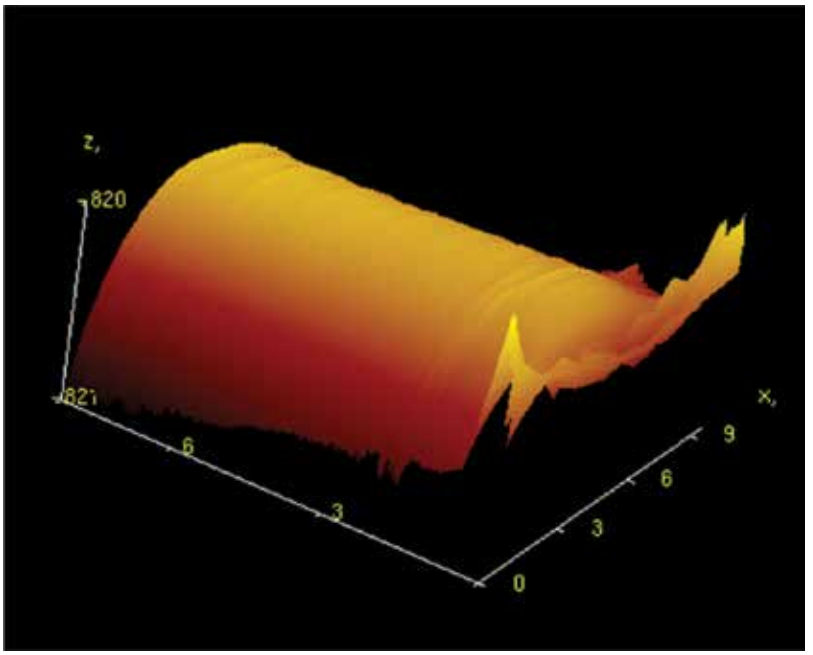

Figure 4. 3D picture of bitumen surface.

http://dx.doi.org/10.5772/intechopen.76877

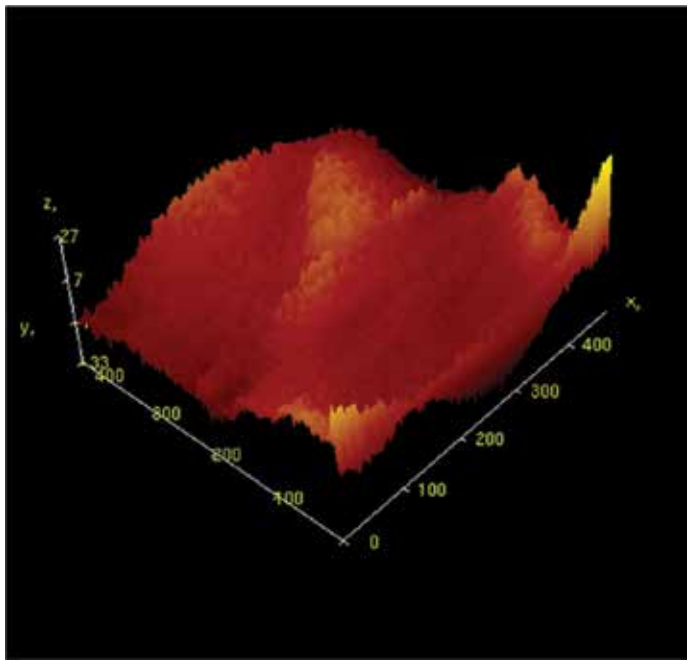

Figure 5. 3D picture of the composite "bitumen-shungite surface".

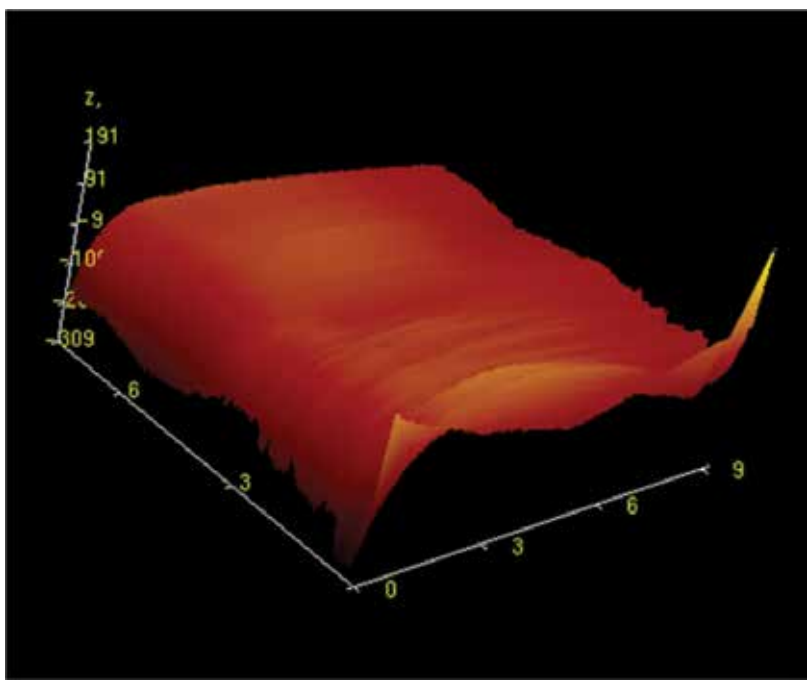

Figure 6. 3D picture of the composite "bitumen-lime stone" surface.

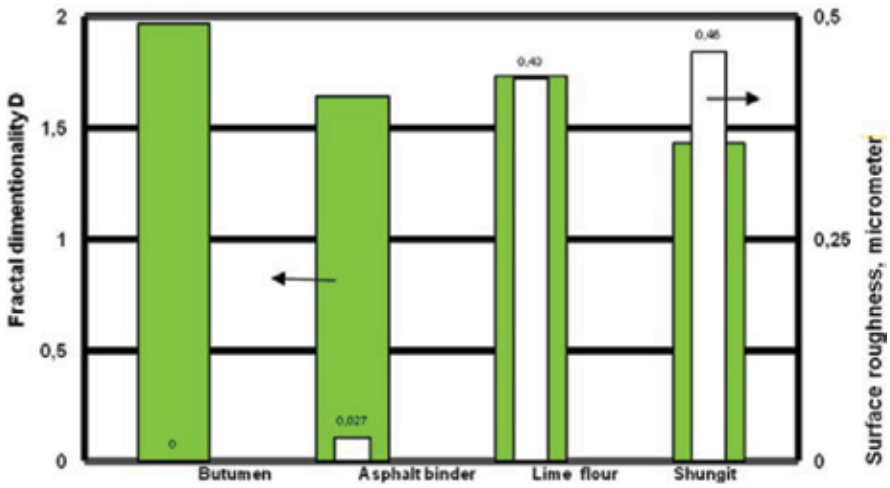

Figure 7. Correlation of the surface roughness and fractal dimensionality characteristics.

Thus the maximal degree of roughness of asphalt concrete binding agent with shungite is 0.027μm (the scan size is 5.0 × 5.0 μm). Fractal dimensionality of the surface is D = 1.64. Composite "bitumen-shungite" surface in 3D is presented in **Figure 5**.

The less surface roughness the nearer the value of surface fractal dimensionality to the criteria "2" that is the material is more dense and homogeneous. Composite "bitumen-lime stone" surface in 3D is given in **Figure 6.**

Correlation of the indicators of the surface roughness and fractal dimensionality characteristics is shown in **Figure 7**.

3. Comparison of reactive ability of shungite and lime stone powders during amalgamation with bitumen

Mineral powder together with bitumen form oriented bitumen layers on mineral grains. These oriented bitumen layers are developed in different degrees. These layers are followed by free bitumen. The qualitative structure of bitumen changes occur in oriented layer as a result of the adsorption processes and bitumen or its separate components diffusion deep into mineral material.

Adsorption is the concentration of substances on a surface or inside a solid body. Not less than two components take part in the process of adsorption.

The nature of such interaction is conditioned not only by the group bitumen structure but also by the properties of mineral powder, its chemical mineralogical composition, grains form, structural peculiarities and surface nature.

http://dx.doi.org/10.5772/intechopen.76877

Active surface centers are on the surfaces of any mineral material. They condition their capacity of reaction and take part in the interaction with organic binding agent.

The presence of the active centers which can absorb practically all organic compounds existing in bitumen provides strong adhesion contacts between binding agents and mineral materials surface.

Chemisorptions are substances adsorption from the surrounding environment by liquid or solid body. It is accompanied by the formation of chemical linkages. Absorption is considered as a substance chemical adsorption by solid body surface that is as chemical adsorption. At chemisorptions there is a linkage formed between atoms (molecules) of adsorbent and adsorbate. Therefore, it can be considered as chemical reaction which is limited by surface layer.

Interaction of binding agents and mineral materials is the most fully appeared during chemisorptions processes taking place on the interface. Herewith the binding components diffuse into pores spaces of mineral materials and there is a physical adsorption of binding surface film which adheres to the stone materials.

In the very work, the reactive properties of the mineral material were considered according to the bitumen amount adsorbed from benzene solutions [9].

The amount of bitumen adsorption from benzene solutions on the surface of mineral powders was defined by the following method:

Bitumen solutions were prepared on the pure chemical nonpolar benzene of four different concentrations: 1, 3, 6, 9 g/l. Weights of tested powders of 5 g each were put into with ground-in stoppers glass flasks of 200 ml capacity and then they were covered with 50 cm^3 of benzene solutions of designed concentrations and agitated on a special plant for an hour.

After agitating, the flasks with the contents were left alone for 24 h. Then the part of the solution was taken out from the flasks and the bitumen concentration was determined by photometer KFK-3 (КФК-3).

The absorption was calculated by the formula:

$$A = \frac{(C_0 - C) \cdot V}{1000 \cdot m} \quad (1)$$

where

Co – initial concentration, kg/m^3;

C – equilibrium concentration, kg/m^3;

V – solution volume, m^3;

M – mineral powder mass, kg

The amount of bitumen chemically connected with the powder surface was defined according to the difference of adsorption and adsorbed bitumen values.

Desorption were conducted by the following method:

The powder left after measuring of adsorption value was covered by 50 sm^3 of pure benzene and agitated on a special plant for an hour. The flasks were left alone for 24 h. After that the samples were taken and the bitumen concentration was determined by photometer KFK-3 (КФК-3).

According to the amount of the powder left on the mineral powder surface, it is possible to reason about the powder surface activity.

The conducted experiment allows to estimate the adsorption properties of the under test mineral materials. The results of the investigations are given in the **Figure 8**.

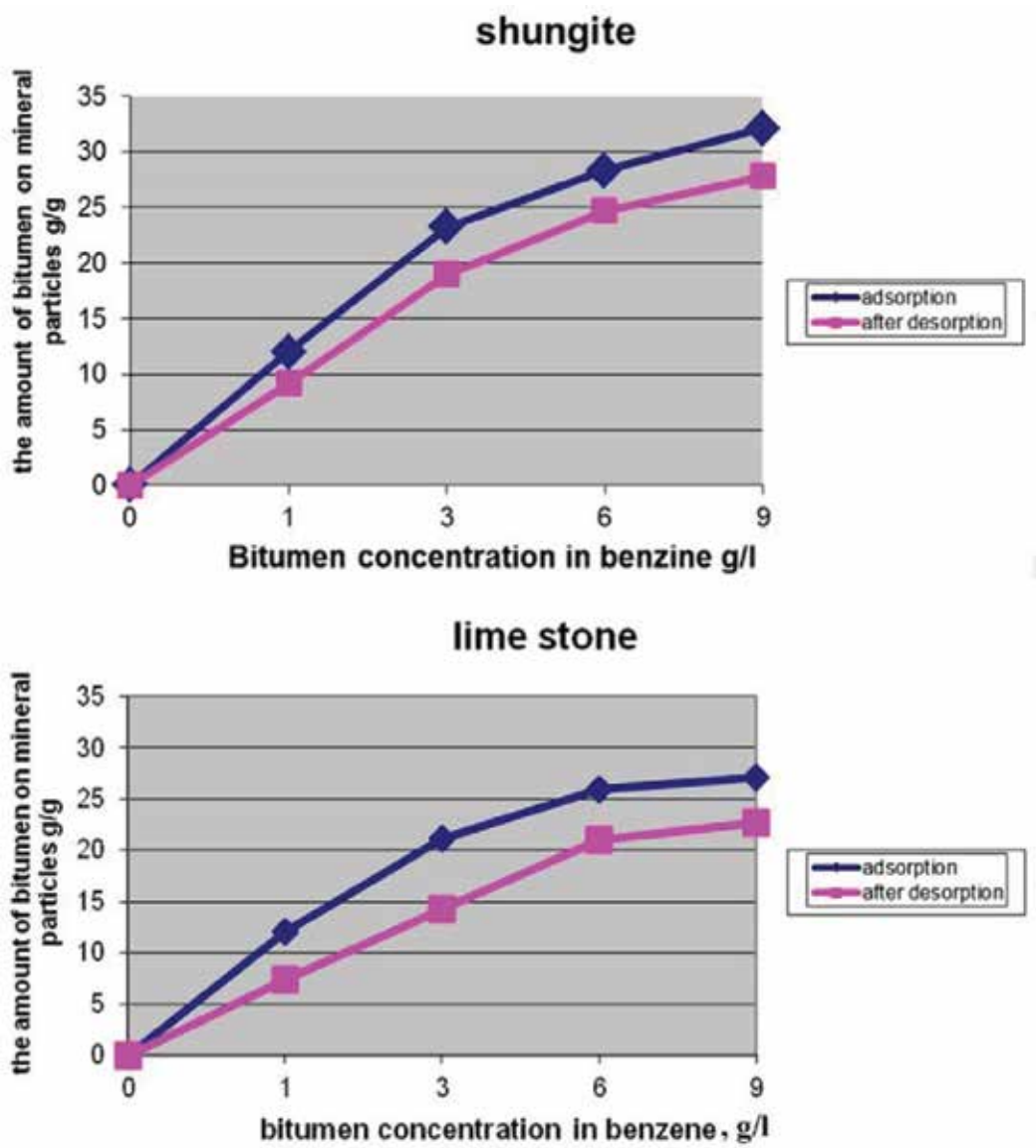

Figure 8. Adsorption–desorption of bitumen on shungite and lime stone surfaces on benzene solutions.

The bigger amount of bitumen is adsorbed on the shungite mineral powder surface than on the lime stone material surface. It was the same at the primary absorption and after the adsorption with benzene. For example, 19 g/g of bitumen are absorbed on shungite surface at bitumen concentration in benzene solution of 3 g/g but 14 g/g of bitumen are absorbed on a lime stone surface, respectively.

The influence of mineral powders on the bitumen structure changing after its desorption from the surface was researched by the spectroscopy method. This method allows investigating mechanism of powders interaction with bitumen, revealing the changes in its structure after adsorption on the mineral powder surface.

It was determined that after bitumen desorption from the shungite surface insignificant amount of organic compounds were left in binding agent. Therefore, they were adsorbed on the surface of shungite mineral powder while their great part on the surface of mineral powder from lime stone was desorbed with benzene. **Figure 8** demonstrate adsorption–desorption of bitumen on shungite and lime stone surfaces on benzene solutions.

The research results of bitumen adsorption and desorption on the surfaces of dispersed materials and bitumen infrared spectrums after the contact with mineral powders show that shungite mineral powder interacts with bitumen more actively than with the lime stone powder (**Figure 8**). The obtained results prove the formation of stable chemisorption bitumen bonds with shungite surface.

4. Infrared spectroscopy

During infrared radiation passing through the substance, the excitation of molecule oscillating movement or their separate fragments takes place. It is observed that the abatement of intensity of the light passed through the sample. The absorption is not in the whole spectrum of incident radiation but only at those wavelengths the energy of which relative to the energy of excitation of oscillations in the molecules under research. Therefore, the wavelengths (or frequency) at which there is maximal absorption of infrared radiation can indicate the presence of these or those functional groups or other fragments in the sample molecular.

5. Shungite mineral powder effect on the asphalt concrete structural-mechanical properties in time

The researchers studied theoretical and practical aspects of shungite mineral powder with account of its interaction with organic binding. The interaction of binding agent with mineral materials depends on chemisorptions processes on their interface. The strength of chemiadsorption bonds between bitumen and mineral powder depends not only on the chemical impact of the bitumen and mineral powder components but also on the mineral powder particles surface state, studied with the microscope (C3M) NanoEducator.

The higher shungite mineral powder porosity than limestone promotes the concentration of the considerable amount of resin in surface microspores. But some amount of oils penetrates the material because of the selective diffusion. That is why structured bitumen films on the shungite particles surface have strong cohesion with them.

Porous filler in shungite bitumen binding agent composition provides the lower temperature of the surface cracking. The tensile strength in such a composition is rather higher than the standard asphalt concrete tensile strength based on dense filler as the friction between the particles is higher due to the greater roughness and specific surface of shungite particles.

The presence of shungite bitumen binding agent in asphalt concrete mix allows increasing surface fracture strength. It is because the chemical activity of shungite particles after their pores filled with bitumen light fractions minimizes internal tension and improves thermal stability of the material.

Shungite particle porosity has better developed specific surface of different mix components as during dry mixing of mineral materials before their integration with bitumen the small mineral powder particles adhere to filler grains. At such processing, a mechanical "modification" of big grains surface which improve bitumen adhesion takes place with them.

Bitumen in thin layer on the mineral particles surface becomes structured, more dense and viscous changing its nature in time. That is why the nature of asphalt concrete mixes based on mineral powder from shungite was defined in different periods at samples conditioning in air: 2, 15, 30, 60 and 90 daily age. Changing of structural mechanical properties of asphalt concrete in time at t + 20°C is presented in **Figure 9**.

The analysis of received results allows determining the following:

in consequence of continuing processes of structure forming the compression strength limits of asphalt concrete based on shungite binding agent at t = 20° (**Figure 9**) and 50°C (**Figure 10**) increases in dependence on sample age conditioning in air. **Figure 10** shows the changing of asphalt concrete structural mechanical properties in time at t + 50°C.

The higher strength limit of asphalt concrete with mineral powder under compression at t = 20 and 50°C than standard asphalt concrete based on lime mineral powder indicates the higher

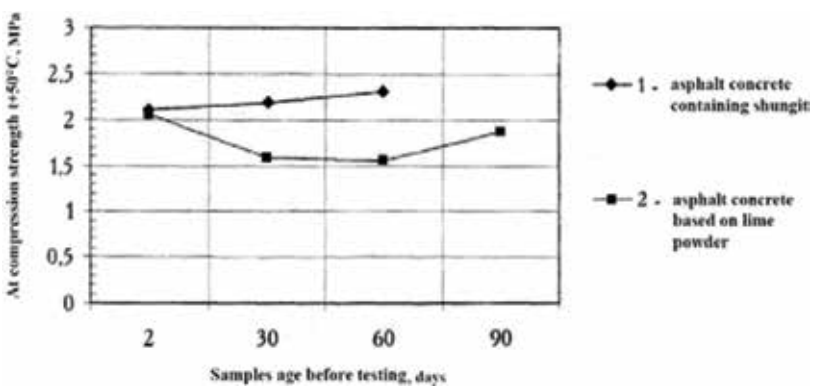

Figure 9. Changing of structural mechanical properties of asphalt concrete in time at t + 20°C.

http://dx.doi.org/10.5772/intechopen.76877

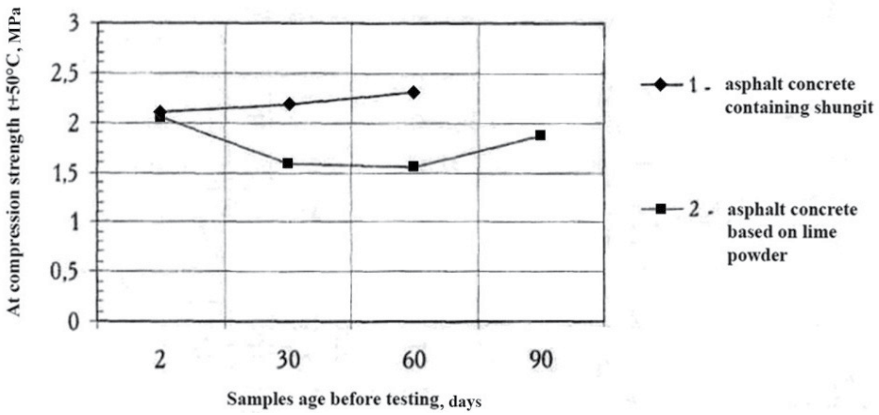

Figure 10. Changing of asphalt concrete structural mechanical properties in time at t + 50°C.

shear strength of asphalt concrete surfaces with shungite bitumen binding agent [4]. It has become usual that the asphalt concrete life service is considerably smaller than theoretically possible according to the abradability conditions. It shows the unconformity of structure – rheological performances of asphalt concrete and its operation conditions. Asphalt concrete during its life duration is affected by different factors: traffic loads, heating, cooling, humidification, and so on. But the normative documents recommend asphalt concrete designing only according to the strength in dependence on traffic load. The possibility of forming shear deformations on asphalt concrete surface in summer time or thermal cracks at negative temperatures is not considered. That is why the deformations excite premature surface destructions more often than the vehicle loads.

Asphalt concrete under different effects is elastic or elastic-viscous, or plastic substance. The theory of elasticity or the theory of plasticity describes only particular cases of asphalt concrete stress state and cannot create the full picture of asphalt concrete operation. Rheology describes asphalt concrete work in deflected mode more objectively.

In rheology, the possibility to describe the stress and deformation in time by differential equations appears. The sphere of these equations definition depends on conditions in which the given materials work. It is suggested that compositional viscous -elastic–plastic material has the total main properties: elasticity, viscosity and plasticity.

While differential equating the main material properties are shown as physically substantiated mechanical models, deformation laws of which are premeditated. In rheology, different simple and complicated models of physical bodies which should correspond to the differential equations situation are used.

While researching rheological characteristics of asphalt concrete based on mineral powders from shungite and limestone, the method by Boguslavsky [10] and Ya. N. Kovalyov was applied. For that target, the height h and the diameter d of asphalt concrete samples before and after the testing and the limit of compression strength were measured.

According to these data, the values of rheological parameters were calculated as follows:

Relaxation time:

$$\Theta = \frac{400 \cdot h \cdot \Delta h^2}{\Delta d^2} \tag{2}$$

Retardation time:

$$\tau = \frac{1000 \cdot \Delta d}{h} \tag{3}$$

Coefficient of elasticity:

$$K = \frac{R \cdot h}{\Delta h} \tag{4}$$

Viscose compliance coefficient:

$$\gamma = \frac{\tau}{K} \tag{5}$$

Viscose coefficient according to Mazwell' s equation:

$$\eta_m = \Theta \cdot K \tag{6}$$

Viscosity of undisturbed structure was defined by the formula.

$$\eta_m = \frac{400 \cdot R \cdot h_1^2 \cdot \Delta h}{\Delta d} \tag{7}$$

Water saturation duration, samples age and freezing cycle number influence rheological characteristics of asphalt concrete were investigated in the road laboratory.

The blanket from crushed stone-mastic mix with shungite mineral powder was constructed in order to satisfy the experiment and study physical-mechanical properties in real operation conditions. Before that, shungite mineral powder of gabbroic-diabase- crushed stone and crushed stone from gabbroic –diabase and bitumen were tested.

The additive based on cellulose filaments Viapor was used as stabilized additive preventing mix segregation and bitumen-shungite binding delimitation at high technologic temperatures. This additive increases the thickness of bitumen film on mineral particles. The mineral proportion of crushed stone-mastic asphalt concrete mix was matched during the research. The composition should provide as follows:

- shear resistance and rut forming resistance at high temperatures;
- water saturation of surface layers at small residual porosity.
- higher crack resistance at surface deformation and under mechanic effects from vehicles.
- high wear resistance.
- uneven surface texture and designed coefficient of adhesion;
- aging resistance.

http://dx.doi.org/10.5772/intechopen.76877

For optimization of composition of crushed stone-mastic and shungite mineral powder, the specific peculiarities of them were considered.

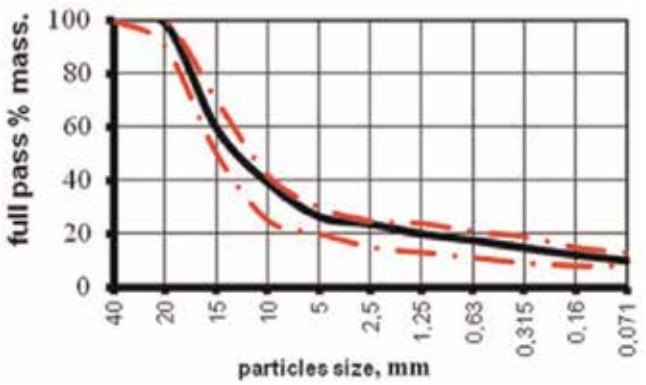

Figure 11. Grain proportion of mineral part of asphalt concrete.

Date of testing	Number of samples	Place of sampling	Layer thickness g(upper /lower) layer)	Surface samples			
			Fact.	Weight of dry sample, g	Weight of dry sample in 30 minutes of aging in water, g	Volume weight g/cm^3	Water saturation, % of volume
1	**2**	**3**	**4**	**5**	**6**	**9**	**10**
01.10.2011 (shungite mineral (powder)	**1**	**1–1 (B)**	5.0	572.20	576.93	2.53	2.36
		1–2 (B)	5.1	920.72	927.76	2.54	3.50
		1–3 (B)	5.0	972.90	976.12	2.58	2.11
	3	**3–1 (B)**	5.3	967.88	970.26	2.57	1.68
		3–2 (B)	5.8	973.60	976.79	2.57	1.26
		3–3 (B)	5.5	1169.82	1171.60	2.56	0.66
	4	**4–1 (B)**	5.0	902.55	905.24	2.58	1.01
		4–2 (B)	5.3	1041.18	1044.03	2.54	1.88
		4–3 (B)	5.1	879.19	884.64	2.54	3.10
01.10.2011 Lime stone mineral powder	**5**	**5–1 (B)**	5.1	868.72	871.10	2.59	1.66
		5–2 (B)	5.0	1152.31	1156.71	2.50	2.46
		5–3 (B)	5.0	871.29	872.98	2.56	1.79
	6	**6–1 (B)**	5.2	909.79	911.48	2.60	1.28
		6–2 (B)	5.7	1420.38	1422.85	2.56	0.81
		6–3 (B)	5.7	1363.83	1366.46	2.55	1.06

Table 2. Physical-mechanical indexes of asphalt-concrete from pilot and control sites.

Shungite	Shungite	Shungite	Shungite	Shungite	Lime stone	Lime stone	Lime stone	Lime stone	Lime stone
30.08.2011	19.10.2012	19.05.2012	03.10.2012	08.05.2013	30.08.2011	19.10.2012	19.05.2012	03.10.2012	08.05.2013
0.390	0.510				0.380	0.450			
0.420	0.560				0.420	0.400			
0.335	0.520				0.44	0.48			
0.382	0.53	0.451	0.389	0.365	0.413	0.443	0.401	0.325	0.309
0.333	0.5	0.437	0.361	0.338	0.379	0.398	0.359	0.315	0.246
0.43	0.56	0.466	0.418	0.393	0.448	0.489	0.443	0.335	0.372

Table 3. The dynamics of adhesion capacity on pilot and control sites.

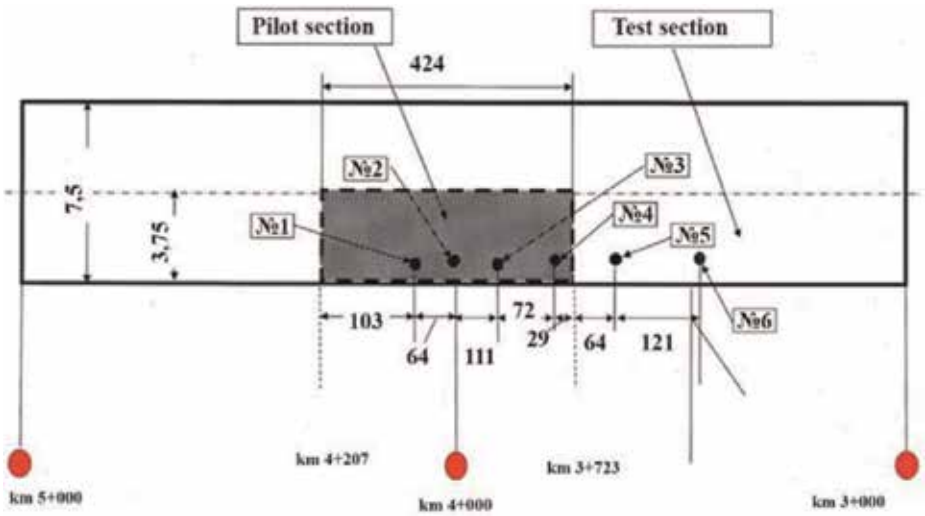

Figure 12. The diagram of sampling on pilot site.

The materials physical-mechanic properties which comply with demands of standard documents were used in asphalt concrete crushed stone-mastic composition.

Granularmetric proportion of crushed-stone asphalt-concrete is demonstrated in **Figure 11**.

After asphalt concrete paving on the pilot site, the blanket has been observed. The adhesion coefficient, evenness, rutting and physical-mechanical properties of asphalt concrete was defined. The results of physical-mechanical properties, adhesion indexes testing are in **Tables 2**, **3**, and the diagram of sampling is in **Figure 12**. Physical-mechanical indexes of asphalt-concrete from pilot and control sites are in **Table 2**.

There is the diagram of sampling on pilot site demonstrated in **Figure 12**.

The coefficient of adhesion is defined at the same time on the pilot site of crushed stone surface with shungite mineral powder and on the control site with lime stone mineral powder. The

http://dx.doi.org/10.5772/intechopen.76877

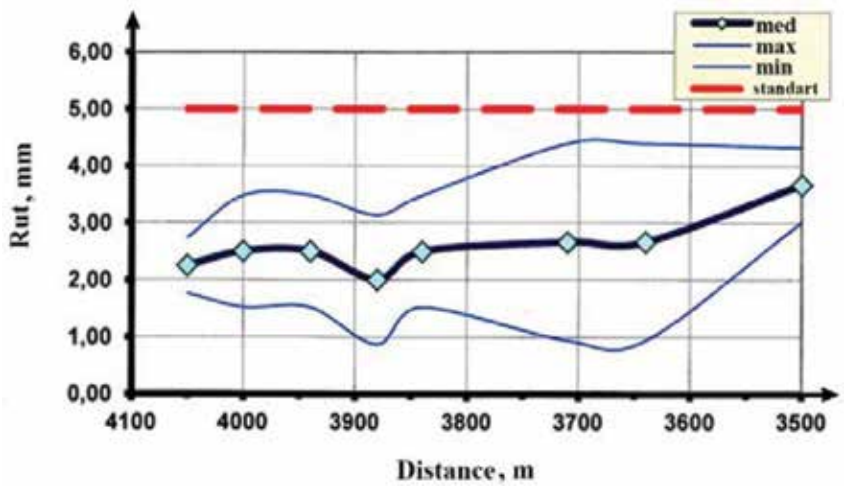

Figure 13. Ruts state on the site with shungite mineral power.

dynamics of adhesion capacity on pilot and control sites are given in **Table 3**, but the ruts state is demonstrated in **Figure 13**.

The monitoring for the state of crushed stone-mastic blanket shows that shungite containing asphalt concrete is in less degree rut prone in comparison with asphalt concrete on lime stone mineral powder.

6. The analysis of traffic load effect on a road blanket

The assessment and prediction of fatigue asphalt concrete properties are the actual problems in assurance of nonrigid road surface reliability.

The effect of fatigue is taken as a process of progressive material destruction by cracks. There are differed three forms of destruction: the beginning of cracks formation; the period of their stable growth and the stage of their intensive growth.

In comparison with the initial period of cracks formation which takes a significant time, the phase of stable cracks growth can be analyzed as the main fatigue process. Cyclic effect of moving vehicles (load) leads to the progressive cracks growing up to the critical depth. A crack increases spontaneously in the third stage which induces the fracture of the material. [11].

The analysis of fatigue performances based on the thermal fluctuation theory of fracture by S.N. Zhurkov shows that fatigue properties of asphalt concrete directly depends on the degree of the plasticity and there is a definite connection between strength and fatigue material properties. There are two different methods of fatigue tests [12]: the test with constant stress amplitude; the test with constant deformation amplitude.

The test of fatigue with constant deformation amplitude is more correct in comparison with the test with constant strain amplitude; as practically, it is not possible to determine the constant stress during the cracks growing and accordingly and the reduction of material area.

Asphalt concrete fatigue fracture in the blanket takes place as a result of cracks formation in the lower tension region and their constant diffusion onto the cover blanket surface. The number of repeated loads necessary for the cracks diffusion onto layer thickness exceeds the number of cycles before the appearance of the first fatigue crack in 20 times. Therefore, the asphalt concrete durability in a blanket exceeds the number of cycles "load-unload" without intervals in which asphalt concrete sample sustains up to fracture in the laboratory in 100 [12] or 200 [13] times.

Operation ability factors of asphalt concrete reliability can be divided into two groups: external and internal.

To the external factors we can refer the environment influence of three types: mechanical, physical-climatic and chemical; to the internal: the indexes of quality, determining the asphalt concrete ability to resist the mentioned types of external one.

The typical fatigue peculiarity is the following: the load factor which is less than the destructive one leads to the progressive durability and degradation of road surface.

Bearing capacity and operation durability of asphalt concrete blanket are more completely characterized by modulus of elasticity and tensile in bending strength.

Dynamic state of road blanket depends on traffic flow concentration and composition and also on the intervals between separate cars.

Traffic loads induce both deflections and oscillations in road blanket are conditioned by momentary elasticity and elastic deflection of road constructions.

While researching bitumen water resistance and adhesion to mineral powders in a laboratory it was proved that bitumen stresses exfoliation from the mineral material surface were comparatively small [14, 15]. In real operation conditions, the additional stresses appearing at traffic movement influence on the wet blanket exceed the thermodynamic ones. Practically, water presses into a blanket in front of the moving wheel and presses out from a blanket after a wheel. The results of such a pumping action are various and difficult for consideration.

At short-term contact of moving wheels with surface, the water pressure in pores of up to 0.05 cm radius is not enough for asphalt concrete fracture but for popcorn mixes it can reach destruction quantity.

If the prolong temperatures are >50°C the deformations of different types appear on an asphalt concrete blanket. The reason is the following: after heat accumulation in asphalt concrete layers, the degradation of bitumen viscosity takes place. According to the second law of thermodynamics (entropy), the grade of the temperature, concentration, barometric pressure always direct from the big value to small one. That is why bitumen starts to move upwards because its concentration is higher inside the asphalt concrete blanket than on the surface. Hereby there is its transition from structured state into the phase of free bitumen. The distance

http://dx.doi.org/10.5772/intechopen.76877

between the mineral material grains increases and the possibility of transmission as a result of wheel load application appears.

It was proved that the mechanism of accelerated fatigue fracture of water saturated asphalt concrete during surface under cyclic dynamic loads is conditioned in certain grade by the appearance of pulse hydrodynamic pressures in water saturated pores of between grains space. Experimental researches of fatigue properties of asphalt concrete while working in the water saturated state show that the service life before the fracture in water saturated state is shorter in 1.5–2.5 times in comparison with the asphalt concrete working in dry state [11, 16]. That is why the formation of pulse hydrodynamic pressures in pores of water saturated asphalt concrete under the moving cars dynamic loads is one of the main mechanisms of asphalt concrete fatigue in watering conditions [14].

7. Previous work reports of dynamic loads on fatigue properties of asphalt concrete

At the car speed of more than 30 km/h the surface load process at the reference point d during a small time interval can be represented as the static load F affecting on the definite blanket volume on the base under the harmonic vibrations. With account of the before mentioned assumption, the authors used the developed in the university (VGASU) method of the prediction of asphalt concrete operational properties based on the results of testing of the beams $4 \times 4 \times 16$ (cm) on the vibration exciter (**Figure 14**).

Vibration exciter provides the production of a frequency and vibrational amplitude from 10 up to 100 Hz and from 0.1 to 5 mm respectively gradually regulated during the operation time. The load onto the sample can change from 2 to 60 kg.

Figure 14. Vibration exciter at the moment of asphalt concrete beams testing.

Analytical dependences able to determine operation period duration under simulation load were taken as the base of method.

The vibrations similar to the harmonic form are modeled on a vibration exciter:

$$A = A_0 \sin(\omega t + \varphi_0) \tag{8}$$

where A – vibrational amplitude at the time moment t:

Ao – maximal amplitude;

φo – initial form.

$\omega = 2\pi f$ - cyclic frequency, where f – vibrational frequency of vibration exciter.

direction of the forces, effecting on asphalt concrete test beam in relaxation stage can be represented in **Figure 14** as:

where F1 – static load weight influencing the asphalt concrete beam.

F2 – elastic force in asphalt concrete beam;

F3 – inertial force during vibration exciter vibrations;

d – arbitrary point of load application.

The process of asphalt concrete fatigue fracture usually has three stages: internal fractures accumulation accompanied by a significant elasticity module reduction; microcracks appearing at small velocity of module elasticity reduction; propagation and progressive development of cracks with strong reduction of elasticity module [3].

The tension acting in the beam section in the bridge span center was calculated by the formula:

$$\sigma = \frac{3P_\partial l}{2bh^2} \tag{9}$$

where P_∂ - dynamic load; l – span between piers; b, h – section size. The value of the relative deformation was defined by the formula:

$$\varepsilon_m = \frac{(n_1 - n_2)}{Km} \cdot 5 \cdot 10^{-6} \tag{10}$$

where n1 и n2 - strain transducer registration for the sample without loading and vibration, and after the loading and vibration; Km– coefficient of strain-sensitivity of a strain transducer.

The values of relative deformation were defined by a strain transducer registrations should be close to the design ones received by the formula:

$$\varepsilon_p = \frac{6fh}{l^2} \tag{11}$$

At adherence to the situation $\varepsilon_p = \varepsilon_m$ the module of elasticity is defined by the formula:

http://dx.doi.org/10.5772/intechopen.76877

$$E_{\text{д}} = \sigma/\varepsilon_m \tag{12}$$

$$\sigma = \frac{3Pl\left(g + 4A_0\pi^2 f^2\right)}{2bh^2} \tag{13}$$

The final formula for dynamic module of elasticity determination is written down as:

$$E_{\text{д}} = \frac{3Pl\left(g + 4A_0\pi^2 f^2\right)K_m}{2bh^2(n_1 - n_2)\cdot 5\cdot 10^{-6}} \tag{14}$$

The assessment of operation reliability caused by operating –climatic effect (T) is implemented by the formula:

$$T = \frac{N_p}{N_{\text{Э}}} \tag{15}$$

where Np - number of asphalt concrete loading cycles up to its dynamic elasticity module abatement in two times; design number of wheels loading application during the year of road blanket service.

$$N_{\text{Э}} = N_{np}K_1K_2 \tag{16}$$

where N_{np} – equated movement intensity; K_1 – coefficient of a car track overlapping; K_2 – coefficient considering portion of design cars in a flow (0.3–0.4).

For the investigation of asphalt concrete cyclic fatigue in a laboratory, the following factors were taken: asphalt concrete water saturation as physical-climatic; aging after heating during 5 h at t 150°C as chemical; asphalt concrete composition formula as internal ones.

Cyclic fatigue under dynamic loads is tested on the specially constructed diagnostic tester in the laboratory providing load application with frequency of 868 min^{-1} in the regime of cyclic bending of the 2.5 × 4 × 16 cm size test beams at the fixed deformation amplitude. The test temperature is 20°C. The fatigue deformation amplitude was registered by the moment of destruction. The deformation amplitude while testing was 0.0021 (the test beam kink was equal to zero).

The use of shungite powder instead of standard mineral powder promotes the growth of asphalt concrete fatigue life especially in the conditions of asphalt concrete water saturation. It may be connected with the higher adhesion of shungite powder.

One of the important properties of asphalt concrete predetermining its durability (during the destruction) is its structural stability in the changing humidity regime and temperature conditions. At water saturation adsorption aqueous layers simplify the formation of new surfaces in asphalt concrete during its deformation reducing the surface energy (Rehbinder's effect). Wedge effect of aqueous layers separating mineral grains and exfoliating bitumen strengthens the destruction effect. The mechanism of accelerated fatigue destruction of water saturated asphalt concrete at surface operation in the regime of cyclic dynamic loads is conditioned by the appearance of hydrodynamic pulsations in filled with water porous. This fact was investigated by Rudensky [17].

Asphalt concrete composition	Aging (Thermal effect)	Number of destruction cycles	
		dry	Water saturated
Granit sieving – 92%, lime-stone mineral powder −8%, bitumen of road oil asphalt 60/90–7.5%	Without heating	14,756	10,416
	After 5 h of heating	17,707	11,488
Granit sieving –92%, shungite mineral powder – 8%, road oil asphalt 60/90–7,	Without heating	17,757	14,322
	After 5 h of heating	20,092	16,297

Table 4. Values of fatigue durability of asphalt concrete samples.

The assessment of asphalt concrete by the method of dynamic effect on the water saturated samples is more corresponding to the operation conditions of the material in road construction than the known methods based on statistic water action. That is why the tests of comparison fatigue of asphalt concrete durability were conducted on dry and water saturated samples. Water saturation of asphalt concrete samples was 1.65–1.66% by volume. Values of fatigue durability of asphalt concrete samples were given in **Table 4**.

The application of shungite material instead of the lime stone mineral powder promotes the growth of asphalt concrete fatigue durability especially in the conditions of water saturation. It connects with high adhesion activity of shungite carbon with shungite carbon containing material [21].

The increase of asphalt concrete fatigue durability with the application of shungite mineral powder as a result of aging (after the heating for 5 h) demonstrates the properties stability under temperature effect. It is clear that it connects with oil migration from pores in carbon containing materials and bitumen film rejuvenation during aging.

8. Asphalt concrete bindings effect

An important structure unit of asphalt concrete that is asphalt concrete binding is generated while mixing mineral filler with organic binding. The nature of asphalt concrete is determined by the quality of the asphalt concrete binding. The properties of the system "bitumen-mineral powder" depend on the properties of binding, chemical-mineral composition and mineral filler dispersion, and also these components proportions [18].

The interaction of bitumen with mineral powder is conditioned not only by the rather developed specific filler surface but also by internal grain surface generated by the branched microspores system. Porous fine dispersed fillers cause strong structuralized influence than dense ones. Micropores differ by the high adsorption potential due to which the significant part of surface active components of bitumen sorbs in them. Therefore, it is possible to suggest that porous mineral fillers will cause strong structuralized influence on bitumen than the traditional materials. It is clear that the interest to porous fillers in asphalt concrete composition is conditioned by this.

http://dx.doi.org/10.5772/intechopen.76877

Mineral powder from shungite (Medvezhjegorskoe deposit) differs from the traditional one from dolomite by bigger porosity of the surface and high developed micropores system and also bitumen of the grade БНД 60/90 of Ryazan НПЗ was investigated. The dispersed raw under study will be correct to test for accordance with the demands [5] asphalt concrete mixes mineral powders. Characteristics of under research fillers properties are shown in **Table 5**.

Mineral powder meets the requirements. But the porosity of the material 20–25% higher than the porosity of lime stone filler and the value of specific surface at the same grain metric proportion is 60–70% higher. So the conclusion is the system of micropores of under research carbon containing raw material is more developed.

The results of the experimental researches of asphalt concrete binding agent. From our point the most informative method of studying the method "bitumen-mineral powder" is the investigation of asphalt concrete binding agent characterized by greater homogeneity of the structure and stability of the properties. Asphalt concrete binding agent was produced from according to the standard method with the before bitumen amount batching. Thus for the mineral powder from shungite the index is 16.2% which is 26% more than traditional lime stone mineral powder has. These data are correlated with the indexes of bitumen proportion in powders. The research results of the physical chemical properties of asphalt concrete binding agent with optimal amount of bitumen are given in **Table 6**.

Coefficient of composite thermal stability and its water resistance are the most interesting among all the data. Therefore, the index of heat resistance of shungite is 14.3% more than while using the traditional mineral powder from lime stone or dolomite. Thermal resistance of mixes and asphalt concrete is characterized by the coefficient of thermal resistance defined as the ratio of ultimate compression strength at t-20°C to the ultimate stress limit at t = 50°C.

As the under research, raw material is porous; the water can penetrate inside the shungite grains and decompose the asphalt concrete binding agent on the bitumen- mineral powder interface if binding agent covers mineral powder surface partially or if the adhesion bonds are weak.

Names of the characteristics	**Mineral powder МП-2**	**Demands of the standard**
	shungite	
Grain proportion, % on mass: Smaller 1.25 mm <0.315 mm <0.071 mm	100 98 80	Not less than 95 from 80 to 95 not less 60
Porosity, %	37	Not more 40
Indexes bitumen capacity, g	48	Not more 80
Humidity, % on mass	0.55	Not more 2.5

Table 5. Characteristics of under research illers properties.

Name of the index	Mineral powder МП-2 shungite	Requirements of established order
Compression strength, М Па: при		
20°C		
20°C in water saturated condition 50°C	4.3	
3.9		
2.7	—	
Water saturation of samples from powder and bitumen mix	0.9	Not less than 0.7
Swelling of samples from powder and bitumen mix, %	1.87	Not more than 3.0
Coefficient of heat resistance	0.63	—

Table 6. Physical chemical properties of asphalt binding agent.

9. Research of structuralized processes in asphalt concrete

The growth of the strength of the samples from shungite is 9.3% compared with the analogical indexes on lime stone [6, 15]. At less density, the growth of strength characteristics in time which attests the process of structurization of asphalt concrete on shungite mineral powder takes place.

This process can be explained from the point of active extraction of bitumen components with mineral powder from shungite. While analyzing the structure of asphalt concrete agent by microscope (C3M) NanoEducator at increase in 1000 and 2000 times (**Figure 15**), it is possible to mention the substance structure vagueness. The following figure present microstructure of asphalt concrete binding agent from (a) shungite (b) lime stone.

It is clear that an original solution of shungite occurs during amalgamation of binder and shungite. Modern image about the material under study is the precondition for such a supposition. It is known that shungite substance is not a simple amorphous carbon but a mix of various carbonic allotropes which have small lattices connected with amorphous carbon [20]. The more so various mixes of compound organic substances are a part of shungite composition. It is 97–99% of water saturated organics of shungite which escapes into the solution together with fullerenes and determine their properties.

Chemical composition of mineral powders from shungite and lime stone is shown in **Table 7**.

10. Conclusions

1. Experimental researches of physical-mechanical properties of asphalt concrete mixes of different types proved the possibility mineral powder from shungite application. So the interaction of bitumen with shungite mineral powder provides the formation of a stable structure of asphalt concrete with the predominance of closed pores.

2. The results of investigation of shungite mineral powder on scan prob. microscope with nanodementional resolution demonstrate the ability of shungite with high adsorption activity in comparison with organic binding promotes its structurization. Together with bitumen it forms the structured dispersed system acting as a binding material in concrete.

3. It is determined that at the result of shungite mineral powder application asphalt concrete has better water resistance and long water saturation properties which provides high corrosion resistance of asphalt concrete carpet in comparison with traditional powder from lime stone rock.

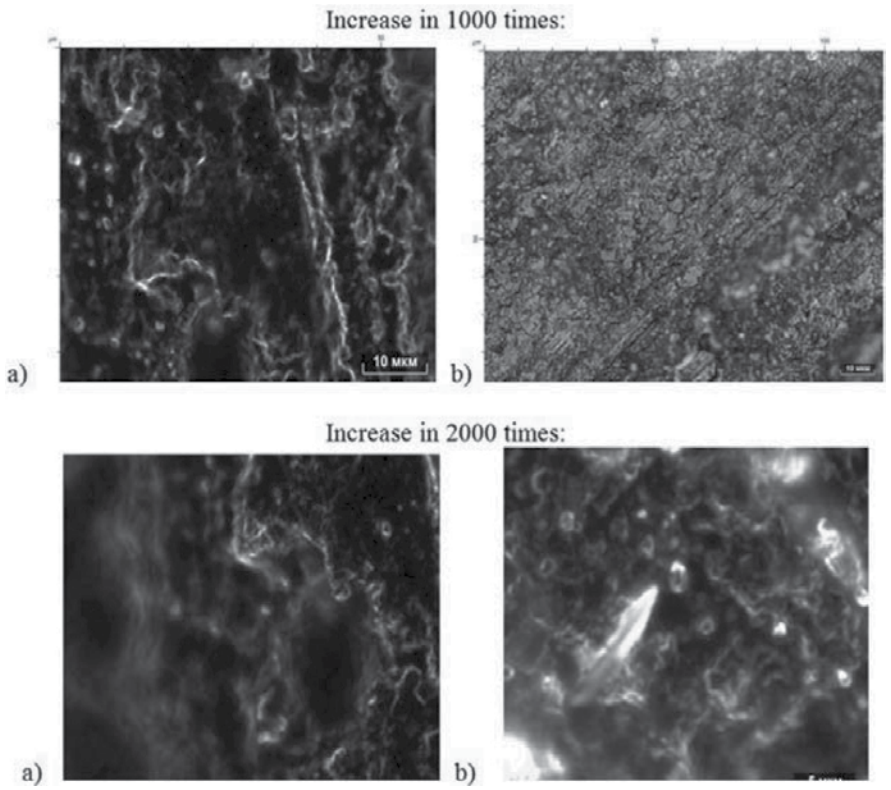

Figure 15. Microstructure of asphalt concrete binding agent from a) shungite b) from lime stone.

Sample	Mass portion, %			
	SiO_2	Al_2O_3	Fe_2O_3	Fe_2O_3
1 (shungite)	45.5	2.3	1.9	1.0
2 (lime stone)	2.1	0.1	1.2	0.8

Table 7. Chemical composition of mineral powders from shungite and lime stone.

4. The use of shungite material instead of lime-stone mineral powder increases the fatigue durability of asphalt concrete especially in the water saturation condition. It connects with the high adhesion activity of shungite carbon containing material.

5. During the process of plot arrangement it was determined that asphalt concrete mix has good placeability and compactability which allows promote designed characteristics of evenness and compacting factor while constructing road carpets.

Author details

Podolsky Vladislav Petrovich[1]*, Lukashuk Alexandr Gennadievich[1],
Tyukov Evgeny Borisovich[1] and Chernousov Dmitry Ivanovich[2]

*Address all correspondence to: tatvikt@mail.ru

1 Department of Road Construction, Operation of Voronezh State Technical University, Voronezh, Russian Federation

2 Stroitelstvo e Expluatatziya Dorog, Solnechnogorsk, Moscow Region, Russian Federation

References

[1] Curl RF, Fullerenes SRE. In the world of science 1991;**12**(1):14-24

[2] Podolsky VlP, Erohin AV. Asphalt concrete resistance with application of mineral powder from carbon consisting materials. Scientific Bulletin of Voronezh State University of Architecture and Civil Engineering. 2008;(9):149-152

[3] Shcherbinina SE, Chernousov DI. Substantiation of application of mineral powder from shungite in asphalt concrete mixes. M.: News in Road Science and Engineering. 2009;**2**:34-35

[4] Podolsky VlP, Chernousov DI. Influence of mineral powder on the changing of asphalt concrete properties in time. International congress. Nauka I innovatzii v stroitelstve. Sovremennye problem stroitelnogo materialovedeniya I technologii. Book 2. Voronezh, 2008;**1**:394-399

[5] Podolsky VlP, Chernousov DI, Tyukov EB, Shiryaeva SM. Influence of different mineral powder on rheological characteristics of asphalt concrete. Bulletin of Central Department of RAACH. Voronezh. 2010;(9):173-184

[6] Podolsky VlP, Chernousov DI. Research of bitumen shungite binding agent on scanning microscope. Voronezh. Scientific bulliten of VGASU. 2010;**4**(20);93-99

[7] Podolsky VlP, Bykova AA, Trufanov EV. Influence of Carbon Consisting Mineral Powder on Operation Ability of Sand Asphalt Concrete. Kazan; 2008:26-30

[8] Podolsky VlP, Lukashuk AG, Chernousov DI. Science-practical results of application of asphalt bitumen binding agent in road construction. 2014;**17**(4):86-95

[9] Podolsky VlP, Vysotskaya MA, Kuznetsov DA, Chernousov DI. Formation of asphalt-binder substance during interaction of shungit mineral powder and bitumen. Scientific Bulletin of VGASU. Construction and Architecture. 2013;(29)75-81

[10] Boguslavsky AM, Sarkha, Efremov LG. Zavisimost dependence of asphalt concrete rheological ability on its composition. Roads. 1977;(8):22-24

[11] Rudensky AV, Radovsky BS, Konovalov SV. About the regularities of fatigue failure of road base. Works by GiprodorNII. 1973;(7):7

[12] Fatigue strength of asphalt-concrete mixtures. Moscow: Express-inform. VINITI RAAS. 1976;**41**:7-19

[13] Basics of a simplified method for calculating bitumen-mineral mixtures. Moscow: Express-inform. VINITI RAAS. 1975;**3**:1-16

[14] Podolsky VlP, Rudensky AV, Chernousov DI, Trufanov EV. Comparison Analysis of Fatigue Durability of Blankets from Asphalt Concrete Mixes Based on Lime Stone and Shungite Powder with Carbon Consisting Material. Moscow: MADI Association of Researches of Asphalt Concrete; 2011. pp. 137-143

[15] Podolsky VP, Chernousov DI, Trufanov EV. Research of fatigue life of asphalt – Concrete based on shungite mineral powder. Scientific Bulletin of VGASU. Construction and Architecture. 2011;**1**(21):80-86

[16] Rudensky AV. The Experience of Asphalt Concrete Blanket Construction in Different Climatic Conditions. Moscow: Transport; 1983. 64p

[17] Rudensky AV. Analysis of asphalt concrete structures with nonstandard performances. GiprodorNII works. 1979;(27):66-78

[18] Gezencvei LB, Boguslavsky AM. Road Asphalt Concrete. L.B. Gorelushev, Moscow: Transport. 1985. 350p

[19] Rysiev OA. Shungite is the stone of life. St. Petersburg: Publishing house “Dilya”; 2010

[20] Chernousov DI. Application of asphalt binding material with shungite in the construction of road surfaces. Voronezh; author's abstract PhD diss; 2011

[21] Podolsky VlP, Trufanov EV, Bykova AA, Kovalyov NS. Effect of Carbonaceous Mineral Powder on Operational Properties of Sand Asphalt-Concrete. Kazan. pp. 26-31

Chapter 6

Evaluation of Structural and Thermal Properties of Rubber and HDPE for Utilization as Binder Modifier

Farzaneh Tahmoorian, Bijan Samali and John Yeaman

Additional information is available at the end of the chapter

http://dx.doi.org/10.5772/intechopen.75535

Abstract

Today, high-performance requirements for asphalt pavements demand enhanced properties for bitumen to withstand the environmental condition and traffic demand. On the other hand, the rapid growth in population and economy results in a continuously increased material consumption, and subsequently waste generation. Among various waste materials, rubber and plastic, including high-density polyethylene (HDPE), constitute some part of the non-biodegradable solid wastes worldwide. Because of the great difficulties in managing the non-biodegradable wastes and the required volume of bitumen, the idea of using plastic and rubber as bitumen modifier in new asphalt mixtures appears to be an effective and meaningful utilization of these materials. As binder plays an important role in the final performance of the asphalt mixture, an understanding of modified binder properties is essential in designing an asphalt mixture. To this point, since compatibility of asphalt mixture with polymer is the most important factor in the blend of polymers and asphalt, the properties of the waste polymers were evaluated in this ongoing research by means of advanced thermal analysis and scanning electron microscope (SEM). This chapter presents the results of this experimental study to evaluate the properties of polymers as potential modifier for virgin bitumen in asphalt mixture.

Keywords: bitumen, modified binder, plastic, rubber, HDPE, TGA, DSC, SEM

1. Introduction

Aggregate and binder are two principal constituents of asphalt mixtures. Although the mechanical and chemical properties of aggregates can vary significantly depending on their

source, the overall durability and other performance characteristics of asphalt mixtures are generally limited by the performance of the asphalt binder. Failure of asphalt pavement due to the asphalt binder can be attributed to three main sources including:

- rutting occurs at high temperatures as asphalt softens and the elasticity of the binder decreases,
- fatigue cracking due to the repeated loading and aging of the pavement, and
- thermal cracking at low temperatures as asphalt becomes brittle.

Failure of asphalt binders is obviously undesirable. Referring to the considerable research in recent years focused on improving the binders' functional properties, the use of polymers as additives greatly improves the performance of bitumen, including elasticity increase, cohesion improvement, and temperature susceptibility reduction, which all subsequently lead to the improvement of asphalt mixture performance in terms of flexibility, cohesion, and deformation resistance at high temperatures. However, the costly nature of polymer modifiers has stimulated research into cheaper and more cost-effective modifiers produced from recycled materials. For these reasons, and as a quite effective way of disposing of the increasing volume of non-biodegradable wastes, which each year are unavoidably generated in different sectors of human activity, polymer wastes like plastic and rubber can be a reasonable potential materials for consideration as binder modifier.

In light of this, the purpose of the present work is to study the characteristics of waste polymers as potential modifier of bitumen. In that sense, as discussed in the following sections, several samples of bitumen and waste polymers were prepared, and a further thermal and microstructural characterization was carried out on these materials.

2. Bitumen

Bitumen is a construction material obtained from crude oil through distillation processes in the petroleum refinery. Bitumen is useful in road construction due to some of its properties such as adhesion, being water proof and durable. The bitumen is principally used in the road construction as a binder where it is mixed with aggregates to produce asphalt mixture. The asphalt mixture must have adequate properties in order to withstand the permanent deformation, fatigue cracking, and thermal cracking, which are the main distress modes of flexible pavements. Therefore, it should have proper stiffness and bearing capacity and must be able to spread load evenly over the pavement layers.

A large number of procedures have described different fractions in bitumen. Based on the most common procedure, bitumen is divided into four generic groups of saturates, aromatics, resins, and asphaltenes, namely SARAs. The molecular weight of these fractions increases in the order S < A < R < A [1].

The structure of bitumen is mostly regarded as a colloidal system. In this system, the asphaltene particles are dispersed into the oily dispersion medium called the maltenes, which is composed of saturates, aromatics, and resins. As illustrated in **Figure 1**, a shell of resins has covered the asphaltene particles. The temperature and equilibrium between the covering part and dissolved part of resins affect the shell thickness [2–4].

http://dx.doi.org/10.5772/intechopen.75535

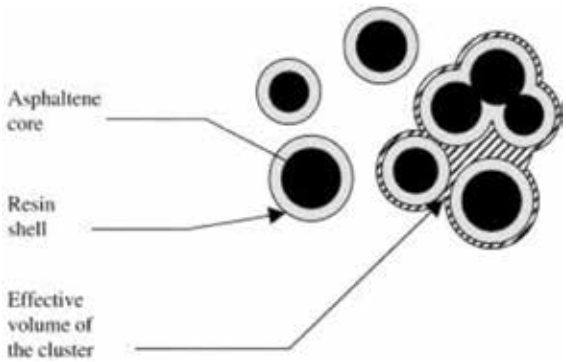

Figure 1. A simplified view of the colloidal structure of bitumen [2].

In 1987, as part of the Superior Performing Asphalt Pavement Program (Superpave), an asphalt binder specification system was developed for evaluation of asphalt performance properties and classification of binders based on its maximum and minimum service temperature. In this specification, the physical properties of an asphalt binder was matched with a performance grade (PG) based on climatic and environmental condition.

In this PG system, two numbers are assigned to each asphalt grade. For example, for asphalt grade of PG 67-22, the first number shows the maximum temperature (in °C) at which the binder can still resist permanent deformation adequately. This number is an average seven-day maximum pavement service temperature. The second number is the minimum temperature at which the binder can perform properly to resist thermal cracking, and hence it is the minimum pavement service temperature. The binders with the maximum temperature ranging from 46 to 82°C and the minimum temperature ranging from −10°C to −46°C (both in increments of 6°) are commercially available, as shown in **Figure 2**. The diagonal line that connects the asphalt grades of PG 82-10 to PG 46-46 is the border between the asphalt grades, which can be produced at refineries and are those produced only by modification (shaded areas). Useful temperature range (UTR) is a measure of the difference between upper and

Upper Specification Temperature, °C \ Lower Specification Temperature, °C	-10	-16	-22	-28	-34	-40	-46
PG 82	-10	-16	-22	-28	-34		
PG 76	-10	-16	-22	-28	-34		
PG 70	-10	-16	-22	-28	-34	-40	
PG 64	-10	-16	-22	-28	-34	-40	
PG 58		-16	-22	-28	-34	-40	
PG 52	-10	-16	-22	-28	-34	-40	-46
PG 46					-34	-40	-46

Figure 2. Performance grades for commercially available binders (after Ref. [5]).

lower service temperatures. The binders produced at refineries without modification have a UTR of not more than 86°C, whereas the modified binder often have a UTR of more than 92°C. Therefore, UTR can be used as an indicator showing the degree of required modification and the cost needed for modification. As UTR increases, this cost increases accordingly [5].

3. Polymer modifiers

The binder characteristics strongly influence the mechanical properties of asphalt mixture. To this point, binder should have a certain mechanical and rheological requirements as follows in order to fulfill the pavement criteria:

- For homogeneous coating of aggregates, the bitumen should be fluid enough at mixing and construction temperatures of about 160°C.
- To resist permanent deformation, the bitumen should be stiff enough at high temperatures (about 60°C depending on the local climate)
- To resist the cracking, the bitumen should be soft enough at lower temperature that pavement experiences (approximately down to −20°C depending on the local climate).

Accordingly, it can be concluded that obtaining bitumen to work well under all aforementioned conditions can be difficult. To surmount this problem, many researchers have tried to develop the asphalt pavement performance by improving the asphalt binder behavior using different modifiers. There are a large varieties of materials, which are often used for modifying the binder, of which polymers are widely known to be easy to use and cost effective. Referring to available literature (for example, see [6–9]), polymer addition may result in both a more flexible binder at low in-service temperature and enhanced properties at high in-service temperature, which significantly prevent the pavement from being deformed. They also improve the adhesive bonding to aggregate particles [10]. Polymers can exist in two different morphologies while in a solid phase:

- Amorphous, in which molecules are randomly oriented within the polymer when the material is cooled in a relaxed state. The cooled state of amorphous materials is highly similar to their molten state. The only difference between these two states is the molecules' distance. These polymers can easily be altered in shape and generally exist in a rubbery state.
- Semicrystalline is an arrangement of ordered molecules with some amorphous regions. As the semicrystalline polymer cools, a portion of the molecular chains forms crystals by folding up into densely packed regions. The polymer is classified as semicrystalline, if more than 35% of the polymer chain forms these crystals. These polymers are stiff and exist in a glassy state.

The degree of crystallinity in a polymer is affected by different factors such as polymer type, additives, and cooling rate. The morphology and degree of crystallinity significantly influence the polymers' properties. Polymers with high degree of crystallinity have a higher glass transition temperature and higher modulus, toughness, stiffness, tensile strength, and hardness. In addition, they have more resistance to solvents but are less resistant to impact strength [11].

http://dx.doi.org/10.5772/intechopen.75535

Today, there are a large varieties of polymers that are often used for modifying the binder. These polymers can be mainly classified into the following categories:

- Elastomers such as rubber can be stretched and then recover their shape when the stretching force is released. Elastomers contribute to the elastic component of binder. The addition of elastomers to the binder results in an increase in the binder stiffness at high temperatures and loading and subsequently will improve the resistance to permanent deformation. However, elastomers will not substantially improve the ability of asphalt mixtures in thermal resistance.
- Plastomers such as polyethylene can form tough, rigid, three-dimensional networks within the bitumen resulting in increase of the initial strength of the bitumen, and subsequently improving the ability of asphalt concrete to resist the heavy loads. Plastomers have less elasticity compared to elastomers as they do not provide an increase in the plastic component of binder while they increase the binder's stiffness at high temperature and loading [12]. Therefore, plastomers can improve the rutting resistance, but they lack the improvements in fatigue resistance, cracking resistance, and low-temperature performance [13] because of increased intermediate and low-temperature stiffness. This makes them inferior to elastomers.

Although modifying the binders will result in the enhancement of binder's properties, using virgin additives as modifier will increase the road construction cost. Therefore, in recent years, many investigations have been conducted on modifying binders using waste materials as additives. Among these waste materials, application of waste plastics and rubbers in certain amount as binder modifier can substantially enhance the stability, strength, fatigue life, and generally the asphalt performance in one hand [14], and on the other hand, it would be an ideal solution for reducing the environmental pollution associated with these non-biodegradable wastes. In light of this, according to the characteristics of elastomers and plastomers, this chapter analyses the characteristics of high-density polyethylene (HDPE) and crumb rubber as potential binder modifier. The tests used to evaluate the polymer properties were thermal analysis by thermogravimetric analysis (TGA) and differential scanning calorimetry (DSC), and microstructure analysis by scanning electron microscopy (SEM).

4. Materials

4.1. Bitumen

Bitumen of C320 was used as a base material for this research, which was kindly supplied by Boral Ltd. This bitumen corresponds to the most common bitumen used in Australia. C320 is classified and manufactured in accordance with AS 2008 (2013) and is suitable for medium to heavy asphalt applications as well as for heavy duty and hot climate seals. The typical characteristics of bitumen C320 are presented in **Table 1**.

As emphasized earlier and shown in **Figure 3**, the complex structure of bitumen is composed of unsaturated structures divided into two main groups of asphaltenes (which are insoluble in n-heptanes) and maltenes. The maltenes are further split into saturates, aromatics, and resins. The proportion of bitumen fractions and the molecular weight of each fraction is presented in **Table 2**.

Characteristics	Unit	Methods	Value
Softening point	°C	AS 2341.18	52
Penetration at 25°C	dmm	As 2341.12	Min 40
Flashpoint	°C	AS 2341.14	Min 250
Viscosity at 60°C	Pa·s	AS 2341.2	320
Viscosity at 135°C	Pa·s	As 2341.2	0.5
Specific Gravity	Kg/m^3	AS 2341.7	1.03

Table 1. Characteristics of the original bitumen.

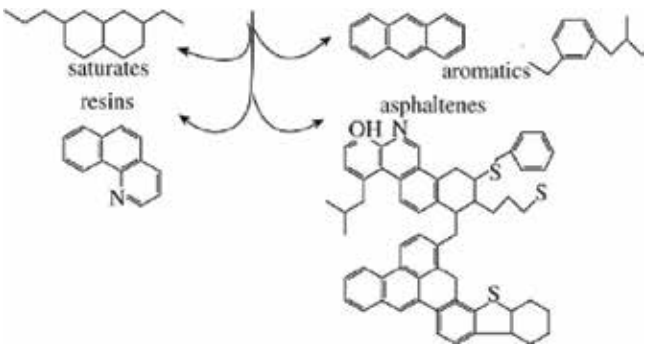

Figure 3. Main compounds in representative structures of the four bitumen fractions [15].

Fraction	Proportion of the overall bitumen	Molecular weight	Description
Asphaltenes	5–25%	600–3000	Substantial effect on bitumen rheological properties
Resins	15–25%	500–1300	Dispersing agent for asphaltenes; their proportion to asphaltenes determines the structural character of the bitumen
Aromatics	40–65%	300–800	Major dispersion medium for asphaltenes
Saturates	5–20%	300–600	Non-polar viscous oil

Table 2. Proportion and molecular weight of bitumen chemical fractions [3, 16–19].

The rheological properties of bitumen are highly affected by the asphaltene content due to its physical parameters such as glass transition and bitumen viscosity [20, 21]. An increase in the asphaltenes content will generally result in harder bitumen with a lower penetration, higher softening point, and higher viscosity [22].

4.2. HDPE

Among plastics, polyethylene (PE) forms the largest portion followed by polyethylene terephthalate (PET). To this point, this study focused on polyethylene and particularly on high-density polyethylene (HDPE). The HDPE used in this research were obtained from plastic recycling plant. As shown in **Figure 4(a)**, the HDPE is in the granular form with the particle size of 2.36 mm. HDPE like other plastics is a polymer consisting of very large molecules made up of smaller units called monomer, which are joined together in a chain by a process called polymerization. Polyethylene is semicrystalline material with a wide range of properties and appropriate resistance to chemicals and fatigue. A molecule of polyethylene has a very simple structure and is composed of a long chain of carbon atoms with two hydrogen atoms attached to them, as shown in **Figure 4(b)**. Sometimes other elements such as oxygen, nitrogen, chlorine, or fluorine are attached to these polymer molecules. These are lightweight molecules with low moisture absorption rates and good resistance to organic solvents.

HDPE is one type of thermoplastics. As most of the thermoplastics can soften at temperature ranging from 130 to 140°C with no gas emission in the temperature range of 130–180°C, they can be a potential option for blending with bitumen in asphalt production because the heating temperature for bitumen ranges from 155 to 165°C in the whole processes for asphalt pavement construction [23]. **Table 3** presents the information regarding the thermal behavior of polyethylene, which emphasizes its suitability as a binder modifier.

In order to find the relevant properties of HDPE, some tests were conducted on this material and the result of these test are presented in **Table 4**.

4.3. Crumb rubber

Crumb rubber used in this research was obtained from tyre recycling plant that processes the car tyres into crumb rubber through the ambient grinding method. The crumb rubber was provided in granule form, as shown in **Figure 5(a)**.

The particle distribution test was performed on crumb rubber. The result of sieve analysis is presented in **Table 5**. The ground tyre rubber has a particle size averaged between 8 and 50 mesh (2.36 and 0.300 mm).

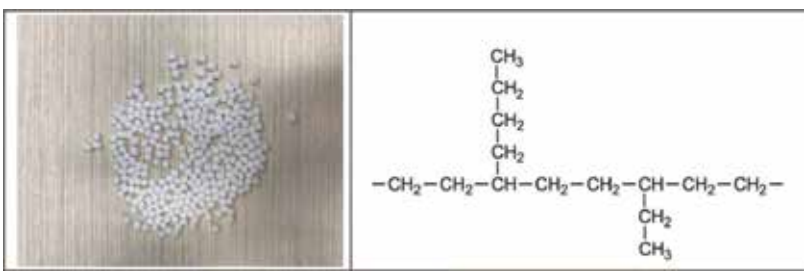

Figure 4. Analyzed material (a) HDPE and (b) chemical structure of HDPE.

Characteristics	Unit	Methods	Reported products
Solubility in water	—	Nil	—
Softening temperature	°C	100–120	No gas
Decomposition temperature	°C	270–350	CH_4, C_2H_6
Ignition temperature range	°C	> 700	CO, CO_2

Table 3. Thermal characteristics of polyethylene [23].

Characteristics	Unit	Methods	Value
Density	g/cm^3	AS 1141.5	0.963
Size	mm	AS 1141.11.1	2.36
Water absorption	%	AS 1141.5	0.0

Table 4. Characteristics of high-density polyethylene (HDPE).

Figure 5. Analyzed material (a) crumb rubber and (b) chemical structure of rubber.

Sieve no.	Sieve size (mm)	Mass retained (%)
4	4.75	0.0
8	2.36	25.7
16	1.18	67.7
30	0.600	6.2
50	0.300	0.4
100	0.150	0.0
200	0.075	0.0

Table 5. Particle size distribution of crumb rubber.

Characteristics	Unit	Methods	Value
Density	g/cm^3	AS 1141.5	0.982
Size	mm	AS 1141.11.1	1.18–2.36
Water absorption	%	AS 1141.5	0.1

Table 6. Characteristics of crumb rubber.

The properties of crumb rubber are presented in **Table 6**, which are obtained from conducting relevant tests on crumb rubber. It should be noted that tyre rubber is typically a composition of three polymers including polyisoprene (natural rubber), polybutadiene, and polystyrene-butadiene [24]. The main compounds in rubber are shown in **Figure 5(b)**.

5. Methodology

In this research, different polymers (i.e., bitumen, HDPE, and crumb rubber) were analyzed based on their calorimetric curve, thermal transition, and their overall quality. The analysis of the materials was performed by means of thermogravimetric analysis (TGA), differential scanning calorimetry (DSC), and scanning electron microscopy (SEM).

5.1. Sample preparation

For performing analysis on polymers, the samples were prepared based on the requirements of equipment. In order to study the thermal behavior of individual polymers, in all cases, a small amount of material (5 to 10 mg) was placed in a measuring pan. To prevent pressure buildup during the test, it was advised to have a small opening in the small pan. After this preparation, the samples were placed in DSC or TGA equipment.

5.2. Analysis methodology

It is expected that the addition of polymers influences the microstructure of binder. In theory, the addition of polymers containing hard segments provides higher strength, whereas the soft segment polymers improve toughness and low-temperature cracking. Since the binder modification depends on the compatibility of bitumen and polymer as modifier, this chapter covers the study of the individual polymers to identify some of their physical and chemical properties, their thermal behavior, and their microstructure. The tests to characterize the analyzed materials were performed in the Advanced Materials Characterization Facility (AMCF) at Western Sydney University, Australia. These tests included thermal analysis, structural characterization, and microstructure analysis, and the main points of testing procedure are represented in the following sections.

5.2.1. Thermal analysis

Thermal analysis corresponds to a group of techniques used to measure the physical and chemical properties of materials as a function of temperature. The measurements can be performed

in different atmospheres including inert atmosphere (nitrogen, argon, helium) or in an oxidative atmosphere (air, oxygen). The gas pressure can also selectively vary in thermal analysis. In this research, the thermal behavior of materials was investigated through DSC and TGA.

5.2.1.1. Differential scanning calorimetry (DSC)

Parameters such as glass transition temperature (T_g), melting point, and the degree of crystallization were monitored by DSC. It should be noted that the glass transition temperature is more important in polymer applications compared to the melting point, because it corresponds to the polymer behavior under ambient conditions.

In this research, DSC analysis was performed according to ASTM E473-85 in an NETZCH DSC 204 F1 to obtain the thermal critical points of materials. The test specimens weighing about 5 mg were heated up at different temperature ranges, depending on polymer type, in an aluminum crucible under an air flow (100 mL/min) at a rate of $10°C \cdot min^{-1}$.

For bitumen, DSC experiments were carried out on about 5 mg samples in aluminum crucibles with perforated covers. Before conducting DSC, the bitumen sample was homogenized at 130°C for about 1 hour and then placed in the DSC equipment. To conduct DSC, first, the samples were cooled from room temperature to −100°C at a heating rate of −10°C/min. The samples were maintained at the low temperature for about 15 minutes to ensure a stabilized initial reading. Then, they were heated up to 200°C at a heating rate of 10°C/min. The DSC thermograph recorded during this heating scan is considered as the first scan. On completing the first scan, the sample was maintained at 200°C for 5 min to remove thermal history and then quickly cooled from 200°C to its starting temperature (−100°C) at a cooling rate of −10°C/min and again held for about 15 min before being reheated to 200°C at a heating rate of 10°C/min. The DSC thermograph recorded during this second heating scan is considered as the second scan. The same procedure was repeated to provide the third heating scan.

For rubber, similar to bitumen, three cycles of cooling and heating were considered as the method of the experiment with the same heating rate of 10°C/min, cooling rate of −50°C/min, and temperature range of −100–200°C. For HDPE, the DSC procedure was the same as bitumen and rubber with an exception of the temperature range, which was considered from −160 to 200°C.

Glass transition and melting point were measured from DSC curves. The percentage of crystallized fraction (CF) was determined from the following equation through dividing the observed melting enthalpy (ΔH_{obs}) by the melting enthalpy of 100% crystalline material (ΔH_o).

$$CF = \frac{(\Delta H_{obs} \times 100)}{\Delta H_o} \quad (1)$$

The values of ΔH_o depend on the material type and can be found in literature. For example, a value of 200 J/g was used by Lesueur et al. [4] and Claudy et al. [25]. Values of 180 and 121 J/g were used by Michon et al. [26] and Lu and Redelius [27], respectively.

5.2.1.2. Thermogravimetric analysis (TGA)

Thermogravimetric analysis (TGA) was performed to study the kinetics and to investigate the degradation process of materials at a higher temperature. In this study, the thermal

decomposition was verified in 5 mg samples in an aluminum crucible under air flow (100 mL/min) heated from 30 to 600°C at a heating rate of 10°C·min^{-1}. The TGA curves and its differential (DTG) were carried out in an NETZSCH STA-449C thermogravimetric analyzer. The onset temperature of the mass loss effect (T_O) and temperature of peak rate of mass loss (T_p) were determined from TGA thermographs.

5.2.1.3. Microstructure characterization

The microstructure of the materials was investigated under scanning electron microscope (SEM). Scanning electron microscopic analysis was done in 6510LV SEM employing between 10 and 20 kW. The specimens in this study were examined with magnifications of 100–1000, and the results of this study with best magnification are presented in the following sections.

6. Results and discussion

6.1. Thermal analysis by DSC

Heating the polymers results in a number of phase changes such as the glass transition (T_g), crystallization transition (T_c), and melting point (T_m). DSC analysis is a useful technique to identify the location of these thermal parameters. In the DSC curves, the sharp peaks are related to the polymer melting and the areas under these peaks provide the heat of fusion (ΔH). Furthermore, the smaller inconsistencies at the lower temperature are most likely related to the glass transition.

In this research, DSC technique is used to investigate the transition temperatures and the crystallization degree of different polymers. Accordingly, the DSC curves were examined to evaluate the physical characteristics of individual materials. It should be noted that for DSC runs, the complete set of heating-cooling process were repeated three times for each polymer, where the first run is usually carried out to remove any impurities and moisture from the sample. In addition, in order to evaluate the transitions accurately, a temperature scan over a wide range temperature is considered for DSC analysis.

In DSC analysis, the thermal parameters for bitumen depend on the refined petroleum source as well as the petroleum refining process. **Figure 6** shows the DSC thermograph of neat bitumen and its corresponding first-derivative curve. The effects detected in the thermograph, as assigned previously (for example, see [28–30]), are described below.

An increase in the heat capacity for neat bitumen can be observed in the DSC curve by an abrupt change in the slope of the curve placed in the low-temperature region (around −30°C) corresponding to the glass transition temperature (T_g) of the bitumen. The glass transition temperature (T_g) is a material's temperature at which all molecular transitional motion is frozen; therefore, the material becomes rigid and brittle at or below this temperature. The glass transition temperature of polymers is one of the most important parameters as it is related to the average molecular weight of polymers and hence provides information about their composition. Moreover, it demonstrates the viscoelastic behavior of polymers at low temperatures [31]. Therefore, the glass transition temperature of neat bitumen is believed to be closely related to the low-temperature performance of asphalts. As shown in **Figure 6**, the middle point of the temperature range where the transition occurs is considered as the

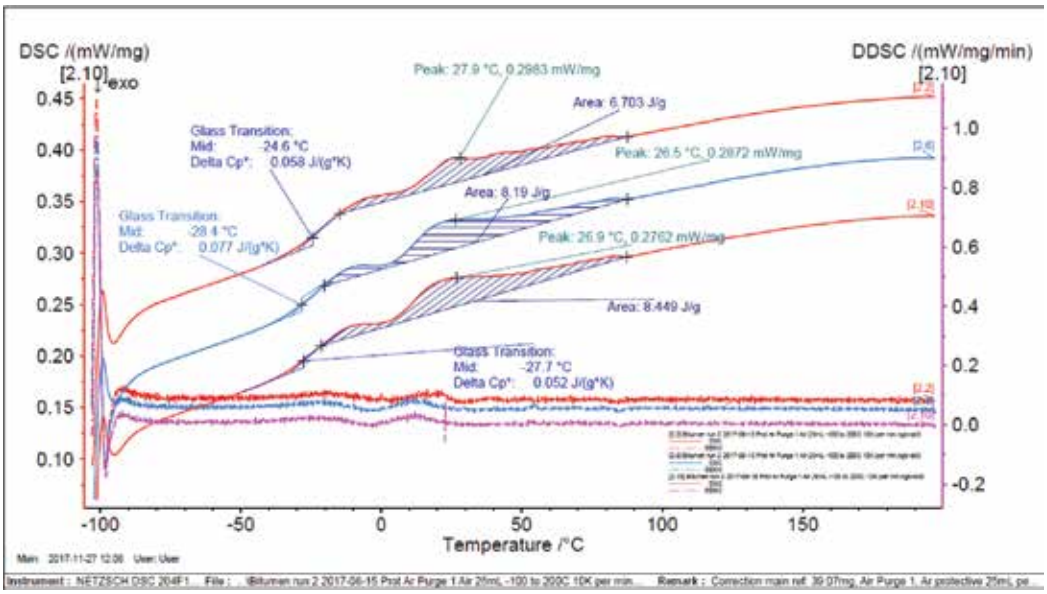

Figure 6. DSC and DDSC thermograms of bitumen.

glass transition temperature. In addition, as shown in **Figure 6**, T_{gonset} of bitumen is at about −40°C. Referring to [32], the T_{gonset} temperature is more closely related to the glass transition temperature of the saturate fraction that has the lowest T_g. The main T_g reflects the characteristics of the glass transition temperature of the majority of components.

At temperature above T_g, an exothermal peak and a broad endothermal peak from about −20 to 85°C is observed. The big exothermal peak next to the glass transition is most likely the result of crystallization of small paraffin molecules, and melting of the crystallites formed during heating or cooling is known as the main reason to produce endothermal peaks in this region [32].

Referring to [31], the exothermic effect just above the T_g in DSC thermographs is negligible, as it has been associated in previous studies (for example, see [28, 30]) with the crystallization of certain molecules, which are not crystallized during cooling.

In addition, referring to the literature (for example, see [25, 28–30, 33]), the dissolution of the crystallized fractions (CF) is the main reason of the enthalpy changes and can be calculated from the area under the peak to a reference enthalpy of dissolution. As shown in **Figure 6**, in order to calculate this parameter, a straight baseline between the end of the glass transition and the end of the endothermic effects is drawn. In this research, the reference enthalpy value of 180 J/g is used for the estimation of the amount of crystallized fraction of bitumen based on previous investigations [1, 4, 15, 25, 26, 33]. The calculation of the crystallizable fraction content shows a value of about 4%, which is considered small. The presence of wax content in bitumen is commonly responsible for the extent of crystallizable fractions, which is the main reason for the problem of pavement exudation and inappropriate thermal susceptibility [15].

To achieve DSC curve for rubber, similar to bitumen, three cycles of cooling and heating were considered as the method of the experiment with the same heating rate of 10°C/min, cooling rate of −10°C/min, and temperature range of −100–200°C.

The DSC thermograph of rubber (**Figure 7**) presented a glass transition temperature (T_g) at −55° C. However, due to amorphous nature of rubber, DSC curve does not present a well-defined melting temperature.

For HDPE DSC analysis, as shown in **Figure 8**, it can be observed that HDPE started to lose its solid form at around −100°C corresponding to the glass transition temperature (T_g) of HDPE. As the temperature increases, a strong endothermic peak average value at 134°C can be observed, which is most likely related to the melting of crystalline domains of HDPE.

The DSC curve of HDPE in second heating cycle is illustrated in **Figure 9**. As can be observed, the energy consumption for melting of crystalline domain of HDPE was 221.1 J/g that occurred between the beginning and end of melting point.

The cooling cycle involves the rate of cooling temperature of 10°C /min. As shown in **Figure 10**, the peak point for HDPE becomes totally solid at around 115°C, which means that the crystallization temperature (Tc) of HDPE, an exothermic peak, is 115°C.

To estimate the amount of crystallized fraction of HDPE, the values of ΔH_o of 287.3 J/g has been found from literature for HDPE (for example, see [34, 35]). The calculation of the crystallizable fraction content for HDPE shows a value of about 76%.

It should be noted that fully crystalline polymers do not exhibit glass transition temperature, and their structure will not change until the melting point. However, according to DSC thermographs, HDPE is considered as semicrystalline polymer.

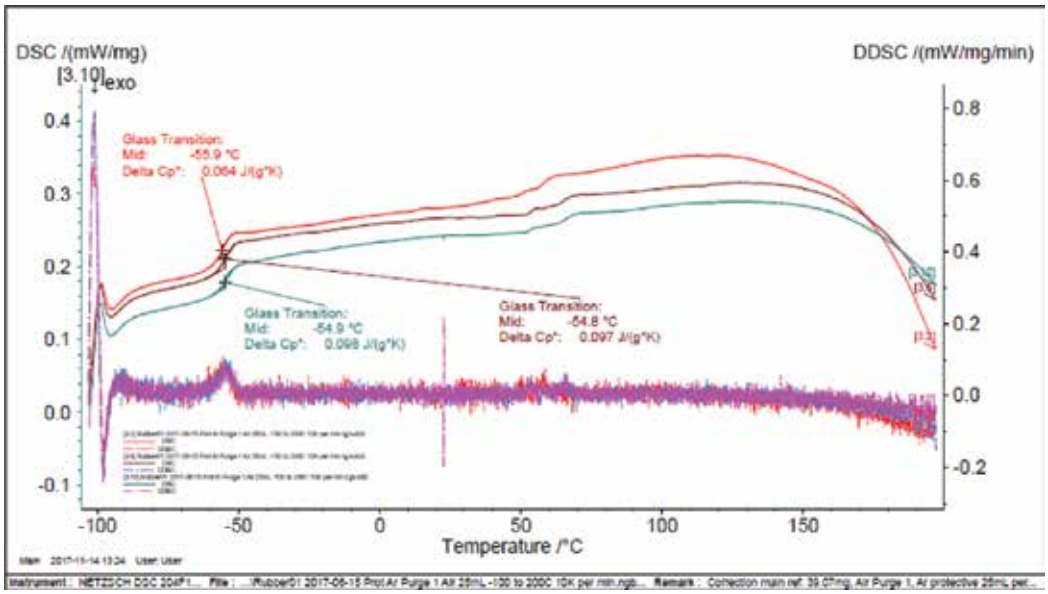

Figure 7. DSC and DDSC thermograms of rubber.

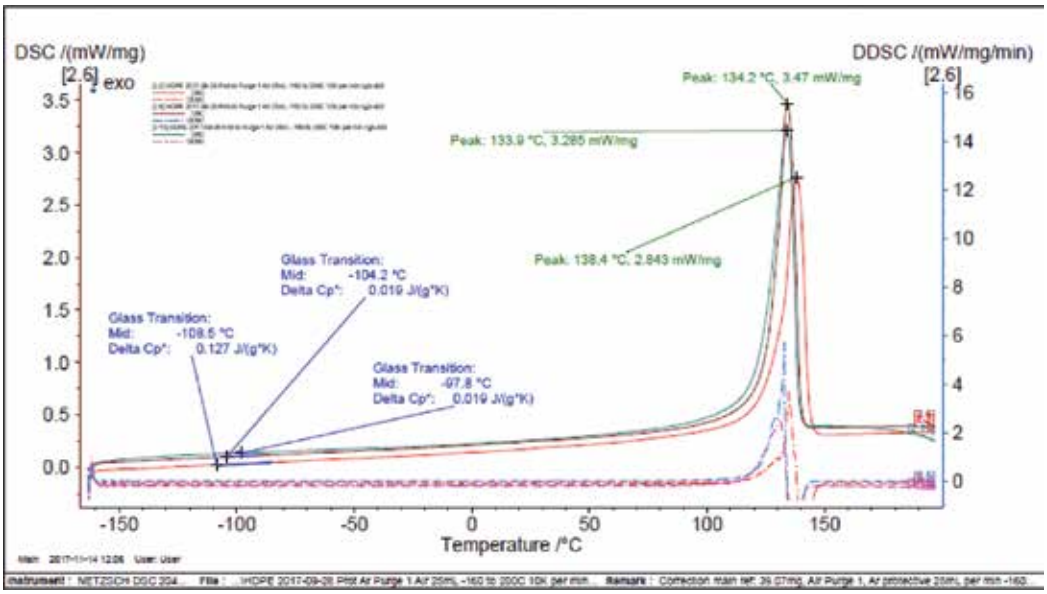

Figure 8. DSC and DDSC thermograms of HDPE for heating cycles.

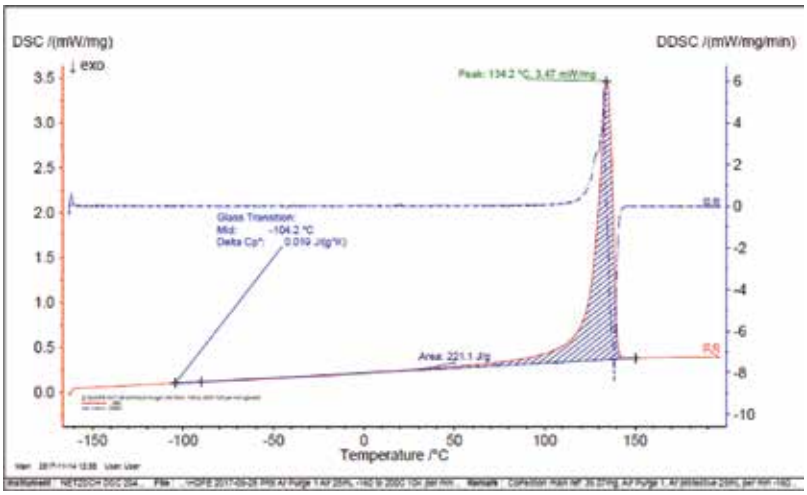

Figure 9. DSC and DDSC thermograms of HDPE for second heating cycle.

In addition, as HDPE has higher molecular weight than bitumen, the melting and crystallization temperature of HDPE is higher to provide more energy for reaching to these points. In addition, the melting and crystallization temperature of HDPE are close to each other, which can be confirmed from literature survey [36].

6.2. Thermal analysis by TGA

The thermal stability of polymers is an important property to be considered for fitting their performance to the proper final application. Thermogravimetric analysis is a good technique

http://dx.doi.org/10.5772/intechopen.75535

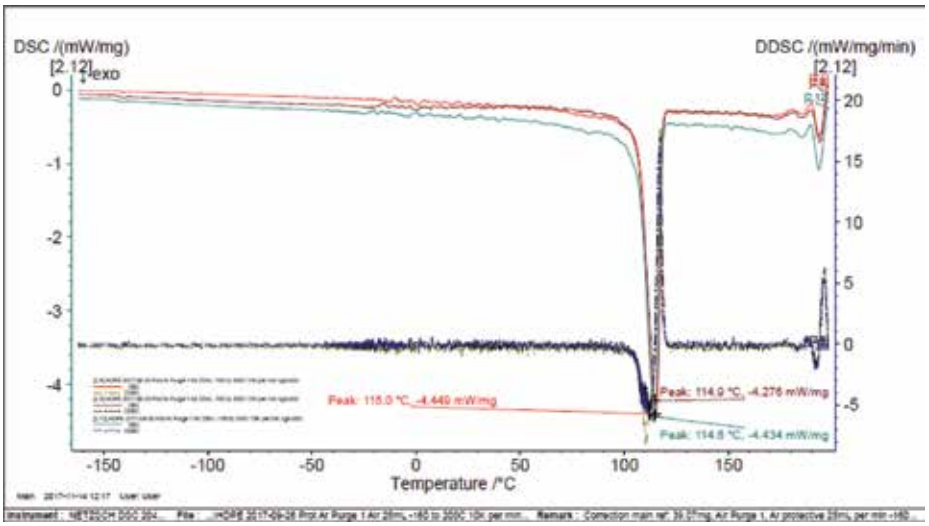

Figure 10. DSC and DDSC thermograms of HDPE for cooling cycles.

to evaluate the thermal stability of materials. Hence, in this research, the thermal stability of three polymers was studied by TGA in air and the main features of the curves including the onset temperatures of the mass loss effects (T_o) and the peak temperatures (T_p) were calculated from the TGA and DTG curves.

For bitumen, the thermogravimetric experiment results for 5 mg samples under air atmosphere over the temperature range of 30–590°C using a total purge gas flow of 100 mL/min and a heating rate of 10°C·min^{-1} show that the onset temperature of the main mass loss effect (T_o) is 370°C, as shown in **Figure 11**.

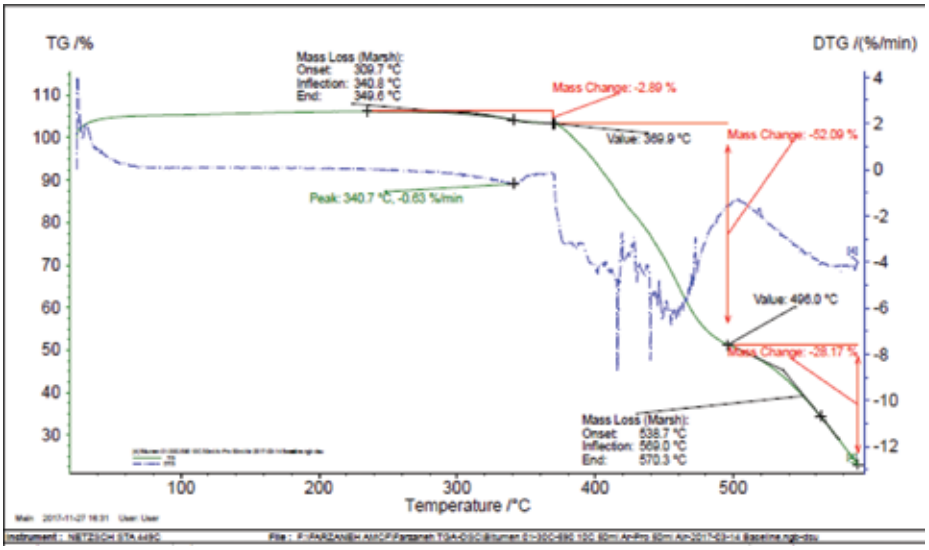

Figure 11. TGA, DTG, and D2TG thermograms of neat bitumen.

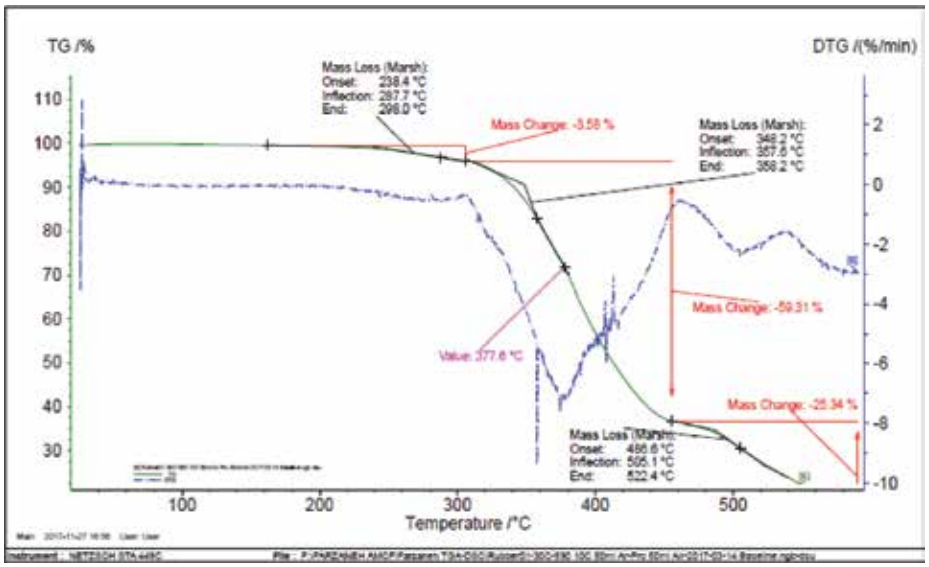

Figure 12. TGA, DTG, and D2TG thermograms of rubber.

Referring to [31], the decomposition of bitumen occurs in at least three steps, considering three temperature ranges, as shown in **Figure 11**. In the temperature range of T < 350°C, the decomposition of saturates and aromatics results in mass loss of bitumen. Over the temperature range of 350 < T < 500°C, resins and aromatics as well as asphaltenes are the main decomposed fractions, and at high temperatures of T > 500°C, the substantial mass change in bitumen occurs as a result of decomposition of asphaltenes. However, resins and aromatics are still decomposed in this range of temperature.

When selecting materials for modifying the binder, it is important that the modifier begins to degrade at a temperature above the bitumen modification temperature or the asphalt production temperature. Otherwise, it will lose its initial properties by the time the modification process is finished. In this research, TGA is used for determination of the degradation temperature of the waste materials, which are used for modifying the binder (i.e., rubber and HDPE). **Figure 12** shows the result of TGA on rubber.

As can be seen, the onset temperature of degradation for rubber is 238°C and the peak temperature of mass loss is 378°C, which can be observed as a peak in the first-derivative curve.

Similar to other polymers, TGA of the HDPE samples was done on approximately 5 mg samples over the range of room temperature to 590°C under air with 100 mL/min flow rate at a heating rate of $10°C \cdot min^{-1}$.

The onset degradation temperature and peak temperature are determined from the derivative TGA curves for HDPE, as shown in **Figure 13**. In this figure, it can be observed that HDPE remains thermally stable up to a temperature of 430°C. After this temperature, HDPE starts to degrade dramatically followed by a substantial step with maximum mass loss rates placing at

http://dx.doi.org/10.5772/intechopen.75535

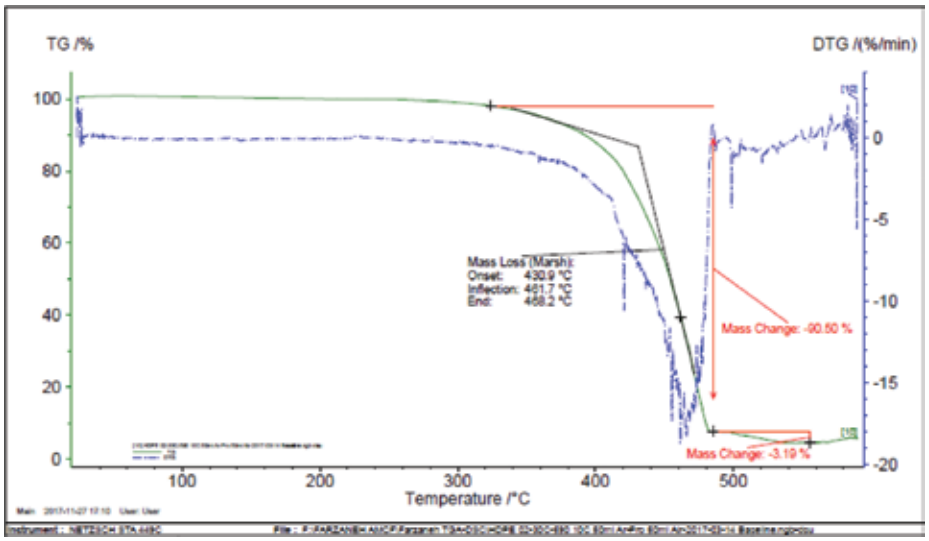

Figure 13. TGA, DTG, and D2TG thermograms of HDPE.

462°C in the DTG curve. This degradation involves a mass loss of about 91% in HDPE due to the thermal cracking of hydrocarbon chains and the production of oxygenated hydrocarbons including CO, CO_2, and H_2O [37]. The degradation ends approximately around 490°C.

6.3. Microstructure analysis by SEM

The analysis of the microstructure of polymers was performed using scanning electron microscope (SEM). The results of the microscopy of as well as the energy dispersive spectroscopy (EDS) analysis on the individual polymers are given in **Figures 14–16**.

As can be observed in **Figure 14**, the surface of bitumen appears as networks of highly entangled strings.

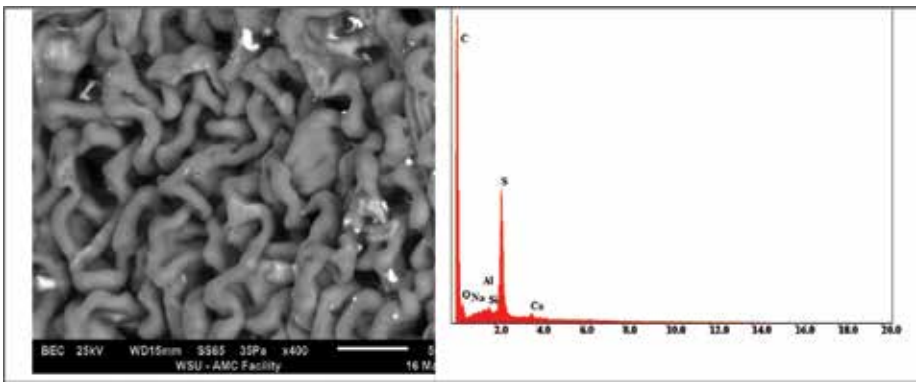

Figure 14. EDS analysis and SEM image of bitumen at 400 magnification.

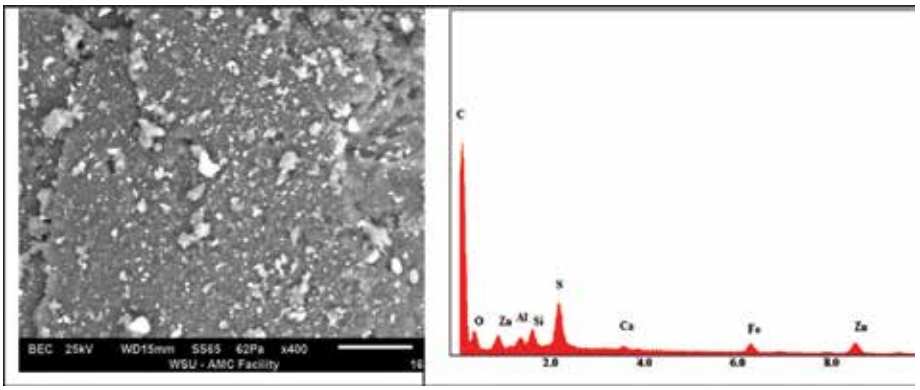

Figure 15. EDS analysis and SEM image of rubber at 400 magnification.

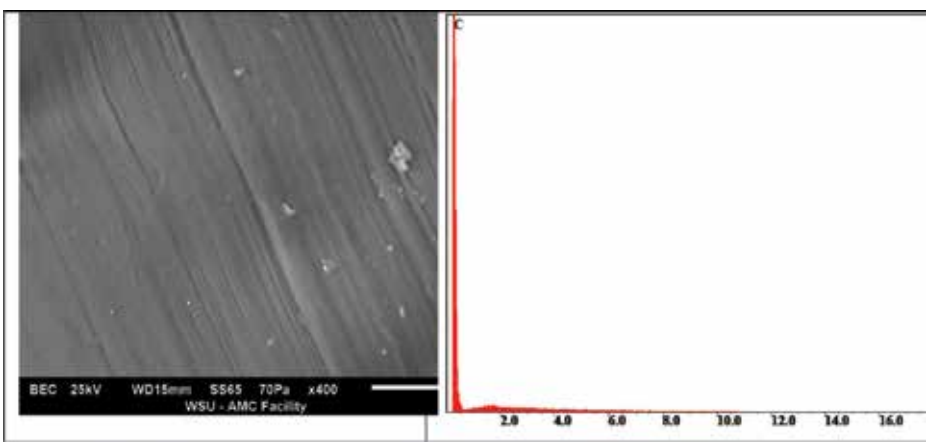

Figure 16. EDS analysis and SEM image of HDPE at 400 magnification.

Figure 15 shows the coarse texture of rubber. The irregular shape and rough texture of rubber can be attributed to its processing method, which is the ambient procedure.

Furthermore, the microstructure of HDPE is shown in **Figure 16**. It should be noted that HDPE has a higher viscosity compared to bitumen. The materials with high viscosity do not separate easily, and therefore, they present in the form of dispersed phase, as can be clearly observed in **Figure 16**.

7. Summary and conclusion

Today, pure bitumen no longer provides suitable performance for pavements due to the current traffic. Therefore, attempts have been made to maximize the effectiveness of asphalt binders selected for construction projects based on a standard asphalt binder classification system. Binder modification technique is used as an alternative to minimize the pavement failures

due to poor performance of asphalt binders, as well as to increase the PG grade of the asphalt binder [38]. Based on these research studies, the utilization of polymers as modifier improves some of the bitumen's properties such as elasticity, cohesion, and temperature susceptibility, which they all subsequently lead to the improvement of asphalt mixture performance.

For these reasons, and as a quite effective way of disposing of the increasing volume of non-biodegradable wastes, which are increasingly generated in societies, plastic wastes and rubbers can be a reasonable potential materials for consideration as binder modifier.

In modification of bitumen with additives, having knowledge about the effects of modifiers on thermal stability is of high importance resulting in manufacturing more thermally stable binders. Accordingly, in this research, the thermal behavior of modifiers and bitumen was studied using TGA, DSC, and SEM facilities. The thermal parameters of T_g and T_m, enthalpy of fusion, ΔH_m, and the percentage of crystallinity, CF (%) of samples can be easily determined from the DSC curves. This information can be useful in understanding the characteristics and the composition of polymers. In addition, many researchers have proposed different equations for estimation of the glass transition temperature of mixture based on the composition and the glass transition of the components of the mixture. All these equations are basically representing the relation between the glass transition temperature of a mixture and those of its components using a basic mathematical form but with minor variations. The glass transition calculated using these equations for the blend of bitumen with 2% HDPE and 8% rubber is −28.8°C. The calculated T_g value for blend is lower than those obtained for neat bitumen, which could be attributed to several effects including certain level of miscibility between the additives (i.e., HDPE and rubber) and bitumen. Thus, using these equations, it may be possible to achieve the formulation of the desired modified binder considering the composition of components and the results of DSC analysis on each component.

Furthermore, in this research, TGA is used in determining the degradation temperature of the waste materials. A modifier that begins to degrade at a temperature below the bitumen modification temperature or the asphalt production temperature is not adequate since it will have lost its initial properties by the time the modification process is finished. In the case of analyzed waste materials, all degrade at temperatures above 200°C and therefore should be adequate for bitumen modification. The main features of TGA curves for individual polymers were discussed in previous sections. From these results, it was observed clearly that HDPE followed by bitumen have higher thermal stability than crumb rubber.

Acknowledgements

The authors would like to acknowledge the Advanced Materials Characterization Facility (AMCF) at Western Sydney University for their expert technical assistance.

Conflict of interest

The authors declare no conflict of interest.

Author details

Farzaneh Tahmoorian[1]*, Bijan Samali[1] and John Yeaman[2]

*Address all correspondence to: f.tahmoorian@westernsydney.edu.au

1 Centre for Infrastructure Engineering, Western Sydney University, Kingswood, NSW, Australia

2 Faculty of Science, Health, Education and Engineering, University of Sunshine Coast, Sippy Downs, Queensland, Australia

References

[1] Claudy P, Létoffé JM, King GN, Planche JP, Brulé B. Characterization of paving asphalts by differential scanning calorimetry. Fuel Science & Technology International. 1991;**9**:71-92

[2] Redelius P. The structure of asphaltenes in bitumen. Road Materials and Pavement Design. 2006;**7**:143-162

[3] Lesueur D. The colloidal structure of bitumen: Consequences on the rheology and on the mechanisms of bitumen modification. Advances in Colloid and Interface Science. 2009;**145**:42-82

[4] Lesueur D, Gerard JF, Claudy P, Letoffe JM, Plance JP, Martin DA. Structure related model to describe asphalt linear viscoelasticity. Journal of Rheology. 1996;**40**(5):813-836

[5] Asphalt Institute, editor. Asphalt Binder Testing MS-25. 2nd ed. USA: Asphalt Institute; 2008

[6] Yeh PH, Nien YH, Chen WC, Liu WT. Evaluation of thermal and viscoelastic properties of asphalt binders by compounding with polymer modifiers. Polym Compos. 2010;**31**:1738-1744

[7] Afroz Sultana SK, Prasad KSB. Utilization of waste plastic as a strength modifier in surface course of flexible and rigid pavements. International Journal of Engineering Resources Applications. 2012;**2**(4):1185-1191

[8] Huang Y, Bird RN, Heidrich O. A review of the use of recycled solid waste materials in asphalt pavements. Journal of Resource Conservation Recycling. 2007;**52**:58-73

[9] Casey D, McNally C, Gibney A, Gilchrist MD. Development of a recycled polymer modified binder for use in stone mastic asphalt. Journal of Resource Conservation Recycling. 2008;**52**(10):1167-1174

[10] Ghuzlan KA, Al-Khateeb GG, Qasem Y. Rheological properties of polyethylene-modified asphalt binder. Athens Journal of Technology and Engineering. 2013. Vol. X, No. Y. pp. 1-14

[11] Farukkawa T. Molecular structure, crystallinity and morphology of polyethylene/polypropylene blends studied by Raman mapping, scanning electron microscopy, wide angle X-ray diffraction, and differential scanning calorimetry. Polymer Science. 2006;**38**:1127-1136

[12] Lavin PEP. Binder Performance. Asphalt Pavements. New York, NY: Spon Press; 2003. Available from: http://www.ARRMAZ.com

[13] Vlachovicova Z, Wekumbura C, Stastna J, Zanzotto L. Creep characteristics of asphalt modified by radial styrene–butadiene-styrene copolymer. Construction Building Material Journal. 2007;**21**:567-577

[14] Verma SS. Roads from plastic waste. Science tech entrepreneur. The Indian Concrete Journal. November 2008:43-44

[15] Lucena MC, Soares SA, Soares JB. Characterization of thermal behavior of polymer-modified asphalt. Materials Research. 2004;**7**:529-534

[16] Read J, Whiteoak D. The Shell Bitumen Handbook. 5th ed. London: Thomas Telford Ltd; 2003

[17] Nellenstyen FJ. The constitution of asphalt. Journal of the Institute of Petroleum Technologists. 1924;**10**:311-325

[18] Airey GD. Chapter 23: Bitumen properties and test methods. In: ICE Manual of Construction Materials. UK: Institution of Civil Engineers; 2009

[19] Paliukaitė M, Vaitkus A, Zofka A. Influence of bitumen chemical composition and ageing on pavement performance. The Baltic Journal of Road and Bridge Engineering. 2015;**10**(1):97-104. DOI: 10.3846/bjrbe.2015.12

[20] Corbett LC. Relationship between composition and physical properties of asphalts. In: Proceedings of the Association of Asphalt Paving Technologists. 1970;**39**:481-498

[21] Halstead JC. Relation of asphalt chemistry to physical properties and specifications. In: Proceedings of the Association of Asphalt Paving Technologists. 1985;**54**:91-117

[22] Scholz TV. Durability of Bituminous Paving Mixtures [PhD thesis]. University of Nottingham; 1995

[23] Gawande A, Zamare G, Renge VC, Tayde S, Bharsakale G. An overview on waste plastic utilization in asphalting of roads. Engineering Research and Studies Journal. 2012;**3**(2):1-5

[24] Quek A, Balasubramanian R. Mathematical modeling of rubber tire pyrolysis. Journal of Analytical and Applied Pyrolysis. 2012;**95**:1-13

[25] Claudy PM, Létoffé JM, Martin D, Planche JP. Thermal behaviour of asphalt cements. Thermochimica Acta. 1998;**324**:203-213

[26] Michon LC, Netzel DA, Turner TF. A C13NMR and DSC study of the amorphous and crystalline phases in asphalts. Energy and Fuels. 1999;**13**:602-610

[27] Lu X, Redelius P. Effect of bitumen wax on asphalt mixture performance. Journal of Construction Building Material. 2007;**21**:1961-1970

[28] Claudy P, Létoffé JM, Germanaud L, King GN, Planche JP, Ramond G, Such C, Buisine JM, Joly G, Edlanio A. Thermodynamic behavior and physicochemical analysis of eight SHRP bitumens. Transportation Research Board. 1993:1-9

[29] Bosselet F, Létoffé JM, Claudy P, Valentin P. Study of the Thermal Behavior of n-Alkanes in Complex Hydrocarbon Media by Differential Calorimetric Analysis. Thermochimica Acta. 1983;**70**:19

[30] Letoffe JM, Claudy P, Kok MV, Garcin M, Volle JL. Crude oils – characterization of waxes precipitated on cooling by DSC and thermomicroscopy. Fuel. 1995;**74**:810

[31] Jiménez-Mateos JM, Quintro LC, Rial C. Characterization of petroleum bitumens and their fractions by thermogravimetric analysis and differential scanning calorimetry. Fuel. 1996;**75**:1691-1700

[32] Harrison IR, Wang G, Hsu TC. A differential scanning calorimetry study of asphalt binders. Strategic Highway Research Program, National Research Council. SHRP-A/UFR-92-612. Washington, DC; 1992

[33] Masegosa Fanego RM, Cañamero P, Sánchez Cabezudo M, Viñas Sánchez MT, Salom Coll C, Gonzáez Prolongo M, Paez A, Ayala M. Thermal behaviour of bitumen modified by sulphur addition. In: 5th Eurasphalt and Eurobitume Congress. 13-15 June 2012; Istanbul. Turkey.pp. 142-148. ISBN 978-972-8692-45-2

[34] Banat R, Fares MM. Thermo-gravimetric stability of high density polyethylene composite filled with olive shell flour. American Journal of Polymer Science. 2015;**5**(3):65-74. DOI: 10.5923/j.ajps.20150503.02

[35] Mirabella FM, Bafna A. Determination of crystallinity of polyethylene/&alpha-olefin copolymers by thermal analysis relationship of the heat of fusion of 100% polyethylene crystal and the density. American Journal of Polymer Science. Part B: Polymer Physics. 2002;**40**:1637-1643

[36] Ashraf A. Thermal analysis of polymers (LDPE, HDPE) by differential scanning calorimetry technique [thesis]. University of Qatar; 2014

[37] Purohit V, Orzel RA. Polypropylene: A literature review of the thermal decomposition products and toxicity. International Journal of Toxicology. 1998;**2**:221-242

[38] Somayaji S. Civil Engineering Materials. Upper Saddle River, NJ: Prentice Hall; 2001

Edited by Jose Luis Rivera-Armenta and Beatriz Adriana Salazar-Cruz

Asphalt modification is an important area in the development of new road and pavement materials. There is an urgent demand for road materials that can minimize fracture at low temperatures and increase resistance to deformation at high temperatures. The function of asphalt is to bind aggregate to protect it from water and other harmful agents. In the beginning asphalt was ideal for this purpose, but recently traffic loads have increased and environmental factors have deteriorated more rapidly than before. Asphalt is a byproduct of crude oil in the refining process, and it is considered a complex heterogeneous mixture of hydrocarbons. Asphalt modification has become an important research area, using several methods and new materials as modifiers.

Published in London, UK

IntechOpen

ISBN 978-1-83881-523-3